Who moved my protein? Mechanisms of Epileptogenesis due to Mutations of Voltage-Gated Sodium Channel *SCN1B*

by

Gustavo A. Patino

A dissertation submitted in partial fulfillment
of the requirements for the degree of
Doctor of Philosophy
(Neuroscience)
in The University of Michigan
2010

Doctoral Committee:

Professor Lori L. Isom, Chair
Professor Miriam H. Meisler
Professor Michael D. Uhler
Associate Professor Geoffrey G. Murphy
Associate Professor Jack M. Parent

DEDICATION

To my family: My loving parents, my amazing brother and my wonderful wife Aubrey

ACKNOWLEDGEMENTS

This work would not have been possible without the help of so many people, both in the personal and professional aspects of my life, who believed in me and encouraged me at every point. I am grateful to all of you.

First and foremost, thanks to my family: To my wonderful wife Aubrey who has been so patient and loving with me during this endeavor. My parents who have always been there for me, and even when in another country always made sure I knew I was not alone in any situation. My brother who is always making sure I am doing good and never hesitated to help me with any of my projects.

I would like to thank my advisor, Dr. Lori L. Isom for her mentorship on becoming a scientist and balancing work and family successfully. Also, for her continuous support in all my ideas and projects over years. Without it, so many of my achievements at Michigan would not have happened. Also, thanks to all the members of the Isom lab that through the years helped me in so many projects and made the lab a great environment in which to work and thrive intellectually.

I am grateful to all the members of my dissertation committee: Dr. Miriam Meisler, Dr. Geoffrey Murphy, Dr. Jack Parent, and Dr. Michael Uhler. I could always count on them to help me with experimental techniques, explain difficult concepts, make sense of some of my data and support various applications to grants and courses throughout the years.

Many teachers also guided me in the years before coming to Michigan and help me form the basis of the scientist I have become so far. I want to mention especially: Dr. Edgar Osuna, Dr. Jaime Toro, Dr. Manuel Yepes, Dr. Aristides Duque, Dr. Carlos Mayor, Dr. Mario Bernal, Dr. José Félix Patiño, Dr. Alfredo Rubiano, Dr. Eugenio Matijasevic, Dr. Eduardo Londoño, Dr. John Duperly, Dr. Jose Rafael Toro and Helena Groot de Restrepo.

After my arrival to Michigan many professors again made sure that I would find here a home in which to learn and thrive. Besides Dr. Isom and the members of my thesis committee I would like to mention first Dr. Peter Hitchcock and Dr. Roger Albin, for

supporting my admission into the program. Dr. Albin also introduced me to life in research, helped focused my research interests and continually advised me on career and life issues. Also I want to thank Dr. Andrew Lieberman, Dr. Jeff Martens, Dr. Mario Delmar, Dr. Mark Russell, Dr. Richard Hume, Dr. Richard Neubig, Dr. Kate Barald, Dr. Steve Fisher, Dr. Gary Huffnagle, Dr. Raymond Ruddon, and Dr. Victoria Booth. Thank you to Dr. Kent Berridge too, for agreeing to be my mentor for the Graduate Teaching Certificate program.

Finally, to all my friends near and far, who have shared the good times and supported me during any hardships. I am indebted to you all, for all the laughter, the tears, the confidences and the quiet moments.

Table of Contents

List of Figures

Figure

List of Tables

Table

Chapter I

Electrophysiology and beyond: Multiple roles of Na^+ Channel β subunits in development and disease

(Portions of this chapter have been published in Neurosci Lett 2010, doi:10.1016/j.neulet.2010.06.050)

Voltage-gated Na^+ channel (VGSC) β subunits are not "auxiliary." These multifunctional molecules not only modulate Na^+ current, but also function as cell adhesion molecules (CAMs) – playing roles in cellular aggregation, migration, invasion, neurite outgrowth, and axonal fasciculation [9, 10]. β subunits are integral members of VGSC signaling complexes at nodes of Ranvier, axon initial segments, and cardiac intercalated disks, regulating action potential propagation through critical intermolecular and cell-cell communication events. At least *in vitro*, many β subunit cell adhesive functions occur both in the presence and absence of pore-forming VGSC α subunits [64, 65, 70], and *in vivo* β subunits are expressed in excitable as well as non-excitable cells [3, 7, 18, 24, 30, 33, 54, 85] [11, 80](O'Malley, submitted), thus β subunits may play important functional roles on their own, in the absence of α subunits. VGSC β1 subunits are essential for life, and appear to be especially important during brain development [6, 9, 17]. Mutations in β subunit genes result in a variety of human neurological and cardiovascular diseases (summarized in **Table I.3**). Moreover, some cancer cells exhibit alterations in β subunit expression during metastasis [7, 18, 24]. In short, these subunits, originally thought of as merely accessory to α subunits, are critical players in their own right in human health and disease.

β Subunits are Immunoglobulin (Ig) Superfamily CAMs

There are four mammalian VGSC β subunit genes, *SCN1B* - *SCN4B*, encoding β1 - β4, respectively. All VGSC β subunits are type I transmembrane proteins, containing an N-terminal signal peptide and a single, heavily glycosylated Ig domain in the extracellular region, a single transmembrane domain, and an intracellular domain **(Figure I.1)**.

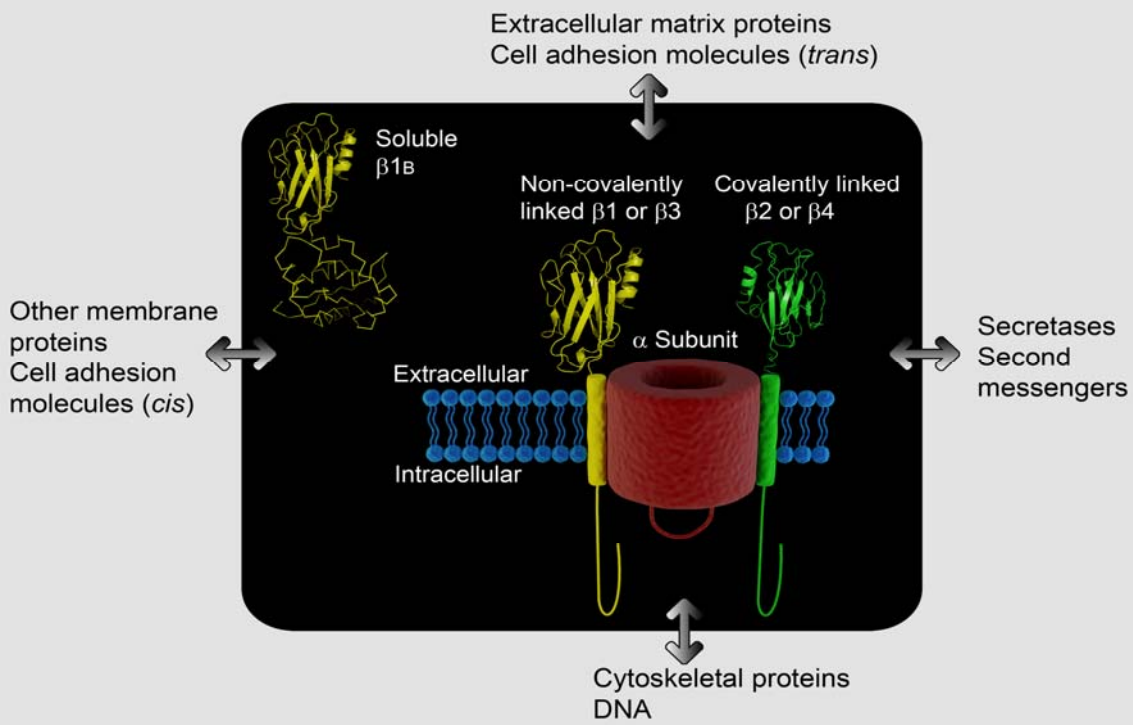

Figure I.1. Subunit structure of VGSCs. VGSCs in the central nervous system are multiprotein complexes composed of a single pore-forming α subunit, one non-covalently-linked β subunit (β1 or β3), and one covalently-linked β subunit (β2 or β4). β1B is a secreted, soluble subunit. In addition, α and β subunits interact with multiple cell adhesion, extracellular matrix, cytoskeletal, and intracellular signal transduction proteins.

VGSC β subunits are enriched in lipid rafts in brain, but are also present in non-raft domains [8, 125]. VGSCs in brain are heterotrimers, containing a single α subunit associated with one non-covalently (β1 or β3) and one covalently (β2 or β4) linked β subunit [38, 39, 76, 80, 128]. *SCN1B* gives rise to two splice variants, β1 and β1B (called

β1A in earlier publications [54]) [95]. β1B is formed through retention of intron 3, with the splice site located following exon 3, encoding the Ig loop domain, and before exon 4, encoding the transmembrane domain [54, 95]. The predicted amino acid sequence of the retained intronic region exhibits very low homology between species [95], however, hydrophobicity analysis of these sequences reveals no transmembrane domains in any species, predicting that β1B is a secreted protein that may function as a ligand for cell adhesion [91]. Multiple *SCN1B* splice variants, including transmembrane and secreted forms, is consistent with other CAMs of the Ig superfamily [49, 99].

Structurally, all of the VGSC β subunits, including the splice variants, belong to the Ig superfamily of CAMs [128] [45]. Interaction of β subunits with other CAMS has been demonstrated for β1, β2, and β3, but not yet for β4, although there is evidence that β4 may function as a CAM in neurite outgrowth [77]. Interestingly, while β1 and β2 display both homophilic and heterophilic cell adhesive interactions, β3 is not a homophilic CAM despite significant homology between β3 and β1 [69], and evidence to date shows only heterophilic interaction of β3 with neurofascin-186 [97]. Within the Ig loop domain of all four β subunits there are multiple N-linked glycosylation sites [44, 45, 80, 128]. The presence of sialic acid in this area is required for Na^+ current modulation by β1 and β2 [47, 48]. The A/A' face of the β1 Ig loop is an important site of interaction with the α subunit [68].

The intracellular domains of β1 and β2 interact with the cytoskeletal proteins $ankyrin_B$ and $ankyrin_G$, and this intracellular region is an additional site of α subunit interaction for β1 and β3 [64, 65, 72, 108]. β1 and β3 contain a YLAI motif in the intracellular domain that predicts internalization through clathrin-coated pits [80]. Phosphorylation of this tyrosine in β1 (Y181) modulates its subcellular localization and ability to associate with ankyrin [66]. Regarding the aminoacid nomenclature of β subunits, it is important to mention that the amino acid sequences for all the β subunits available on NCBI and Uniprot contain a signal peptide with the initiator methionine

designated amino acid #1. This nomenclature is also followed in studies reporting pathogenic human mutations in genes encoding the β subunits. In contrast, in much of the literature discussing structural domains of β subunits amino acid #1 is defined to be the first residue after cleavage of the signal peptide. Lengths of the signal peptide and the first amino acids of the mature protein for each β subunit are summarized in **Table I.1**.

Table I.1. Length of signal peptides and identity of the first aminoacid after it in VGSC β subunits.

β Subunit	Length of signal peptide (aminoacids)	First aminoacid after signal peptide	Reference
β1	19	Glycine (G)	[44]
β1B	19	Glycine (G)	[95]
β2	29	Methionine (M)	[45]
β3	24	Valine (V)	[80]
β4	30	Leucine (L)	[128]

β3 contains a tyrosine in the position corresponding to β1Y181, but its phosphorylation or its ability to associate with ankyrin has not been demonstrated [69]. In the intracellular domain of β4, the sequence KKLITFILKKT may function as an open-channel blocker allowing resurgent Na^+ current [2, 5, 34].

All four VGSC β subunit proteins are substrates for sequential cleavage by the β-site amyloid precursor protein-cleaving enzyme 1 (BACE1) and γ-secretase [125]. β2 can also be cleaved by the α-secretase ADAM10 [56]. Processing of β subunits by BACE1 or α-secretase at cleavage sites in the extracellular juxtamembrane region results in ectodomain shedding, leaving membrane-bound C-terminal fragments (CTFs) [56, 125]. Evidence suggests that the shed ectodomain of β1 may function as a soluble ligand for cell adhesion to promote neurite outgrowth [20, 64]. The CTFs are further processed by γ-secretase at intracellular sites, resulting in free small intracellular domains (ICDs) [56, 125]. Pharmacological inhibition of β2 cleavage by γ-secretase

reduces cell-cell adhesion and migration [56] and β4 processing by BACE1 increases neurite outgrowth [77], predicting that proteolytic processing events are critical to the *in vivo* functioning of these subunits. The β2 ICD localizes to the nucleus and increases *Scn1a* mRNA and $Na_v1.1$ protein levels, suggesting that this fragment may function as a transcriptional regulator of VGSC α subunits [55]. Although all four β subunits are BACE substrates in *in vitro* assays, *in vivo* processing by BACE1 has only been confirmed for β2 and β4 in the mouse CNS [125], suggesting that this role may be specific to subunits that are covalently linked to α.

β Subunits Are Expressed In Excitable And Non-Excitable Tissues

All four β subunits, including β1B, are widely expressed in the soma of neurons of the mammalian brain and spinal cord [6, 17, 54, 80, 95, 128]. β1 is also highly expressed in the axon initial segment of cortical and hippocampal pyramidal neurons and cerebellar Purkinje neurons[124]. β1, β2 and β4 are present at optic and sciatic nerve nodes of Ranvier [16, 17, 29, 50, 92](O'Malley, submitted). β3 is not found at nodes in optic nerve or spinal cord (O'Malley, submitted). Interestingly, while β1 is present at the majority of nodes in optic nerve and spinal cord, β2 and β4 are expressed in subsets of nodes in these areas (O'Malley, submitted). These data suggest that the VGSC subunit composition at nodes can be αβ1β2 or αβ1β4, resulting in differential electrical and cell adhesive effects. In addition to nodes, β1 is present in the axon initial segment of cerebellar Purkinje neurons and cerebellar granule neurons (CGNs), and in CGN growth cones where it is postulated to contribute to neurite outgrowth [6]. β1 and β2 are expressed in mammalian retinal ganglion cells [50], and scn1ba (β1) protein in zebrafish is present in multiple types of retinal cells [29]. β1B, β2, and β3 are present at the soma of subpopulations of large and small DRG neurons [12, 54, 93, 95], and their differential expression may predict subtle variations in neuronal firing properties. β1B and β3 are also present in peripheral nerve fibers [12, 95]. Finally, β subunits are expressed in glia.

Scn1b mRNA is expressed in Schwann cells and astrocytes [3, 33, 85] and *Scn2b* mRNA is detected in cerebral and spinal cord astrocytes [84]. β1 and β4, but not β2 or β3, are detected in Bergmann glia [20]. All four β subunit proteins are expressed in oligodendrocyte precursor cells (O'Malley, submitted). The zebrafish protein scn1bb (β1) is expressed in optic nerve myelin, in spinal cord radial glía, and in Schwann cells [30]. Thus, β subunits are expressed in excitable as well as non-excitable cells in brain, suggesting that they may play cell adhesive roles in the absence of an associated α subunit *in vivo*.

In addition to brain, all four VGSC β subunits are expressed in heart [43, 51, 62]. β1 and β1B are present in atrial and ventricular tissues [28, 54]. β3 is present in ventricular cardiomyocytes, but not in atrial cells [28]. β2 and β4 are expressed in ventricular myocytes, but their presence in atrial tissue has not been studied. All four β subunits are expressed in the sinoatrial (SA) node [63]. β1 is also expressed at low levels in atrioventricular (AV) node and His bundle, and abundantly in Purkinje fibers [26]. In the ventricles, non-phosphorylated β1, β3, and β2 co-localize at the t-tubules, along with the α subunits $Na_v1.1$, $Na_v1.3$ and $Na_v1.6$. Tyrosine phosphorylated β1, β2, and β4 are found at intercalated disks of ventricular cardiomyocytes with $Na_v1.5$ [22, 62, 66]. *Scn3b* mRNA is detected in both the SA and AV nodes [67], while *SCN1B* mRNA encoding β1B is expressed in both ventricles and the Purkinje fibers [122].

β subunits are expressed in skeletal and smooth muscle. In skeletal muscle, RT-PCR experiments detect mRNAs for all mammalian β subunits [11, 128]. Immunohistochemistry experiments show zebrafish scn1ba in skeletal muscle [29]. The mRNAs for *SCN1B*, *SCN2B* and *Scn4b*, but not *SCN3B*, are present in smooth muscle cells [94, 105]. In addition, β1B protein is expressed in endothelial cells [54]. *SCN1B* and *SCN4B* mRNA are expressed in other non-excitable tissues, including lung, kidney, liver, placenta, prostate, and thyroid [11]. *Scn3b* mRNA is also present in kidney and liver [80]. These data again suggest non-conducting roles for β subunits *in vivo*. Importantly,

because levels of VGSC β subunit mRNA and protein rarely correlate [60], expression of these subunits at the protein level must be confirmed in future studies.

There is little information regarding the factors that control β subunit transcription, although it is known that β subunit expression in the CNS is developmentally regulated. mRNAs for β1B and β3 predominate in fetal brain, with levels decreasing (but not disappearing) during late gestation and after birth. In contrast, levels of β1 and β2 mRNA increase progressively and become dominant over β1B and β3 after birth [45, 54, 101, 106]. A similar temporal characterization has not been carried out for β4. β2 is present in murine optic nerve nodes of Ranvier during early postnatal development [16, 50]. At later time points, β1 is also present in these structures [17], although early expression of β1 at nodes has not been investigated. Levels of *Scn1b* mRNA in the heart increase toward the end of gestation and after birth, and this increase is, at least in part, dependent on the prepartum surge in cortisol [27]. Silencing of the voltage-gated K^+ channel subunit KChIP2 in neonatal ventricular cardiomyocytes reduces the levels of *Scn1b* mRNA and protein [21]. In *Scn3b* null mice there is a selective ventricular (but not atrial) increase in *Scn1b* mRNA [35, 36]. Increased *Scn3b* expression is repressed by the RE1-silencing transcription factor (REST) [89] and is induced by p53 [1]. Taken together these studies indicate that the genes encoding VGSC β subunits are subject to multiple mechanisms of control, including possible modulation by other ion channel subunits.

β subunits interact with multiple cytoskeletal, cell adhesion, signal transduction, and extracellular matrix proteins

β subunits modulate Na^+ current as integral members of the VGSC signaling complex and, as such, associate with multiple pore-forming α subunits [22, 66, 76, 108]. In addition, these multifunctional proteins interact both in *cis* and in *trans* with multiple CAMs, with components of the extracellular matrix, and with intracellular cytoskeletal and signaling molecules. A summary of those interactions is presented in **Table I.2**, with

the majority of these studies focusing on β1. Similar studies have not been carried out for β1B, however, because β1 and β1B share the extracellular Ig domain, it is safe to assume that these two CAMs share many, if not all, extracellular binding partners.

β1 subunits associate with multiple CAMs, including contactin, neurofascin-186 and -155, NrCAM, N-cadherin, and β2 [52, 66, 70, 71, 97]. β2 does not associate with contactin, but does associate with β1 and the extracellular matrix proteins, tenascin-C and tenascin-R [109] [70]. Transfected fibroblasts expressing β1 or β2 are repelled by substrates containing tenascin-R, suggesting initial binding and recognition of this extracellular matrix molecule by these β subunits [126]. Some information is known regarding the β1-binding domains of these partners. For example, neurofascin-186 interacts with β1 through its first Ig-like domain and second fibronectin type III-like domain [97]. Contactin binds the β1 Ig loop through its fibronectin-like domain [70]. β2 associates with the fibronectin type III repeats 1-2, A, B, and 6-8 of tenascin-C and fibronectin type III repeats 1-2 and 6-8 of tenascin-R [109]. Functionally, the cysteine-rich amino-terminal domain of tenascin-R, termed EGF-L, is responsible for tenascin-R's repellent effect on β1- or β2-expressing cells. The tenascin-R epidermal growth factor-like repeats and fibronectin-like repeats 6-8 are critical for the initial adhesion of β1- or β2-expressing cells [126].

Trans homophilic β1-β1 or β2-β2 association results in the recruitment of ankyrin to points of cell contact [64]. The key residue in the interaction between the intracellular domain of β1 and ankyrin is β1Y181. Phosphorylation of this tyrosine abolishes the ability of β1 to associate with $ankyrin_B$ or $ankyrin_G$ and is postulated to be a mechanism regulating β1 subcellular localization [65, 71]. Association of the β1 intracellular domain with receptor phosphotyrosine phosphatase β may provide a yin-yang mechanism of phosphorylation and dephosphorylation [96]. Indirect evidence suggests that β1 may

Table I.2. VGSC β subunit protein-protein interactions

	β SUBUNITS			EXTRACELLULAR MATRIX PROTEINS		CYTOSKELETAL PROTEINS		OTHER ION CHANNELS	ENZYMES	CELL ADHESION MOLECULES				
	β1	**β2**	**β3**	**TN-C**	**TN-R**	**Ankyrin$_G$**	**Ankyrin$_B$**	**Kv4.2 / Kv4.3**	**RPTPβ**	**Contactin**	**NF-155**	**NF-186**	**N-Cadherin**	**Nr CAM**
β1	*trans* [64]	*trans* [70]	(-) [70]		(+) [126]	Non-phosphorylated β1 [64, 65, 71]	Non-phosphorylated β1 [66]	(+) [21]	(+) [96]	*cis* [52, 71] *trans* [70]	*trans* [70]	*cis* [97] *trans* [70]	(+) [66]	*cis, trans* [70]
β2	*trans* [70]	*trans* [64]		(+) [109, 126]	(+) [109, 126]	(+) [64]			(-) [96]	(-) [52]		(-) [97]		
β3	(-) [70]		(-) [69]							(-) [69]		*cis* [97] *trans* [70]		
β4	*cis* [2]													

Abbreviations: NF: neurofascin, RPTPβ: receptor tyrosine phosphatase β, TN: tenascin.

associate with the lipid raft kinase fyn in response to extracellular *trans* β1-β1 adhesion [8]. β1 and β2 also participate in *trans* heterophilic extracellular interactions and some of these interactions require the intracellular domain of at least one of the partners. For example, the intracellular domains of NrCAM and β2, respectively, are necessary for the extracellular association of these CAMs with β1, suggesting inside-out signaling mechanisms [70].

VGSC β subunits can associate with other ion channels. In neonatal rat ventricular myocardium β1 and $Na_v1.5$ associate with the voltage-gated K^+ channel subunits $K_V4.2$ and $K_V4.3$, and the accessory subunit KChIP2 [21]. These results suggest that Na^+ and K^+ channels may physically communicate to regulate action potential conduction and that β subunits may act as key junctional components of multi-channel complexes in excitable cells *in vivo*.

What do β subunits do?

1. β subunits modulate Na^+ current:

A large body of literature exists to show that β subunits modulate Na^+ current in transfected cells *in vitro*. While this approach has yielded valuable structure-function information, these data may have little relevance to the *in vivo* situation. Evidence shows that given α-β subunit combinations yield different electrophysiological results in different cell backgrounds. For example, β1 shifts the voltage dependence of $Na_v1.2$-expressed Na^+ current in the negative direction in 1610 Chinese hamster lung cells but in the positive direction in HEK cells [46]. β1-mediated effects on $Na_v1.5$ have been particularly difficult to resolve using heterologous systems. Some groups have reported no effect of β1 on $Na_v1.5$, while other studies have found significant changes in the characteristics of Na^+ current. However, which electrophysiological parameter was modulated, as well as the extent of modulation, varied between studies (see [73] for a more detailed discussion). These differing effects may be due to the presence of varying levels of

endogenous β subunits in different cell lines [78, 79] and/or the differential expression of other endogenous VGSC interacting or modifying proteins. Excitable cells express multiple VGSC α subunit genes in specific complexes of signaling, cytoskeletal, and adhesion molecules in particular subcellular domains, e.g. [6, 14, 22, 50, 83] a situation that cannot be mimicked using a heterologous system. Importantly, while co-expression of β subunits, especially β1, produces significant changes in Na^+ current characteristics in heterologous systems, mouse models tell us otherwise. For example, even though *Scn1b* null mice have a severe neurological phenotype, there are so far only subtle, cell type specific changes reported in Na^+ current [2, 6, 17, 92, 114]. Thus, heterologous systems have revealed little useful information regarding the effects of β subunits, especially β1, on Na^+ current *in vivo*.

β subunit modulation of Na^+ current *in vivo* is cell type specific and subtle, yet may result in significant changes in electrical excitability in brain. *Scn1b* null CGNs exhibit reduced resurgent Na^+ current that likely contributes to the ataxic phenotype of these mice [6]. Minor changes in hippocampal excitability in *Scn1b* null mice may contribute to severe seizures [92]. A portion of *Scn2b* null hippocampal neurons show negative shifts in the voltage dependence of inactivation [16, 114], while in small-fast DRG neurons there is slowing of Na^+ current activation and inactivation with no change in voltage-dependence [60]. In wildtype hippocampal neurons transfected with β4, persistent current is increased. β4-expressing neurons from *Scn1b* and *Scn1b/Scn2b* null mice show slowed entry into inactivated states [2]. Data from this study suggest that β1 and β4 may play antagonistic roles in hippocampus *in vivo*, with the former favoring inactivation, and the latter favoring activation. Because increased VGSC availability may facilitate action potential firing, these results suggest a mechanism for seizure susceptibility of both mice and humans with mutated β1 subunits [2].

In the heart Na^+ current gating abnormalities have been documented for *Scn1b* null mice [59], *Scn3b* null mice [36], and a strain of mice (129P2) that are cardiac-

specific *Scn4b* hypomorphs [98]. *Scn1b* null ventricular myocytes show increased transient and persistent Na^+ current with no changes in other electrophysiological parameters. *Scn3b* null ventricular myocytes show a hyperpolarizing shift in the voltage-dependence of current inactivation. *Scn4b* null mice have not been developed, however, ventricular cardiomyocytes from 129P2 mice exhibit a depolarizing shift of the voltage-dependence of current activation when compared to cells isolated from the FVB/N strain that expresses high levels of β4 [98].

The gating modulating properties of β subunits are also important for the response of α subunits to VGSC blockers, as shown *in vivo* for flecainide with β3 [37], *ex vivo* for carbamazepine with β1 and β2 [114], and *in vitro* for phenytoin with β1 [61], and lidocaine with β1 and β3 [57].

The interaction of β subunits with other CAM, cytoskeletal, or signaling molecules may also influence Na^+ current. For example, β1 association with contactin or NrCAM results in increased current density *in vitro* and *in vivo* [52, 70]. β1 and β2 are ankyrin binding proteins. $Ankyrin_B$ null mice exhibit reduced Na^+ current density and abnormal Na^+ current kinetics [15], suggesting that β subunits may play important roles in the VGSC-ankyrin complex. These interactions may be particularly critical at the nodes of Ranvier. *Scn1b* null mice show reduced numbers of nodes, dysmyelination, and disruption of axo-glial cell-cell contacts [17]. While $Na_v1.6$, contactin, caspr, and K^+ channels are normally localized to nodes in these mice, association between VGSCs and contactin, and possibly ankyrin, neurofascin, and NrCAM, are disrupted. It is proposed that loss of these critical β1 subunit-dependent protein-protein interactions leads to instability of the nodal complex [17, 53]. Finally, β1 and $Na_v1.6$ reciprocally modulate each other in terms of neurite outgrowth, subcellular localization, and regulation of resurgent Na+ current in CGNs [6].

2. β subunits modulate channel cell surface expression:

β subunits, especially β2, increase Na^+ current density in heterologous systems by enhancing the trafficking of α subunits to the plasma membrane. In contrast to discrepancies in Na^+ current modulation *in vitro* vs. *in vivo* for β1, this β2-mediated effect holds up to *in vivo* scrutiny. α subunit association with β2 and concomitant plasma membrane insertion are the final steps in VGSC biosynthesis in primary brain neurons, suggesting that β2 is critical for establishment and maintenance of channel cell surface expression and excitability [103, 104] Experiments in *Scn2b* null neurons supports this conclusion. In *Scn2b* null mice acutely dissociated hippocampal neurons have Na^+ current density that is ~50% of wildtype. *Scn2b* null embryonic neuronal cultures exhibit a ~50% reduction in cell surface ^{3}H-saxitoxin (STX) binding compared to wildtype. No difference was observed comparing ^{3}H-STX binding to lysed neuronal cultures, indicating that the absence of β2 had no effect on overall VGSC expression, but specifically on VGSC cell surface trafficking [16]. Like most of the effects of β subunits described in this chapter, the ability of β2 to increase Na^+ current density is cell-type specific, since neurons from the dentate gyrus of *Scn2b* null mice have similar Na^+ current densities as their wild-type littermates [114]. *Scn2b* null small-fast dorsal root ganglia (DRG) neurons have significantly decreased protein expression of $Na_v1.1$ and $Na_v1.7$ and subsequent reduction in tetrodotoxin (TTX)-sensitive Na^+ current density compared to wildtype, but unchanged TTX-resistant Na^+ currents [60], suggesting that the effects of β2 may be specific to TTX-sensitive channels.

In the CNS β1 may be required for the expression or subcellular localization of specific VGSC α subunits in specific cell types. *Scn1b* null hippocampal neurons in the CA3 region express decreased levels of Nav1.1 and increased levels of Nav1.3 compared to wildtype, as assessed by immunofluorescence [17]. Subpopulations of *Scn1b* null CGNs exhibit reduced expression of $Na_v1.6$ channels, but increased levels of $Na_v1.1$ channels, at axon initial segments compared to wildtype [6].

Cell surface expression of $Na_v1.5$ in the heart may be mediated by its association with β3, as in *Scn3b* null ventricular cardiomyocytes Na^+ current density is reduced [36]. Despite coimmunoprecipitation experiments using rodent heart lysates demonstrating association between β1 and $Na_v1.5$, as well as data showing increased current density upon co-expression of β1 with $Na_v1.5$ in some heterologous systems,*Scn1b* null heart levels of *Scn5a* mRNA and $Na_v1.5$ are increased [59], again suggesting that in vitro experiments may fail to predict the *in vivo* situtation. β1 may affect the expression of other, TTX-sensitive, VGSC α subunits in the heart, as *Scn1b* null heart lysates have increased ^{3}H-saxitoxin binding [59]. It is possible that BACE1 cleavage of β1 normally results in dampened VGSC transcription in the heart. In the absence of β1 VGSC gene expression may lose this regulation, resulting in channel over-expression.

The mechanism by which β subunits promote VGSC α subunit cell surface expression is not well understood, although some information is known. $Na_v1.8$ contains an endoplasmic reticulum retention (ER) signal in its first intracellular loop that is masked by the intracellular domain of β3 when the two subunits are associated, facilitating exit of the α subunit from the ER [129]. In spite of this, β3 does not promote the cell surface expression of $Na_v1.8$ in this system, suggesting that other factors are required. Evidence suggests that β1 may act as a chaperone to facilitate proper folding of mutant $Na_v1.1$ subunits associated with epilepsy, allowing them to pass the quality control mechanisms of the ER [100]. However, β1 does not appear to enhance the expression of wildtype $Na_v1.1$ at the cell surface *in vitro* [92, 100].

3. β subunits modulate cellular migration, neurite extension, and axonal fasciculation:

As is true for other CAMs, VGSC β subunits are critical for cellular migration, neurite outgrowth, and axonal fasciculation. Forced expression of β1 and β2 mediate migration of fibroblasts away from a tenascin-R substrate [126]. β1 also modulates the migration and invasion of cancer cells, as described below. β1 and β4 promote neurite

extension in a cell type-dependent manner [20, 77]. In the mouse neuroblastoma cell line Neuro2a β4 promotes neurite outgrowth and branching [77]. In mouse CGNs β1 promotes neurite outgrowth, β2 inhibits neurite outgrowth, and β4 has no detectable effect [20]. We have shown that β1-mediated neurite outgrowth requires β1-β1 *trans* interactions: β1 expressed at the CGN cell surface must interact with another β1 subunit that is located either on the cell surface of an adjacent neuron or glial cell (likely Bergmann glia in the cerebellum) [20]. In addition, β1-mediated neurite outgrowth in CGNs requires the presence of $Na_v1.6$ at the axon initial segment, TTX-sensitive Na^+ current, the CAM contactin, and fyn kinase [6, 8]. Requirements for contactin are complicated by the finding that *Cntn* null mice are *Scn1b* hypomorphs in the brain, thus the reported results may have reflected a difference in β1 cell surface expression. *Scn1b* null mice exhibit significant defasciculation of the corticospinal tract at the level of the pyramidal decussation, abnormal migration of CGNs from the external germinal layer, and defasciculation of cerebellar parallel fibers [9]. These cerebellar defects may contribute to the ataxic phenoype of these mice [17]. Zebrafish *scn1bb* morphants exhibit defasciculation of the olfactory nerve [30]. Taken together, these data suggest that VGSC β subunits are critical modulators of brain development.

In heart the differential subcellular localization of β subunits in ventricular myocytes may affect mechanical and electrical coupling through cell adhesive and electrophysiological modulation. At the intercalated disk β subunits, especially β1, may interact with other CAMs (e.g. N-cadherin or connexin-43 [66]) and cytoskeletal molecules to stabilize intercellular junctions critical for mechanical and electrical coupling [22, 62, 66]. In addition, association of β subunits with $Na_v1.5$ at this location (and possibly with voltage-gated K^+ channel subunits [21]) likely influences the propagation of action potentials through the ventricular tissue. β subunits located at t-tubules may associate with TTX-sensitive VGSCs and $ankyrin_B$ to modulate excitation-contraction coupling [22, 62, 66].

The roles of β subunits in cell migration, adhesion, and neurite extension depend not only on extracellular CAM interactions, but also on intracellular signal transduction events. β1-mediated neurite outgrowth in CGNs requires fyn kinase [8], suggesting that extracellular β1-β1 cell adhesion results in intracellular activation of fyn and initiation of a tyrosine phosphorylation signal transduction cascade. Blockade of processing of β2 by γ-secretase inhibits cell adhesion and cell migration [56]. These data suggest that intracellular β2-ankyrin interactions may first need to be interrupted by γ-secretase cleavage of the β2 ICD for cytoskeletal remodeling to occur.

What is the role of β subunits in disease?

1. Evidence from mouse models:

Given the multifunctional nature of β subunits in the normal organism, what are the morphological and behavioral consequences of their functional disruption? While *Scn2b* and *Scn3b* null mice show some abnormalities, both of these models, as well as their heterozygous counterparts, have relatively normal life spans and behaviors [16, 36]. *Scn2b* null mice have a ~50% loss of cell surface TTX-sensitive VGSCs in central and peripheral neurons [16, 60]. This results in a reduction in the amplitude of compound action potentials and an increased action potential threshold in optic nerve, increased susceptibility to seizures induced by the muscarinic acetylcholine receptor agonist pilocarpine, increased sensitivity to thermal stimuli, and decreased sensitivity in some models of neuropathic pain. The phenotype of *Scn3b* null mice, as reported, appears to be mild and limited to cardiac abnormalities, as discussed below. The apparent lack of a neurological phenotype in these mice may suggest that *Scn1b* can compensate for *Scn3b* in brain. On the other hand, *Scn1b* null mice have a severe and complex phenotype that includes retarded growth, ataxia, spontaneous seizures, and lethality between the second and third postnatal week [17]. These results suggest that the remaining β subunit genes cannot compensate for the loss of *Scn1b*. *Scn1b* null

mice have been proposed to represent a novel model for Dravet Syndrome (also called Severe Myoclonic Epilepsy of Infancy) [92]. In contrast, *Scn1b*$^{+/-}$ mice have a normal phenotype [17]. Surprisingly, in spite of an extensive literature describing significant electrophysiological effects of β1 co-expression with VGSC α subunits in heterologous systems, only subtle changes in Na^+ current have been described in *Scn1b* null neurons, as described above [17, 92, 114]. Taken together, these results suggest that the cell adhesive functions of β1 may be more important than their effects on current modulation in brain *in vivo*.

β subunits are also important for proper cardiac function. Isolated *Scn1b* null ventricular myocytes exhibit increased transient and persistent Na^+ current and action potential prolongation resulting in prolonged QT and longer RR intervals in intact heart [59]. In contrast, *Scn3b* null ventricular myocytes exhibit shortened action potentials and a decreased effective refractory period. Hearts from these animals show slower heart rates, longer sinus node recovery times, longer P wave and PR interval durations, and a high tendency for induced atrial tachycardia and fibrillation, and ventricular tachycardia [35, 36]. Ventricular cardiomyocytes isolated from 129P2 mice, which are cardiac-specific *Scn4b* hypomorphs, exhibit slowed upstroke velocities and prolonged action potentials compared to myocytes isolated from the FVB/N strain. This results in increased PQ and QRS intervals, although no arrhythmias could be induced with the use of flecainide [98]. No cardiac characterization of *Scn2b* null mice has been performed. Taken together, these mouse models suggest that β1, β2, β3 and β4 are all required for normal excitability *in vivo*.

2. Human inherited arrhythmia and epilepsy:

VGSC β subunits are involved in a number of human diseases, either as a primary cause, as a downstream target, or as a modifying factor. **Table I.3** summarizes the diseases that have been linked to β subunits and the experimental models used to

demonstrate this association. **Figure I.2** shows the amino acid location of β subunit mutations reported in the literature and one being reported in the third chapter of the present work. To date, all diseases associated with β subunit mutations are episodic, or paroxysmal, disorders that show variable penetrance and expressivity (see references in **Table I.3**).

In all but one case the mutations reported are heterozygous in humans [92], which, for loss-of-function mutations, contrasts with findings described above that *Scn1b*$^{+/-}$, *Scn2b*$^{+/-}$, and *Scn3b*$^{+/-}$ mice are phenotypically normal.

Mutations in *SCN1B*, *SCN2B*, *SCN3B*, and *SCN4B* are associated with cardiac arrhythmia, including atrial, ventricular, and conduction system diseases [112, 115, 122]. Mutations associated with sudden infant death syndrome (SIDS) are also included in this section, as *in vitro* studies using heterologous systems have found abnormalities in their electrophysiological modulation of $Na_v1.5$ [112]. To attempt to understand the mechanisms by which these mutations cause arrhythmia, wildtype and mutant cDNAs have been expressed with $Na_v1.5$ in heterologous systems. However, these results are complicated by the problems discussed above.

In vitro, all β1 mutations associated with arrhythmia result in the loss of the ability of β1 to increase Na^+ current density [121, 122]. Their effects on other currents parameters, however, are less consistent. β1p.R85H abolishes β1-mediated modulation of the voltage dependence of current activation and inactivation. β1p.E87G abolishes the effect of β1 on voltage-dependence of activation but not on inactivation. β1p.D153N conserves the effects of the wildtype subunit on voltage-dependence [121, 122]. Co-expression of β1p.E87G with wildtype β1 and $Na_v1.5$ results in currents that are indistinguishable from currents generated by co-expression of mutant β1 and $Na_v1.5$, suggesting that β1p.E87G might have a dominant-negative function [122]. As discussed above, other studies have found no effect at all of wildtype β1 on $Na_v1.5$ in various heterologous systems [73], adding another layer of complexity to understanding

Table I.3. Human diseases associated with β subunits.

β Subunit	Disease	Relationship	Model	Reference
β1	Conduction disease	Causal	Human	[122]
	Atrial fibrillation	Causal	Human	[121]
	Long QT syndrome	Causal	Mouse	[59]
	Febrile seizures	Causal	Human, Mouse	[4, 87, 102, 117, 118, 124]
	Dravet Syndrome	Causal	Human, Mouse	[17, 92]
	Temporal lobe epilepsy	Causal	Human	[102]
	Traumatic nerve injury	Downstream target	Human	[19]
$\beta1_B$	Brugada syndrome	Causal / Modifying factor	Human	[82, 122]
	Conduction Disease	Causal	Human	[122]
β2	Atrial fibrillation	Causal	Human	[121]
	Multiple sclerosis	Modifying factor	Mouse	[81]
	Post-traumatic neuropathic pain	Downstream target	Mouse	[93]
	Inflammatory pain	Modifying factor	Mouse	[60]
	Traumatic nerve injury	Downstream target	Human	[19]
β3	Idiopathic ventricular fibrillation	Causal	Human	[115]
	Sudden infant death syndrome	Causal	Human	[112]
	Brugada syndrome	Causal	Human	[43]
	Atrial fibrillation	Causal	Human	[119]
	Conduction disease	Causal	Mouse	[36]
	Temporal lobe epilepsy without hippocampal sclerosis	Causal vs. Downstream target	Human	[116]
	Traumatic nerve injury	Downstream target	Human	[12]
	Cancer	Modifying factor	Mammalian cell lines	[1]
	Non-syndromic oral clefts	Causal	Human	[90]
β4	Long QT syndrome	Causal	Human	[75]
	Sudden infant death syndrome	Causal	Human	[112]
	Huntington's disease	Downstream target	Human, Mouse	[88]

the role of *SCN1B* mutations in heart *in vivo*. To date there is one reported *SCN1B* arrhythmia mutation that specifically affects the β1B splice variant. β1Bp.W179X abolishes all effects of wildtype β1B on $Na_v1.5$ expressed current [122].

Similar to arrhythmia mutations in *SCN1B*, mutations identified in *SCN2B* and *SCN3B* affect Na^+ current density expressed by $Na_v1.5$, while the effects on other current parameters are variable. The two reported *SCN2B* mutations associated with atrial fibrillation affect the same residue in the β2 signal peptide, arginine-28 [121]. Whereas wildtype β2 neither modifies the current density nor voltage-dependence of activation of $Na_v1.5$, both of these mutations decrease the current density and shift the voltage-dependence of activation towards more depolarized potentials, suggesting gain-of-function. Regarding the voltage-dependence of inactivation, β2p.R28W abolishes the effect of wildtype β2 while β2p.R28Q conserves it [121].

β3 does not affect the density of $Na_v1.5$-expressed current, but all of the reported arrhythmia mutations in *SCN3B* are reported to dramatically reduce the current density, suggesting gain-of-function [43, 112, 115, 119]. In addition, β3p.V54G completely abolishes the effects of wildtype β3 on the voltage-dependence of inactivation [115]. β3p.V36M does not change it, but increases the level of persistent current [112]. β3p.L10P, located in the signal peptide, shifts the voltage-dependence of inactivation towards more hyperpolarized potentials compared to wildtype β3 and prolongs the kinetics of recovery from inactivation [43]. Unlike the aforementioned reports, in the paper describing β3p.A130V even the wild-type β3 had no effect on the voltage-dependence of inactivation of $Na_v1.5$ [119], despite the fact that all of these papers have used HEK derived cell lines as their heterologous system. β3p.V54G and β3p.L10P are trafficking deficient mutants, resulting in the intracellular retention of $Na_v1.5$ with a subsequent reduction in current density [43, 115]. β3p.A130V is not a trafficking-deficient mutant, thus the reduction of sodium current is due to a predominantly electrophysiological effect on Nav1.5 [119].

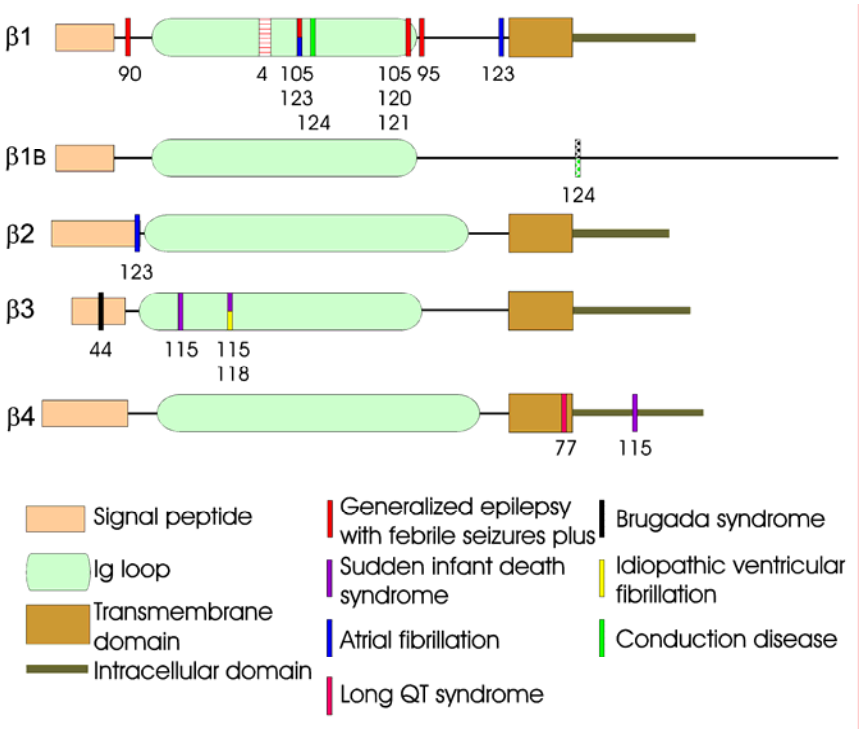

Figure I.2. Localization of human epilepsy and cardiac arrhythmia mutations in VGSC β subunits. Colored bars indicate the position of amino acids affected by reported genetic mutations. Solid bars represent missense mutations, dotted bars represent nonsense mutations, and striped bars indicate deletions. The conventions in the lower panel depict the symbols used for the structural domains of the β subunits (left) and the color code for the diseases associated with the mutations (right).

At the moment it is unknown if β3p.V36M is trafficking-deficient. β3p.A130V acts is able to act as a dominant-negative mutant [119], while β3p.V54G does not [115]; No such characterization has been performed for β3p.L10P and β3p.V36M.

While all reported arrhythmia mutations affecting β1, β2, and β3 are located in the extracellular domains of these subunits, those identified in β4 are located in the transmembrane or intracellular domains [75, 112], perhaps suggesting *in vivo* functioning of β4 in heart that does not involve cell adhesion. Neither the mutations, nor wildtype β4 affect the density of Nav1.5-expressed current. However, both mutants, β4p.S206L and β4p.L179F, abolish the effect of wildtype β4 on the voltage-dependence of inactivation, resulting in increased window current and enhanced levels of persistent current [75, 112]. β4p.L179F also alters the kinetics of recovery from inactivation [75].

Expression of β4p.S206L in isolated adult rat ventricular myocytes using adenoviral vectors resulted in increased persistent Na^+ current and prolongation of the action potential [112].

In summary, results from heterologous systems suggest that mutations affecting β1, β2 and β3 may alter the cardiac action potential through their effects on Na^+ current density. In contrast, mutations in β4 appear to result in changes in the level of persistent Na^+ current. Confirmation that such changes actually occur in cardiac myocytes has been performed for only some of these mutations [112]. In addition a microsatellite polymorphism in the untranslated region of *SCN1B* intron three (within the part of the intron that is retained in β1B) may be a risk factor, but is not by itself a cause, for Brugada syndrome [82].

Of the four VGSC β subunits genes, to date only mutations in *SCN1B* have been reported to cause epilepsy (**Figure I.2**). At least two different studies have purposefully screened *SCN2B* for mutations in epileptic patients with no positive results [40, 117]. No such studies have been reported for *SCN3B*. Interestingly, all epileptic syndromes associated with *SCN1B* mutations thus far include febrile seizures as part of the symptomatology, assigning them to the disease spectrum of genetic epilepsy with febrile seizures plus (GEFS+) [4, 87, 92, 102, 117, 118]. Most studies characterizing these mutants have been performed in heterologous systems, and thus results must be interpreted with caution. The study by Patino et al [92] provides a summary of the results of these studies. It is important to note that the majority of these *SCN1B* mutations are loss-of-function [2, 74, 92, 111, 127]. Three of these mutants (β1p.R125C, β1p.R85H, β1p.R85C) have been shown to be trafficking deficient [92, 127]. Whereas the β1p.C121W mutant is able to traffic to the cell surface in heterologous systems (Patino and Isom, unpublished data), a knock-in mouse model of this mutation showed an absence of β1 at the axon initial segment of pyramidal cells. Mice homozygous for the mutation exhibited spontaneous seizures, tremor,growth retardation and died by the

fourth week of life [124]. In all cases but one [92], the GEFS+ patients described carry a single mutant *SCN1B* allele, making the data difficult to resolve with the normal phenotype of *Scn1b*$^{+/-}$ mice [4, 102, 117, 118], although the mice heterozygous for the β1p.C121W had a lower threshold for temperature-induced seizures and more severe convulsive episodes [124]. It is likely that genetic background as well as epigenetic factors play important roles in the phenotypes of these mutant alleles in human families.

At this point it is important to remember that β subunits also modulate the response of α subunits to medications used to treat both epilepsy (phenytoin and carbamazepine) and cardiac arrhythmias (flecainide and lidocaine), as was mentioned before.

3. Is there a role for β subunits in neuroprotection or neurodegeneration?

Rodent models of nerve injury have suggested a protective role for β2 in neuropathology. β2 expression is increased in peripheral axons and cell bodies in both the spared nerve injury and spinal nerve ligation models of neuropathic pain. Consistent with this, the behavioral response to these models is significantly attenuated in *Scn2b* null mice [93]. In addition, *Scn2b* null mice have a reduced response to the formalin model of inflammatory pain [60]. In the Experimental Allergic Encephalomyelitis (EAE) mouse model of Multiple Sclerosis *Scn2b* null mice exhibit significantly attenuated symptoms, mortality, and axonal loss when compared to wildtype littermates [81]. The proposed mechanism for this neuroprotective phenotype is blockade of $Na_v1.6$ up-regulation along demyelinated axons in the absence of β2, resulting in attenuation of the known rise in persistent Na^+ current, and subsequent prevention of reverse activation of Na^+/Ca^{2+} exchange and activation of damaging Ca^{2+} signaling cascades in the axon that lead to degeneration [123]. In support of this, brains of wildtype mice with EAE show higher levels of $Na_v1.6$ than *Scn2b* null mice under the same conditions [81].

Mouse strains that express huntingtin protein with expanded polyglutamine repeats are models of Huntington's disease (HD). In two of these models, HD190QG and R6/2, brain levels of *Scn4b* mRNA are reduced. This change is reflected in the protein levels of β4 in the basal ganglia of R6/2 mice, as well as in human HD patients. In R6/2 mice the reduction in β4 precedes the appearance of motor symptoms. It has been proposed that, in light of its neurite outgrowth promoting ability, a reduction in β4 may cause neurite degeneration as well as alter Na^+ current [88].

4. β subunits and cancer:

The role of β subunits as CAMs appears to be critical for their involvement in certain types of cancer, and may be independent of their electrophysiological function. Most interestingly, β subunits may be involved in cellular metastasis and invasion in breast cancer. β1 is highly expressed in the weakly metastatic breast cancer cell line, MCF-7. In contrast, its expression levels are very low in the strongly metastatic line, MDA-MB-231. Knock-down of β1 using siRNA in MCF-7 cells resulted in reduced cellular adhesion ability and enhanced cellular migration, suggesting that β1 expression may limit the metastatic potential in this cancer type [18]. A previous study showed that the expression of a neonatal splice variant of $Na_v1.5$ is positively correlated with the *in vitro* metastatic behavior of MDA-MB-231 cells [7]. MCF-7 cells exhibit low levels of this $Na_v1.5$ splice variant. β1 knock-down increases $Na_v1.5$ expression and stimulates cellular migration, implicating β1 in a regulatory role. Cellular migration resulting from this increase in VGSC expression is blocked by TTX [18]. As in neurons, the effects of β1 in cancer cells may be cell type specific, as strongly metastatic prostate cancer cell lines express higher levels of *SCN1B* mRNA than weakly metastatic lines [24]. Also, as is a theme throughout this review, cell line data must be interpreted with caution and hypotheses tested using *in vivo* models and patient samples.

Some disease associations suggest novel functions of β subunits. One study found using *in vitro* methods that β3 can induce apoptosis and enhance the response to anticancer drugs [1]. In one study a robust association was found between *SCN3B* SNP markers and non-syndromic oral clefts, one of the most common birth defects, but the mechanism of this association was not clear [90].

Conclusions and future directions

An exciting direction in ion channel research focuses on the finding that voltage-gated ion channels are multi-functional. In addition to regulating electrical excitability through ion conduction, some voltage-gated ion channels contribute to processes as diverse as intracellular signaling, transcriptional regulation, scaffolding, and cell adhesion without requiring changes in ion flux [8, 9, 58]. Data presented here demonstrate clear roles for VGSC β subunits in the regulation of VGSC cell surface expression, localization, Na^+ current modulation, action potential conduction, and cell adhesion. While many drugs targeting VGSC α subunits are in common use [13, 23, 41, 42, 86, 107], the potential of VGSC β subunits as therapeutic targets has not been considered. Moreover, therapeutic targeting of the non-conducting functions of VGSCs may be critical. Previous work has centered on the functional roles of VGSC β subunits in current modulation. Interestingly, while β subunits clearly modulate Na^+ current in heterologous systems *in vivo* models indicate that this may not be their most important role. It is critical that we now challenge our previously held concepts and take a fresh look at the biology of these multi-functional subunits.

Patients with *SCN1B* mutations have GEFS+ spectrum epilepsy disorders, including the milder GEFS+, more severe temporal lobe epilepsy, and Dravet Syndrome, a catastrophic pediatric epileptic encephalopathy that includes mental retardation [92]. Importantly, there is a significant comorbidity of neuropsychiatric disease and seizures [25, 32] and anti-epileptic therapies targeting VGSCs are effective in mood disorders

[113]. Taken together, this suggests a shared pathophysiology between these diseases [32]. Bipolar disorder is linked genetically to *ANK3*, encoding ankyrin$_G$, a protein that is critical for VGSC targeting and localization in neurons [31]. VGSC β1 and β2 are ankyrin$_G$ binding proteins [65]. *SCN8A*, encoding Na$_v$1.6 that associates with β1 and β2 and is also an ankyrin$_G$ binding protein, is another susceptibility gene for bipolar disorder [120]. *Scn1b* null mice have neuronal migration, pathfinding, and fasciculation defects in the cerebellum [6, 9]. Recent data suggest that cerebellar output targets multiple non-motor areas in the prefrontal cortex and posterior parietal cortex associated with behaviors such as attention, memory, learning, and emotion [110]. Thus, a possible novel direction for β subunit research is the idea that mutations in *SCN1B* may be linked to mood disorders as well as epilepsy. Because *SCN1B* plays important roles in neuronal pathfinding and VGSC expression, disruptions in its expression during development and early childhood may lead to a spectrum of childhood and adolescent neurological and neuropsychiatric diseases. *In vivo* data suggest that the primary role of *SCN1B* in brain is cell adhesion, further, that disruptions in *SCN1B*-mediated cell adhesive interactions result in pathology. This may be the case for other β subunits as well. β subunit function may be modulated in the future by interfering with or enhancing cell adhesive interactions, such that patients with β subunit gene mutations might be effectively treated with small molecules that mimic or alter these interactions. In conclusion, important advances in the therapy of diseases that are associated with VGSC β subunit loss- or modulation-of-function may be achieved by targeting β subunits directly.

In the following chapters I will present my work describing the experiments that led to a number of significant findings described in this introduction. Specifically, my thesis work focuses on characterizing the structure and physiology of the β1B splice variant. In addition, I describe two novel human *SCN1B* mutations associated with epilepsy that cause protein trafficking defects.

Bibliography

[1] K. Adachi, M. Toyota, Y. Sasaki, T. Yamashita, S. Ishida, M. Ohe-Toyota, R. Maruyama, Y. Hinoda, T. Saito, K. Imai, R. Kudo, T. Tokino, Identification of SCN3B as a novel p53-inducible proapoptotic gene, Oncogene 23 (2004) 7791-7798.

[2] T.K. Aman, T.M. Grieco-Calub, C. Chen, R. Rusconi, E.A. Slat, L.L. Isom, I.M. Raman, Regulation of persistent Na current by interactions between beta subunits of voltage-gated Na channels, J Neurosci 29 (2009) 2027-2042.

[3] E. Aronica, D. Troost, A.J. Rozemuller, B. Yankaya, G.H. Jansen, L.L. Isom, J.A. Gorter, Expression and regulation of voltage-gated sodium channel beta1 subunit protein in human gliosis-associated pathologies, Acta Neuropathol 105 (2003) 515-523.

[4] D. Audenaert, L. Claes, B. Ceulemans, A. Lofgren, C. Van Broeckhoven, P. De Jonghe, A deletion in SCN1B is associated with febrile seizures and early-onset absence epilepsy, Neurology 61 (2003) 854-856.

[5] J.S. Bant, I.M. Raman, Control of transient, resurgent, and persistent current by open-channel block by Na channel beta4 in cultured cerebellar granule neurons, Proceedings of the National Academy of Sciences of the United States of America 107 (2010) 12357-12362.

[6] W.J. Brackenbury, J.D. Calhoun, C. Chen, H. Miyazaki, N. Nukina, F. Oyama, B. Ranscht, L.L. Isom, Functional reciprocity between Na+ channel Nav1.6 and beta1 subunits in the coordinated regulation of excitability and neurite outgrowth, Proceedings of the National Academy of Sciences of the United States of America 107 (2010) 2283-2288.

[7] W.J. Brackenbury, A.M. Chioni, J.K. Diss, M.B. Djamgoz, The neonatal splice variant of Nav1.5 potentiates in vitro invasive behaviour of MDA-MB-231 human breast cancer cells, Breast Cancer Res Treat 101 (2007) 149-160.

[8] W.J. Brackenbury, T.H. Davis, C. Chen, E.A. Slat, M.J. Detrow, T.L. Dickendesher, B. Ranscht, L.L. Isom, Voltage-gated Na+ channel beta1 subunit-mediated neurite outgrowth requires Fyn kinase and contributes to postnatal CNS development in vivo, J Neurosci 28 (2008) 3246-3256.

[9] W.J. Brackenbury, M.B. Djamgoz, L.L. Isom, An emerging role for voltage-gated Na+ channels in cellular migration: regulation of central nervous system development and potentiation of invasive cancers, Neuroscientist 14 (2008) 571-583.

[10] W.J. Brackenbury, L.L. Isom, Voltage-gated Na+ channels: potential for beta subunits as therapeutic targets, Expert Opin Ther Targets 12 (2008) 1191-1203.

[11] L. Candenas, M. Seda, P. Noheda, H. Buschmann, C.G. Cintado, J.D. Martin, F.M. Pinto, Molecular diversity of voltage-gated sodium channel alpha and beta subunit mRNAs in human tissues, Eur J Pharmacol 541 (2006) 9-16.

[12] M.A. Casula, P. Facer, A.J. Powell, I.J. Kinghorn, C. Plumpton, S.N. Tate, C. Bountra, R. Birch, P. Anand, Expression of the sodium channel beta3 subunit in injured human sensory neurons, Neuroreport 15 (2004) 1629-1632.

[13] W.A. Catterall, S. Dib-Hajj, M.H. Meisler, D. Pietrobon, Inherited neuronal ion channelopathies: new windows on complex neurological diseases, J Neurosci 28 (2008) 11768-11777.
[14] W.A. Catterall, A.L. Goldin, S.G. Waxman, International Union of Pharmacology. XLVII. Nomenclature and structure-function relationships of voltage-gated sodium channels, Pharmacological reviews 57 (2005) 397-409.
[15] V.S. Chauhan, S. Tuvia, M. Buhusi, V. Bennett, A.O. Grant, Abnormal cardiac Na(+) channel properties and QT heart rate adaptation in neonatal ankyrin(B) knockout mice, Circulation research 86 (2000) 441-447.
[16] C. Chen, V. Bharucha, Y. Chen, R.E. Westenbroek, A. Brown, J.D. Malhotra, D. Jones, C. Avery, P.J. Gillespie, 3rd, K.A. Kazen-Gillespie, K. Kazarinova-Noyes, P. Shrager, T.L. Saunders, R.L. Macdonald, B.R. Ransom, T. Scheuer, W.A. Catterall, L.L. Isom, Reduced sodium channel density, altered voltage dependence of inactivation, and increased susceptibility to seizures in mice lacking sodium channel beta 2-subunits, Proceedings of the National Academy of Sciences of the United States of America 99 (2002) 17072-17077.
[17] C. Chen, R.E. Westenbroek, X. Xu, C.A. Edwards, D.R. Sorenson, Y. Chen, D.P. McEwen, H.A. O'Malley, V. Bharucha, L.S. Meadows, G.A. Knudsen, A. Vilaythong, J.L. Noebels, T.L. Saunders, T. Scheuer, P. Shrager, W.A. Catterall, L.L. Isom, Mice lacking sodium channel beta1 subunits display defects in neuronal excitability, sodium channel expression, and nodal architecture, J Neurosci 24 (2004) 4030-4042.
[18] A.M. Chioni, W.J. Brackenbury, J.D. Calhoun, L.L. Isom, M.B. Djamgoz, A novel adhesion molecule in human breast cancer cells: voltage-gated Na+ channel beta1 subunit, Int J Biochem Cell Biol 41 (2009) 1216-1227.
[19] K. Coward, A. Jowett, C. Plumpton, A. Powell, R. Birch, S. Tate, C. Bountra, P. Anand, Sodium channel beta1 and beta2 subunits parallel SNS/PN3 alpha-subunit changes in injured human sensory neurons, Neuroreport 12 (2001) 483-488.
[20] T.H. Davis, C. Chen, L.L. Isom, Sodium channel beta1 subunits promote neurite outgrowth in cerebellar granule neurons, The Journal of biological chemistry 279 (2004) 51424-51432.
[21] I. Deschenes, A.A. Armoundas, S.P. Jones, G.F. Tomaselli, Post-transcriptional gene silencing of KChIP2 and Navbeta1 in neonatal rat cardiac myocytes reveals a functional association between Na and Ito currents, J Mol Cell Cardiol 45 (2008) 336-346.
[22] J. Dhar Malhotra, C. Chen, I. Rivolta, H. Abriel, R. Malhotra, L.N. Mattei, F.C. Brosius, R.S. Kass, L.L. Isom, Characterization of sodium channel alpha- and beta-subunits in rat and mouse cardiac myocytes, Circulation 103 (2001) 1303-1310.
[23] S.D. Dib-Hajj, J.A. Black, S.G. Waxman, Voltage-gated sodium channels: therapeutic targets for pain, Pain Med 10 (2009) 1260-1269.
[24] J.K. Diss, S.P. Fraser, M.M. Walker, A. Patel, D.S. Latchman, M.B. Djamgoz, Beta-subunits of voltage-gated sodium channels in human prostate cancer: quantitative in vitro and in vivo analyses of mRNA expression, Prostate Cancer Prostatic Dis 11 (2008) 325-333.
[25] T.J. Dixon-Salazar, L.C. Keeler, D.A. Trauner, J.G. Gleeson, Autism in several members of a family with generalized epilepsy with febrile seizures plus, Journal of child neurology 19 (2004) 597-603.
[26] J.N. Dominguez, F. Navarro, D. Franco, R.P. Thompson, A.E. Aranega, Temporal and spatial expression pattern of beta1 sodium channel subunit during heart development, Cardiovascular research 65 (2005) 842-850.

[27] A.I. Fahmi, A.J. Forhead, A.L. Fowden, J.I. Vandenberg, Cortisol influences the ontogeny of both alpha- and beta-subunits of the cardiac sodium channel in fetal sheep, J Endocrinol 180 (2004) 449-455.
[28] A.I. Fahmi, M. Patel, E.B. Stevens, A.L. Fowden, J.E. John, 3rd, K. Lee, R. Pinnock, K. Morgan, A.P. Jackson, J.I. Vandenberg, The sodium channel beta-subunit SCN3b modulates the kinetics of SCN5a and is expressed heterogeneously in sheep heart, The Journal of physiology 537 (2001) 693-700.
[29] A.J. Fein, L.S. Meadows, C. Chen, E.A. Slat, L.L. Isom, Cloning and expression of a zebrafish SCN1B ortholog and identification of a species-specific splice variant, BMC genomics 8 (2007) 226.
[30] A.J. Fein, M.A. Wright, E.A. Slat, A.B. Ribera, L.L. Isom, scn1bb, a zebrafish ortholog of SCN1B expressed in excitable and nonexcitable cells, affects motor neuron axon morphology and touch sensitivity, J Neurosci 28 (2008) 12510-12522.
[31] M.A. Ferreira, M.C. O'Donovan, Y.A. Meng, I.R. Jones, D.M. Ruderfer, L. Jones, J. Fan, G. Kirov, R.H. Perlis, E.K. Green, J.W. Smoller, D. Grozeva, J. Stone, I. Nikolov, K. Chambert, M.L. Hamshere, V.L. Nimgaonkar, V. Moskvina, M.E. Thase, S. Caesar, G.S. Sachs, J. Franklin, K. Gordon-Smith, K.G. Ardlie, S.B. Gabriel, C. Fraser, B. Blumenstiel, M. Defelice, G. Breen, M. Gill, D.W. Morris, A. Elkin, W.J. Muir, K.A. McGhee, R. Williamson, D.J. MacIntyre, A.W. MacLean, C.D. St, M. Robinson, M. Van Beck, A.C. Pereira, R. Kandaswamy, A. McQuillin, D.A. Collier, N.J. Bass, A.H. Young, J. Lawrence, I.N. Ferrier, A. Anjorin, A. Farmer, D. Curtis, E.M. Scolnick, P. McGuffin, M.J. Daly, A.P. Corvin, P.A. Holmans, D.H. Blackwood, H.M. Gurling, M.J. Owen, S.M. Purcell, P. Sklar, N. Craddock, Collaborative genome-wide association analysis supports a role for ANK3 and CACNA1C in bipolar disorder, Nat Genet 40 (2008) 1056-1058.
[32] J.J. Gargus, Ion channel functional candidate genes in multigenic neuropsychiatric disease, Biol Psychiatry 60 (2006) 177-185.
[33] J.A. Gorter, E.A. van Vliet, F.H. Lopes da Silva, L.L. Isom, E. Aronica, Sodium channel beta1-subunit expression is increased in reactive astrocytes in a rat model for mesial temporal lobe epilepsy, Eur J Neurosci 16 (2002) 360-364.
[34] T.M. Grieco, J.D. Malhotra, C. Chen, L.L. Isom, I.M. Raman, Open-channel block by the cytoplasmic tail of sodium channel beta4 as a mechanism for resurgent sodium current, Neuron 45 (2005) 233-244.
[35] P. Hakim, N. Brice, R. Thresher, J. Lawrence, Y. Zhang, A.P. Jackson, A.A. Grace, C.L. Huang, Scn3b knockout mice exhibit abnormal sino-atrial and cardiac conduction properties, Acta Physiol (Oxf) 198 (2010) 47-59.
[36] P. Hakim, I.S. Gurung, T.H. Pedersen, R. Thresher, N. Brice, J. Lawrence, A.A. Grace, C.L. Huang, Scn3b knockout mice exhibit abnormal ventricular electrophysiological properties, Prog Biophys Mol Biol 98 (2008) 251-266.
[37] P. Hakim, R. Thresher, A.A. Grace, C.L. Huang, Effects of flecainide and quinidine on action potential and ventricular arrhythmogenic properties in Scn3b knockout mice, Clin Exp Pharmacol Physiol (2010).
[38] R.P. Hartshorne, W.A. Catterall, The sodium channel from rat brain. Purification and subunit composition, The Journal of biological chemistry 259 (1984) 1667-1675.
[39] R.P. Hartshorne, D.J. Messner, J.C. Coppersmith, W.A. Catterall, The saxitoxin receptor of the sodium channel from rat brain. Evidence for two nonidentical beta subunits, The Journal of biological chemistry 257 (1982) 13888-13891.
[40] K. Haug, T. Sander, K. Hallmann, B. Rau, J.S. Dullinger, C.E. Elger, P. Propping, A. Heils, The voltage-gated sodium channel beta2-subunit gene and idiopathic generalized epilepsy, Neuroreport 11 (2000) 2687-2689.
[41] H.C. Hemmings, Jr., Neuroprotection by Na+ channel blockade, J Neurosurg Anesthesiol 16 (2004) 100-101.

[42] H.C. Hemmings, Jr., Sodium channels and the synaptic mechanisms of inhaled anaesthetics, Br J Anaesth 103 (2009) 61-69.
[43] D. Hu, H. Barajas-Martinez, E. Burashnikov, M. Springer, Y. Wu, A. Varro, R. Pfeiffer, T.T. Koopmann, J.M. Cordeiro, A. Guerchicoff, G.D. Pollevick, C. Antzelevitch, A mutation in the beta 3 subunit of the cardiac sodium channel associated with Brugada ECG phenotype, Circ Cardiovasc Genet 2 (2009) 270-278.
[44] L.L. Isom, K.S. De Jongh, D.E. Patton, B.F. Reber, J. Offord, H. Charbonneau, K. Walsh, A.L. Goldin, W.A. Catterall, Primary structure and functional expression of the beta 1 subunit of the rat brain sodium channel, Science 256 (1992) 839-842.
[45] L.L. Isom, D.S. Ragsdale, K.S. De Jongh, R.E. Westenbroek, B.F. Reber, T. Scheuer, W.A. Catterall, Structure and function of the beta 2 subunit of brain sodium channels, a transmembrane glycoprotein with a CAM motif, Cell 83 (1995) 433-442.
[46] L.L. Isom, T. Scheuer, A.B. Brownstein, D.S. Ragsdale, B.J. Murphy, W.A. Catterall, Functional co-expression of the beta 1 and type IIA alpha subunits of sodium channels in a mammalian cell line, The Journal of biological chemistry 270 (1995) 3306-3312.
[47] D. Johnson, E.S. Bennett, Isoform-specific effects of the beta2 subunit on voltage-gated sodium channel gating, The Journal of biological chemistry 281 (2006) 25875-25881.
[48] D. Johnson, M.L. Montpetit, P.J. Stocker, E.S. Bennett, The sialic acid component of the beta1 subunit modulates voltage-gated sodium channel function, The Journal of biological chemistry 279 (2004) 44303-44310.
[49] D.C. Jones, A. Roghanian, D.P. Brown, C. Chang, R.L. Allen, J. Trowsdale, N.T. Young, Alternative mRNA splicing creates transcripts encoding soluble proteins from most LILR genes, Eur J Immunol 39 (2009) 3195-3206.
[50] M.R. Kaplan, M.H. Cho, E.M. Ullian, L.L. Isom, S.R. Levinson, B.A. Barres, Differential control of clustering of the sodium channels Na(v)1.2 and Na(v)1.6 at developing CNS nodes of Ranvier, Neuron 30 (2001) 105-119.
[51] S.G. Kaufmann, R.E. Westenbroek, C. Zechner, A.H. Maass, S. Bischoff, J. Muck, E. Wischmeyer, T. Scheuer, S.K. Maier, Functional protein expression of multiple sodium channel alpha- and beta-subunit isoforms in neonatal cardiomyocytes, J Mol Cell Cardiol 48 (2010) 261-269.
[52] K. Kazarinova-Noyes, J.D. Malhotra, D.P. McEwen, L.N. Mattei, E.O. Berglund, B. Ranscht, S.R. Levinson, M. Schachner, P. Shrager, L.L. Isom, Z.C. Xiao, Contactin associates with Na+ channels and increases their functional expression, J Neurosci 21 (2001) 7517-7525.
[53] K. Kazarinova-Noyes, P. Shrager, Molecular constituents of the node of Ranvier, Mol Neurobiol 26 (2002) 167-182.
[54] K.A. Kazen-Gillespie, D.S. Ragsdale, M.R. D'Andrea, L.N. Mattei, K.E. Rogers, L.L. Isom, Cloning, localization, and functional expression of sodium channel beta1A subunits, The Journal of biological chemistry 275 (2000) 1079-1088.
[55] D.Y. Kim, B.W. Carey, H. Wang, L.A. Ingano, A.M. Binshtok, M.H. Wertz, W.H. Pettingell, P. He, V.M. Lee, C.J. Woolf, D.M. Kovacs, BACE1 regulates voltage-gated sodium channels and neuronal activity, Nat Cell Biol 9 (2007) 755-764.
[56] D.Y. Kim, L.A. Ingano, B.W. Carey, W.H. Pettingell, D.M. Kovacs, Presenilin/gamma-secretase-mediated cleavage of the voltage-gated sodium channel beta2-subunit regulates cell adhesion and migration, The Journal of biological chemistry 280 (2005) 23251-23261.
[57] P.W. Lenkowski, B.S. Shah, A.E. Dinn, K. Lee, M.K. Patel, Lidocaine block of neonatal Nav1.3 is differentially modulated by co-expression of beta1 and beta3 subunits, Eur J Pharmacol 467 (2003) 23-30.

[58] I.B. Levitan, Signaling protein complexes associated with neuronal ion channels, Nature neuroscience 9 (2006) 305-310.
[59] L.F. Lopez-Santiago, L.S. Meadows, S.J. Ernst, C. Chen, J.D. Malhotra, D.P. McEwen, A. Speelman, J.L. Noebels, S.K. Maier, A.N. Lopatin, L.L. Isom, Sodium channel Scn1b null mice exhibit prolonged QT and RR intervals, J Mol Cell Cardiol 43 (2007) 636-647.
[60] L.F. Lopez-Santiago, M. Pertin, X. Morisod, C. Chen, S. Hong, J. Wiley, I. Decosterd, L.L. Isom, Sodium channel beta2 subunits regulate tetrodotoxin-sensitive sodium channels in small dorsal root ganglion neurons and modulate the response to pain, J Neurosci 26 (2006) 7984-7994.
[61] P.T. Lucas, L.S. Meadows, J. Nicholls, D.S. Ragsdale, An epilepsy mutation in the beta1 subunit of the voltage-gated sodium channel results in reduced channel sensitivity to phenytoin, Epilepsy research 64 (2005) 77-84.
[62] S.K. Maier, R.E. Westenbroek, K.A. McCormick, R. Curtis, T. Scheuer, W.A. Catterall, Distinct subcellular localization of different sodium channel alpha and beta subunits in single ventricular myocytes from mouse heart, Circulation 109 (2004) 1421-1427.
[63] S.K. Maier, R.E. Westenbroek, T.T. Yamanushi, H. Dobrzynski, M.R. Boyett, W.A. Catterall, T. Scheuer, An unexpected requirement for brain-type sodium channels for control of heart rate in the mouse sinoatrial node, Proceedings of the National Academy of Sciences of the United States of America 100 (2003) 3507-3512.
[64] J.D. Malhotra, K. Kazen-Gillespie, M. Hortsch, L.L. Isom, Sodium channel beta subunits mediate homophilic cell adhesion and recruit ankyrin to points of cell-cell contact, The Journal of biological chemistry 275 (2000) 11383-11388.
[65] J.D. Malhotra, M.C. Koopmann, K.A. Kazen-Gillespie, N. Fettman, M. Hortsch, L.L. Isom, Structural requirements for interaction of sodium channel beta 1 subunits with ankyrin, The Journal of biological chemistry 277 (2002) 26681-26688.
[66] J.D. Malhotra, V. Thyagarajan, C. Chen, L.L. Isom, Tyrosine-phosphorylated and nonphosphorylated sodium channel beta1 subunits are differentially localized in cardiac myocytes, The Journal of biological chemistry 279 (2004) 40748-40754.
[67] C. Marionneau, B. Couette, J. Liu, H. Li, M.E. Mangoni, J. Nargeot, M. Lei, D. Escande, S. Demolombe, Specific pattern of ionic channel gene expression associated with pacemaker activity in the mouse heart, The Journal of physiology 562 (2005) 223-234.
[68] K.A. McCormick, L.L. Isom, D. Ragsdale, D. Smith, T. Scheuer, W.A. Catterall, Molecular determinants of Na+ channel function in the extracellular domain of the beta1 subunit, The Journal of biological chemistry 273 (1998) 3954-3962.
[69] D.P. McEwen, C. Chen, L.S. Meadows, L. Lopez-Santiago, L.L. Isom, The voltage-gated Na+ channel beta3 subunit does not mediate trans homophilic cell adhesion or associate with the cell adhesion molecule contactin, Neuroscience letters 462 (2009) 272-275.
[70] D.P. McEwen, L.L. Isom, Heterophilic interactions of sodium channel beta1 subunits with axonal and glial cell adhesion molecules, The Journal of biological chemistry 279 (2004) 52744-52752.
[71] D.P. McEwen, L.S. Meadows, C. Chen, V. Thyagarajan, L.L. Isom, Sodium channel beta1 subunit-mediated modulation of Nav1.2 currents and cell surface density is dependent on interactions with contactin and ankyrin, The Journal of biological chemistry 279 (2004) 16044-16049.
[72] L. Meadows, J.D. Malhotra, A. Stetzer, L.L. Isom, D.S. Ragsdale, The intracellular segment of the sodium channel beta 1 subunit is required for its efficient association with the channel alpha subunit, Journal of neurochemistry 76 (2001) 1871-1878.

[73] L.S. Meadows, L.L. Isom, Sodium channels as macromolecular complexes: implications for inherited arrhythmia syndromes, Cardiovascular research 67 (2005) 448-458.
[74] L.S. Meadows, J. Malhotra, A. Loukas, V. Thyagarajan, K.A. Kazen-Gillespie, M.C. Koopman, S. Kriegler, L.L. Isom, D.S. Ragsdale, Functional and biochemical analysis of a sodium channel beta1 subunit mutation responsible for generalized epilepsy with febrile seizures plus type 1, J Neurosci 22 (2002) 10699-10709.
[75] A. Medeiros-Domingo, T. Kaku, D.J. Tester, P. Iturralde-Torres, A. Itty, B. Ye, C. Valdivia, K. Ueda, S. Canizales-Quinteros, M.T. Tusie-Luna, J.C. Makielski, M.J. Ackerman, SCN4B-Encoded Sodium Channel {beta}4 Subunit in Congenital Long-QT Syndrome, Circulation (2007).
[76] D.J. Messner, W.A. Catterall, The sodium channel from rat brain. Separation and characterization of subunits, The Journal of biological chemistry 260 (1985) 10597-10604.
[77] H. Miyazaki, F. Oyama, H.K. Wong, K. Kaneko, T. Sakurai, A. Tamaoka, N. Nukina, BACE1 modulates filopodia-like protrusions induced by sodium channel beta4 subunit, Biochemical and biophysical research communications 361 (2007) 43-48.
[78] O. Moran, F. Conti, P. Tammaro, Sodium channel heterologous expression in mammalian cells and the role of the endogenous beta1-subunits, Neuroscience letters 336 (2003) 175-179.
[79] O. Moran, M. Nizzari, F. Conti, Endogenous expression of the beta1A sodium channel subunit in HEK-293 cells, FEBS letters 473 (2000) 132-134.
[80] K. Morgan, E.B. Stevens, B. Shah, P.J. Cox, A.K. Dixon, K. Lee, R.D. Pinnock, J. Hughes, P.J. Richardson, K. Mizuguchi, A.P. Jackson, beta 3: an additional auxiliary subunit of the voltage-sensitive sodium channel that modulates channel gating with distinct kinetics, Proceedings of the National Academy of Sciences of the United States of America 97 (2000) 2308-2313.
[81] H.A. O'Malley, A.B. Shreiner, G.H. Chen, G.B. Huffnagle, L.L. Isom, Loss of Na+ channel beta2 subunits is neuroprotective in a mouse model of multiple sclerosis, Mol Cell Neurosci 40 (2009) 143-155.
[82] R. Ogawa, R. Kishi, A. Takagi, I. Sakaue, H. Takahashi, N. Matsumoto, K. Masuhara, K. Nakazawa, S. Kobayashi, F. Miyake, H. Echizen, A novel microsatellite polymorphism of sodium channel beta1-subunit gene (SCN1B) may underlie abnormal cardiac excitation manifested by coved-type ST-elevation compatible with Brugada syndrome in Japanese, Int J Clin Pharmacol Ther 48 (2010) 109-119.
[83] I. Ogiwara, H. Miyamoto, N. Morita, N. Atapour, E. Mazaki, I. Inoue, T. Takeuchi, S. Itohara, Y. Yanagawa, K. Obata, T. Furuichi, T.K. Hensch, K. Yamakawa, Na(v)1.1 localizes to axons of parvalbumin-positive inhibitory interneurons: a circuit basis for epileptic seizures in mice carrying an Scn1a gene mutation, J Neurosci 27 (2007) 5903-5914.
[84] Y. Oh, Y.J. Lee, S.G. Waxman, Regulation of Na+ channel beta 1 and beta 2 subunit mRNA levels in cultured rat astrocytes, Neuroscience letters 234 (1997) 107-110.
[85] Y. Oh, S.G. Waxman, The beta 1 subunit mRNA of the rat brain Na+ channel is expressed in glial cells, Proceedings of the National Academy of Sciences of the United States of America 91 (1994) 9985-9989.
[86] R. Onkal, M.B. Djamgoz, Molecular pharmacology of voltage-gated sodium channel expression in metastatic disease: clinical potential of neonatal Nav1.5 in breast cancer, Eur J Pharmacol 625 (2009) 206-219.

[87] A. Orrico, L. Galli, S. Grosso, S. Buoni, R. Pianigiani, P. Balestri, V. Sorrentino, Mutational analysis of the SCN1A, SCN1B and GABRG2 genes in 150 Italian patients with idiopathic childhood epilepsies, Clin Genet 75 (2009) 579-581.
[88] F. Oyama, H. Miyazaki, N. Sakamoto, C. Becquet, Y. Machida, K. Kaneko, C. Uchikawa, T. Suzuki, M. Kurosawa, T. Ikeda, A. Tamaoka, T. Sakurai, N. Nukina, Sodium channel beta4 subunit: down-regulation and possible involvement in neuritic degeneration in Huntington's disease transgenic mice, Journal of neurochemistry 98 (2006) 518-529.
[89] A. Pance, F.J. Livesey, A.P. Jackson, A role for the transcriptional repressor REST in maintaining the phenotype of neurosecretory-deficient PC12 cells, Journal of neurochemistry 99 (2006) 1435-1444.
[90] J.W. Park, J. Cai, I. McIntosh, E.W. Jabs, M.D. Fallin, R. Ingersoll, J.B. Hetmanski, M. Vekemans, T. Attie-Bitach, M. Lovett, A.F. Scott, T.H. Beaty, High throughput SNP and expression analyses of candidate genes for non-syndromic oral clefts, J Med Genet 43 (2006) 598-608.
[91] G. Patino, W.J. Brackenbury, L.L. Isom, The β1B splice variant of the voltage-gated sodium channel SCN1B is a soluble protein with a possible role in axon pathfinding Program No. 517.12. 2009 Neuroscience Meeting Planner. Chicago, IL: Society for Neuroscience, 2009. Online.
[92] G.A. Patino, L.R. Claes, L.F. Lopez-Santiago, E.A. Slat, R.S. Dondeti, C. Chen, H.A. O'Malley, C.B. Gray, H. Miyazaki, N. Nukina, F. Oyama, P. De Jonghe, L.L. Isom, A functional null mutation of SCN1B in a patient with Dravet syndrome, J Neurosci 29 (2009) 10764-10778.
[93] M. Pertin, R.R. Ji, T. Berta, A.J. Powell, L. Karchewski, S.N. Tate, L.L. Isom, C.J. Woolf, N. Gilliard, D.R. Spahn, I. Decosterd, Upregulation of the voltage-gated sodium channel beta2 subunit in neuropathic pain models: characterization of expression in injured and non-injured primary sensory neurons, J Neurosci 25 (2005) 10970-10980.
[94] O. Platoshyn, C.V. Remillard, I. Fantozzi, T. Sison, J.X. Yuan, Identification of functional voltage-gated Na(+) channels in cultured human pulmonary artery smooth muscle cells, Pflugers Arch 451 (2005) 380-387.
[95] N. Qin, M.R. D'Andrea, M.L. Lubin, N. Shafaee, E.E. Codd, A.M. Correa, Molecular cloning and functional expression of the human sodium channel beta1B subunit, a novel splicing variant of the beta1 subunit, European journal of biochemistry / FEBS 270 (2003) 4762-4770.
[96] C.F. Ratcliffe, Y. Qu, K.A. McCormick, V.C. Tibbs, J.E. Dixon, T. Scheuer, W.A. Catterall, A sodium channel signaling complex: modulation by associated receptor protein tyrosine phosphatase beta, Nature neuroscience 3 (2000) 437-444.
[97] C.F. Ratcliffe, R.E. Westenbroek, R. Curtis, W.A. Catterall, Sodium channel beta1 and beta3 subunits associate with neurofascin through their extracellular immunoglobulin-like domain, J Cell Biol 154 (2001) 427-434.
[98] C.A. Remme, B.P. Scicluna, A.O. Verkerk, A.S. Amin, S. van Brunschot, L. Beekman, V.H. Deneer, C. Chevalier, F. Oyama, H. Miyazaki, N. Nukina, R. Wilders, D. Escande, R. Houlgatte, A.A. Wilde, H.L. Tan, M.W. Veldkamp, J.M. de Bakker, C.R. Bezzina, Genetically determined differences in sodium current characteristics modulate conduction disease severity in mice with cardiac sodium channelopathy, Circulation research 104 (2009) 1283-1292.
[99] G. Rougon, O. Hobert, New insights into the diversity and function of neuronal immunoglobulin superfamily molecules, Annu Rev Neurosci 26 (2003) 207-238.
[100] R. Rusconi, R. Combi, S. Cestele, D. Grioni, S. Franceschetti, L. Dalpra, M. Mantegazza, A rescuable folding defective Nav1.1 (SCN1A) sodium channel mutant causes GEFS+: common mechanism in Nav1.1 related epilepsies?, Human mutation 30 (2009) E747-760.

[101] S. Sashihara, C.A. Greer, Y. Oh, S.G. Waxman, Cell-specific differential expression of Na(+)-channel beta 1-subunit mRNA in the olfactory system during postnatal development and after denervation, J Neurosci 16 (1996) 702-713.
[102] I.E. Scheffer, L.A. Harkin, B.E. Grinton, L.M. Dibbens, S.J. Turner, M.A. Zielinski, R. Xu, G. Jackson, J. Adams, M. Connellan, S. Petrou, R.M. Wellard, R.S. Briellmann, R.H. Wallace, J.C. Mulley, S.F. Berkovic, Temporal lobe epilepsy and GEFS+ phenotypes associated with SCN1B mutations, Brain 130 (2007) 100-109.
[103] J. Schmidt, S. Rossie, W.A. Catterall, A large intracellular pool of inactive Na channel alpha subunits in developing rat brain, Proceedings of the National Academy of Sciences of the United States of America 82 (1985) 4847-4851.
[104] J.W. Schmidt, W.A. Catterall, Biosynthesis and processing of the alpha subunit of the voltage-sensitive sodium channel in rat brain neurons, Cell 46 (1986) 437-444.
[105] M. Seda, F.M. Pinto, S. Wray, C.G. Cintado, P. Noheda, H. Buschmann, L. Candenas, Functional and molecular characterization of voltage-gated sodium channels in uteri from nonpregnant rats, Biol Reprod 77 (2007) 855-863.
[106] B.S. Shah, E.B. Stevens, R.D. Pinnock, A.K. Dixon, K. Lee, Developmental expression of the novel voltage-gated sodium channel auxiliary subunit beta3, in rat CNS, The Journal of physiology 534 (2001) 763-776.
[107] J.P. Smits, M.T. Blom, A.A. Wilde, H.L. Tan, Cardiac sodium channels and inherited electrophysiologic disorders: a pharmacogenetic overview, Expert Opin Pharmacother 9 (2008) 537-549.
[108] J. Spampanato, J.A. Kearney, G. de Haan, D.P. McEwen, A. Escayg, I. Aradi, B.T. MacDonald, S.I. Levin, I. Soltesz, P. Benna, E. Montalenti, L.L. Isom, A.L. Goldin, M.H. Meisler, A novel epilepsy mutation in the sodium channel SCN1A identifies a cytoplasmic domain for beta subunit interaction, J Neurosci 24 (2004) 10022-10034.
[109] J. Srinivasan, M. Schachner, W.A. Catterall, Interaction of voltage-gated sodium channels with the extracellular matrix molecules tenascin-C and tenascin-R, Proceedings of the National Academy of Sciences of the United States of America 95 (1998) 15753-15757.
[110] P.L. Strick, R.P. Dum, J.A. Fiez, Cerebellum and nonmotor function, Annu Rev Neurosci 32 (2009) 413-434.
[111] P. Tammaro, F. Conti, O. Moran, Modulation of sodium current in mammalian cells by an epilepsy-correlated beta 1-subunit mutation, Biochemical and biophysical research communications 291 (2002) 1095-1101.
[112] B.H. Tan, K.N. Pundi, D.W. Van Norstrand, C.R. Valdivia, D.J. Tester, A. Medeiros-Domingo, J.C. Makielski, M.J. Ackerman, Sudden infant death syndrome-associated mutations in the sodium channel beta subunits, Heart Rhythm (2010).
[113] M.E. Thase, T. Denko, Pharmacotherapy of mood disorders, Annu Rev Clin Psychol 4 (2008) 53-91.
[114] M. Uebachs, T. Opitz, M. Royeck, G. Dickhof, M.T. Hostmann, L.L. Isom, H. Beck, Efficacy loss of the anticonvulsant carbamazepine in mice lacking sodium channel β subunits via paradoxical effects on persistent sodium currents, J Neurosci (2010) In press.
[115] C.R. Valdivia, A. Medeiros-Domingo, B. Ye, W.K. Shen, T.J. Algiers, M.J. Ackerman, J.C. Makielski, Loss-of-function mutation of the SCN3B-encoded sodium channel {beta}3 subunit associated with a case of idiopathic ventricular fibrillation, Cardiovascular research (2010).
[116] K.L. van Gassen, M. de Wit, M. van Kempen, W.S. van der Hel, P.C. van Rijen, A.P. Jackson, D. Lindhout, P.N. de Graan, Hippocampal Nabeta3 expression in patients with temporal lobe epilepsy, Epilepsia 50 (2009) 957-962.

[117] R.H. Wallace, I.E. Scheffer, G. Parasivam, S. Barnett, G.B. Wallace, G.R. Sutherland, S.F. Berkovic, J.C. Mulley, Generalized epilepsy with febrile seizures plus: mutation of the sodium channel subunit SCN1B, Neurology 58 (2002) 1426-1429.
[118] R.H. Wallace, D.W. Wang, R. Singh, I.E. Scheffer, A.L. George, Jr., H.A. Phillips, K. Saar, A. Reis, E.W. Johnson, G.R. Sutherland, S.F. Berkovic, J.C. Mulley, Febrile seizures and generalized epilepsy associated with a mutation in the Na+-channel beta1 subunit gene SCN1B, Nat Genet 19 (1998) 366-370.
[119] P. Wang, Q. Yang, X. Wu, Y. Yang, L. Shi, C. Wang, G. Wu, Y. Xia, B. Yang, R. Zhang, C. Xu, X. Cheng, S. Li, Y. Zhao, F. Fu, Y. Liao, F. Fang, Q. Chen, X. Tu, Q.K. Wang, Functional dominant-negative mutation of sodium channel subunit gene SCN3B associated with atrial fibrillation in a Chinese GeneID population, Biochemical and biophysical research communications (2010).
[120] X. Wang, A.V. Koulov, W.A. Kellner, J.R. Riordan, W.E. Balch, Chemical and Biological Folding Contribute to Temperature-Sensitive DeltaF508 CFTR Trafficking, Traffic (Copenhagen, Denmark) (2008).
[121] H. Watanabe, D. Darbar, D.W. Kaiser, K. Jiramongkolchai, S. Chopra, B.S. Donahue, P.J. Kannankeril, D.M. Roden, Mutations in sodium channel beta1- and beta2-subunits associated with atrial fibrillation, Circ Arrhythm Electrophysiol 2 (2009) 268-275.
[122] H. Watanabe, T.T. Koopmann, S. Le Scouarnec, T. Yang, C.R. Ingram, J.J. Schott, S. Demolombe, V. Probst, F. Anselme, D. Escande, A.C. Wiesfeld, A. Pfeufer, S. Kaab, H.E. Wichmann, C. Hasdemir, Y. Aizawa, A.A. Wilde, D.M. Roden, C.R. Bezzina, Sodium channel beta1 subunit mutations associated with Brugada syndrome and cardiac conduction disease in humans, The Journal of clinical investigation 118 (2008) 2260-2268.
[123] S.G. Waxman, Mechanisms of disease: sodium channels and neuroprotection in multiple sclerosis-current status, Nat Clin Pract Neurol 4 (2008) 159-169.
[124] V.C. Wimmer, C.A. Reid, S. Mitchell, K.L. Richards, B.B. Scaf, B.T. Leaw, E.L. Hill, M. Royeck, M.T. Horstmann, B.A. Cromer, P.J. Davies, R. Xu, H. Lerche, S.F. Berkovic, H. Beck, S. Petrou, Axon initial segment dysfunction in a mouse model of genetic epilepsy with febrile seizures plus, The Journal of clinical investigation 120 (2010) 2661-2671.
[125] H.K. Wong, T. Sakurai, F. Oyama, K. Kaneko, K. Wada, H. Miyazaki, M. Kurosawa, B. De Strooper, P. Saftig, N. Nukina, beta Subunits of voltage-gated sodium channels are novel substrates of beta-site amyloid precursor protein-cleaving enzyme (BACE1) and gamma-secretase, The Journal of biological chemistry 280 (2005) 23009-23017.
[126] Z.C. Xiao, D.S. Ragsdale, J.D. Malhotra, L.N. Mattei, P.E. Braun, M. Schachner, L.L. Isom, Tenascin-R is a functional modulator of sodium channel beta subunits, The Journal of biological chemistry 274 (1999) 26511-26517.
[127] R. Xu, E.A. Thomas, E.V. Gazina, K.L. Richards, M. Quick, R.H. Wallace, L.A. Harkin, S.E. Heron, S.F. Berkovic, I.E. Scheffer, J.C. Mulley, S. Petrou, Generalized epilepsy with febrile seizures plus-associated sodium channel beta1 subunit mutations severely reduce beta subunit-mediated modulation of sodium channel function, Neuroscience 148 (2007) 164-174.
[128] F.H. Yu, R.E. Westenbroek, I. Silos-Santiago, K.A. McCormick, D. Lawson, P. Ge, H. Ferriera, J. Lilly, P.S. DiStefano, W.A. Catterall, T. Scheuer, R. Curtis, Sodium channel beta4, a new disulfide-linked auxiliary subunit with similarity to beta2, J Neurosci 23 (2003) 7577-7585.
[129] Z.N. Zhang, Q. Li, C. Liu, H.B. Wang, Q. Wang, L. Bao, The voltage-gated Na+ channel Nav1.8 contains an ER-retention/retrieval signal antagonized by the beta3 subunit, J Cell Sci 121 (2008) 3243-3252.

Chapter II

A functional null mutation of *SCN1B* in a patient with Dravet Syndrome

(This chapter has been published in J Neurosci 2009; 29: 10764-10778)

Introduction

Patients with Dravet syndrome (OMIM 607208, Severe Myoclonic Epilepsy of Infancy) typically exhibit prolonged febrile seizures in the first year of life. Subsequently, multiple types of febrile and afebrile seizures occur. Seizures are difficult to control, often requiring polytherapy. Cognitive development is normal until approximately two years of age, when it slows or stagnates. All patients exhibit some level of mental retardation. Patients often exhibit other neurological abnormalities, including ataxia and pyramidal signs. Risk of death is high in this group, including patients with sudden unexpected death in epilepsy (SUDEP) [19, 69].

40 to 85% percent of Dravet syndrome patients have mutations in *SCN1A* [10, 33, 46], the gene encoding voltage-gated sodium channel $Na_v1.1$. In most patients mutations are acquired *de novo* [23, 32], although in some they are inherited [24, 44]. Sodium channels are multimeric protein complexes essential for action potential generation in excitable cells, including neurons. Sodium channels are composed of a central, pore-forming α subunit and two β subunits: a non-covalently-linked β1 or β3 subunit, and a disulfide-linked β2 or β4 subunit [8, 11]. In the central nervous system the most abundant α subunits are $Na_v1.1$, $Na_v1.2$, and $Na_v1.6$ [11]. Therefore it is not surprising that mutations in genes encoding these subunits lead to epilepsy.

Sodium channel β1 subunits modulate channel voltage-dependence and gating as well as channel cell surface expression [28-30]. β1 also participates in cell-cell and cell-matrix adhesion [6, 7]. β1-mediated homophilic cell adhesion *in vitro* results in cellular aggregation,

ankyrin recruitment, and neurite outgrowth [17, 37, 38]. *In vivo*, the loss of β1 results in spontaneous seizures, ataxia, and aberrant neuronal pathfinding and fasciculation [6, 14]. *SCN1B*, encoding β1 [28], gives rise to at least two splice variants, β1 and β1B, that differ in their carboxyl-terminal domains [31, 50].

Heterozygous mutations in *SCN1B* have been reported in patients with Genetic Epilepsy with Febrile Seizures Plus type 1 (GEFS+1). Other genes implicated in GEFS+ include: *SCN1A* (GEFS+2), *GABRG2* (GEFS+3), *GABRD* (GEFS+5) and *SCN9A* (GEFS+7) (OMIM 604233) [3, 9, 54, 64, 65, 71]. GEFS+ is an epilepsy syndrome that includes mild to severe forms of epilepsy, with Dravet syndrome classified on the most severe side of the spectrum. All GEFS+ patients with *SCN1B* mutations reported to date fall in the mild to moderate range of seizure severity, comprising febrile seizures, febrile seizures plus, early-onset absence epilepsy, mild to moderate generalized epilepsies and focal epilepsies. Here we report the first case of Dravet syndrome caused by a *SCN1B* homozygous mutation and explore the mechanisms by which this mutation may cause disruptions in the control of electrical excitability.

Materials and Methods

1. Genetic analysis:

Mutation analysis of the 6 exons and intron-exon boundaries of *SCN1B* was performed on genomic DNA of the patient by PCR sequencing. Primer sequences can be obtained upon request. Purified PCR products were subsequently sequenced using the ABI BigDye Terminator cycle sequencing kit v3.1 and analyzed on an ABI 3730 automated sequencer (PE Applied Biosystems). Automated variation (SNPs and indels) discovery was performed using novoSNP [66]. Pyrosequencing with the PSQ^{TM}96 System (Pyrosequencing AB) was used to confirm the presence of the mutation in the patient and to exclude it from the parents and a panel of 92 control individuals, of which 40 were of Moroccan origin, similar to the patient's family. DNA was extracted from

peripheral blood of all participants. The Commission for Medical Ethics of the University of Antwerp approved this study and participants or their legal representative signed an informed consent.

Mutations were numbered according to the published cDNA sequence (accession number NM_001037) with nucleotide +1 corresponding to the A of the ATG translation initiation codon and the nomenclature followed the MDI/HGVS Mutation Nomenclature Recommendations [18].

To test for homozygosity we genotyped 4 STR-markers distributed over 5 Mb surrounding *SCN1B*. The markers were amplified in one multiplex PCR reaction and analyzed on an ABI 3730 automated sequencer (PE Applied Biosystems).

2. Animals:

Female *Xenopus laevis* frogs were obtained from Xenopus I (Ann Arbor, MI), and housed in cages filled with distilled water and protected from light. Frog chow was available *ad libitum*. Recovery of oocytes was performed as described below and previously [22]. Frogs were allowed to recover at least two weeks between surgeries, and consecutive surgeries took place on opposite sides of the abdomen for each individual frog.

Scn1b$^{-/-}$ and *Scn1b*$^{+/+}$ mice, congenic on the C57BL/6 background for at least 15 generations, were generated from *Scn1b*$^{+/-}$ mice as described [14]. Animals were housed in the Unit for Laboratory Animal Medicine at the University of Michigan. All procedures were performed in accordance with University of Michigan guidelines for animal use and care.

3. Antibodies:

Primary antibodies used in these studies were: anti- $\beta1_{intra}$ (1:1000 dilution) [13, 48], anti-V5 monoclonal antibody (1:2000, AbD Serotec), or anti-α-tubulin monoclonal

antibody (1:10000, Cedarlane Laboratories). The specificity of the anti- $\beta1_{intra}$ has been reported previously using Western blot analysis of *Scn1b*$^{+/+}$ and *Scn1b*$^{-/-}$ brain membranes [13]. To test the specificity of anti- $\beta1_{intra}$ using immunofluorescence, we labeled *Scn1b*$^{+/+}$ and *Scn1b*$^{-/-}$ optic nerve nodes of Ranvier as in [14] (**Figure II.1.A** and **B**). *Scn1b*$^{+/+}$ nerves showed β1 immunofluorescence in the nodal gap with caspr marking the paranodal regions, as expected. In contrast, *Scn1b*$^{-/-}$ nerves showed paranodal caspr staining but no β1 signal in the nodes. To test the specificity of the anti-V5 antibody, membrane preps from rat or *Scn1b*$^{-/-}$ mouse brains, V5-tagged p.R125C-transfected or untransfected 1610 cells ([14, 67]) were analyzed by Western Blot, as described below. No immunoreactive bands were detected in rat or mouse brain or untransfected cells. In contrast, V5-tagged p.R125C was detected in the transfected cells by the anti-V5 antibody (**Figure II.1.C**). Secondary antibodies used in these studies were HRP-conjugated goat anti-rabbit or anti-mouse (Pierce, Rockford, IL) diluted 1:2000, and Alexa Fluor 568 anti-rabbit (Molecular Probes, Eugene, OR). Cell nuclei were counterstained with 4',6-diamidino-2-phenylinodole (DAPI) (10 µg/ml; Sigma, Saint Louis, MO)

4. Expression vectors:

p.R125C cDNA was generated by PCR using human β1 cDNA in pcDNA3 as the template while simultaneously introducing the mutation by site-directed mutagenesis. For the experiments in mammalian cells, p.R125C cDNA was inserted into pcDNA3.1 Hygro(+), as was the human β1 cDNA (β1WT), and the sequences of both constructs were confirmed. From these plasmids, cDNAs were amplified by PCR to remove the stop codon and then inserted into pcDNA3.1/V5-HIS using the pcDNA3.1/V5-HIS TOPO TA Expression Kit (Invitrogen, Carlsbad, CA), according to the manufacturer's instructions, to produce the V5-His tagged subunits.

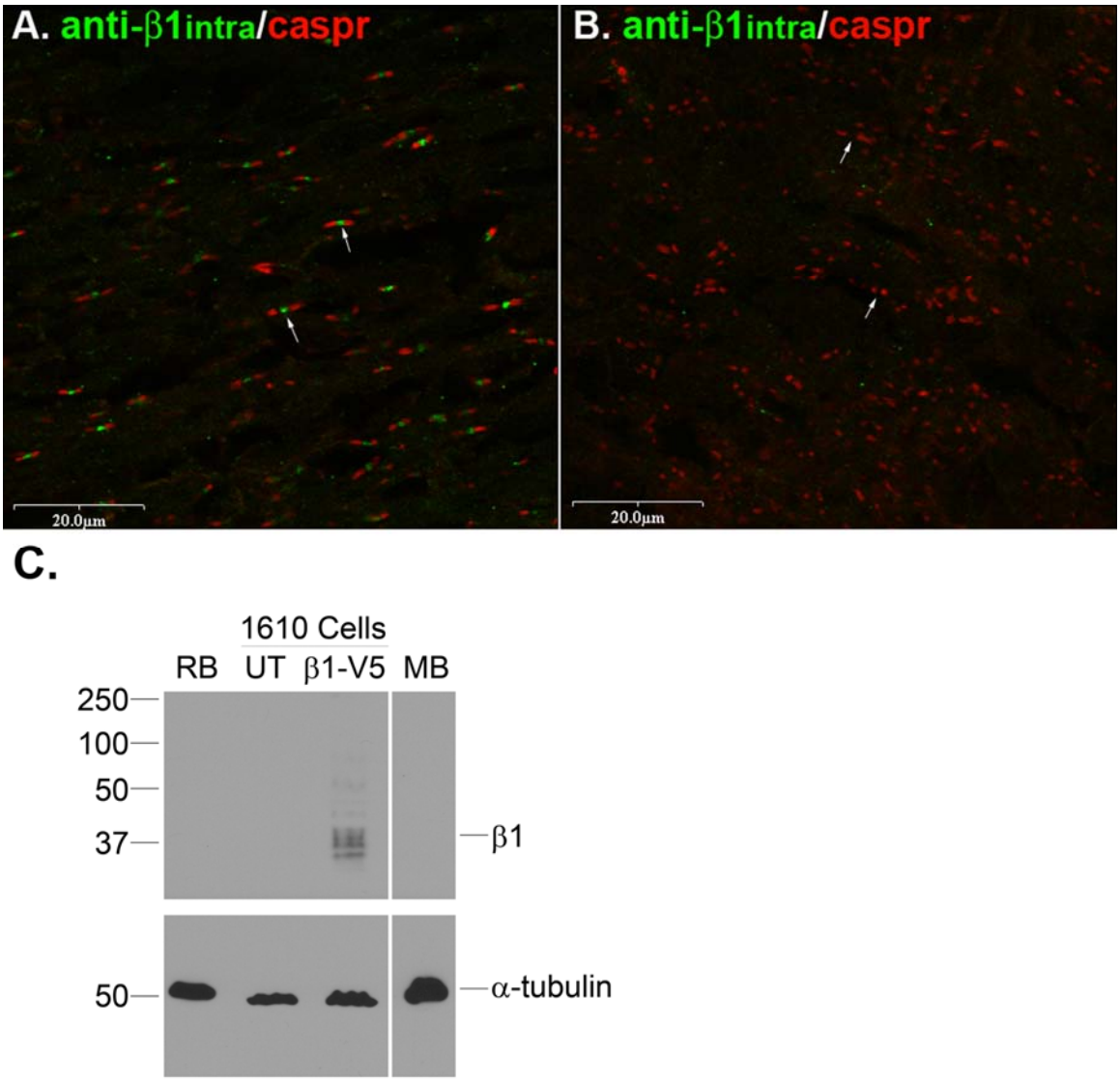

Figure II.1. Specificity of anti- $\beta1_{intra}$ antibody. (**A**) Anti-$\beta1_{intra}$ labels nodes of Ranvier in optic nerve. *Scn1b+/+* optic nerves were prepared and stained for immunofluorescence as in [14]. Green: anti- $\beta1_{intra}$. Red: anti-caspr (Neuromab). (**B**) As in (**A**), but *Scn1b-/-* optic nerves were stained in place of WT. Arrows in (**A**) and (**B**) indicate positions of nodes of Ranvier. (**C**) **Specificity of the anti-V5 antibody.** Rat (RB) or *Scn1b-/-* mouse (MB) brain membrane preparations, untransfected 1610 cells (UT) or p.R125C-V5-transfected 1610 cells were analyzed by Western blot with anti-V5 antibody. No immunoreactive bands were detected in anysample except for 1610 cells stably transfected with V5-tagged p.R125C. Arrow indicated position of β1 immunoreactive band. Molecular weight markers are in KDa.

For oocyte expression, p.R125C cDNA was inserted into pSP64t-BXN [42]. β1WT-pSP64t-BXN was generated as previously described [42]. The plasmid encoding rat $Na_v1.2$ has been described previously [22].

5. Cell Lines:

All cell lines were maintained at 37°C with 5% CO_2 with the exception of the 27°C growth experiment, as indicated. HEK-293 cells expressing human $Na_v1.1$ (HEKh$Na_v1.1$) were obtained from Glaxo-Smith-Kline under a Materials Transfer Agreement and maintained in DMEM supplemented with 10% heat inactivated fetal bovine serum (HI-FBS), 200 μg/ml G418, 0.1% non-essential amino acids, 100 U + 100 μg/ml penicillin/streptomycin, and 0.25 μg/ml Fungizone (all from Invitrogen). HEKr$Na_v1.1$ cells are HEK-293 derived and stably express the rat $Na_v1.1$ subunit. These cells were cultured in MEM with Earle's salts, supplemented with 10% HI-FBS, 1% Glutamax, 1% sodium pyruvate, 1% non-essential amino acids mix, 100 U + 100 μg/ml penicillin/streptomycin, 400 μg/ml Zeocin, 0.25 μg/ml Fungizone (all from Invitrogen). Untransfected HEK cells were maintained in this medium in the absence of Zeocin. SNaIIa cells are derived from Chinese hamster lung 1610 cells and stably express the rat $Na_v1.2$ subunit [67]. They were cultured in DMEM with low glucose, L-glutamine and sodium pyruvate; supplemented with 5% HI-FBS, 100 U + 100 μg/ml penicillin/streptomycin, 400 μg/ml G418, 0.25 μg/ml Fungizone. 1610 cells were maintained in this medium in the absence of G418. All cells were transfected with Fugene 6 transfection reagent (Roche) according to the manufacturer's instructions.

For electrophysiology experiments using transient transfection, 2 μg of the cDNAs encoding wildtype or mutant β1 subunits were co-transfected with 0.5 μg of Enhanced Green Fluorescent Protein (EGFP), using pEGFP-N3 (Clontech), as a marker. 24 hours later the cells were passaged into 35 mm Petri dishes (Falcon). 24 to 48 h later, whole-cell patch-clamp recordings were performed at room temperature,

using an Axopatch 200B amplifier (Axon Instruments). The presence or absence of EGFP did not affect the results obtained (data not shown). Cells were visualized using an epi-fluorescence-equipped inverted microscope (Zeiss Axovert 25). For biochemical experiments using transient transfections 3 µg of the cDNAs encoding wildtype or mutant β1 subunits were transfected into HEKhNa$_v$1.1 cells. 24-48 hours post-transfection the cells were trypsinized and processed for whole-cell lysates or cell surface biotinylation experiments as described below.

To generate stable cell lines, 2.5 µg of β1 cDNAs were transfected and 24 h later cell were passed into new medium containing selective antibiotics (400 µg/ml Hygromycin (Invitrogen) for untagged β1 subunit cDNAs, or 400 µg/ml G418 for V5 epitope-tagged β1 subunit cDNAs). The cells were then incubated for several days until cell colonies were visible, when they were isolated and grown until reaching 95% confluence as in [30]. Cell clones were then passaged for biochemical and electrophysiological characterization.

6. Whole-cell patch clamp analysis:

Micropipettes were obtained from capillary glass tubing (Warner Instruments, Hamden, CT) using a horizontal P-97 puller (Sutter Instrument, Novato, CA). Electrode resistance was between 1.5 and 3.5 MΩ. Voltage pulses were applied and data recorded using Clampex 9.2 and a Digidata 1322A digitizer (Axon Instruments). Pipette and whole-cell capacitance were fully compensated and the series resistance compensation was set to approximately 80% with the lag set no greater than 15 µs. Residual linear currents were subtracted using the p/4 procedure on-line, except for current rundown recordings. Signals were low pass filtered at 5 kHz and data sampled at 40 kHz online. Extracellular solution contained (in mM): 130 NaCl, 4 KCl, 1.5 $CaCl_2$, 1 $MgCl_2$,5 glucose, 10 HEPES. Intracellular solution (in mM): 20 CsF, 95 CsCl, 10 NaCl, 10 EGTA, 10 HEPES. To determine the sodium current amplitude and voltage-dependence of

activation, currents were evoked by depolarization to different 250 ms test pulses (from -120 to -70 mV at 10 mV intervals, from -70 to -10 mV at 5 mV intervals, and from -10 to 50 mV at 10 mV intervals) from a holding potential of -90 mV and a hyperpolarizing -120 mV, 500 ms prepulse. Peak currents were normalized to cell capacitance and used to plot current density/V curves and to calculate conductance ($g=I/(V-V_{rev})$ where V is the test potential and V_{rev} is the measured reversal potential). Voltage-dependence of inactivation was determined by applying a 50 ms test pulse of 0 mV after 250 ms prepulses to the same voltages as described for the voltage-dependence of activation. Peak currents were normalized to the peak current amplitude. Normalized voltage conductance and inactivation curves were fit with the Boltzmann equation $1/[1+\exp(V-V_{1/2})/k]$, where $V_{1/2}$ is the membrane potential in the midpoint of the curve, and k is a slope factor. To asses the time course of recovery from inactivation a pulse to 0 mV for 20 ms was followed by a recovery interpulse of variable duration (from 0.2 ms to 750 ms) to -110 mV and then a 20 ms test pulse to 0 mV to determine the fraction of recovered channels. Peak currents during the test pulse were normalized to the peak current during the corresponding prepulse, and plotted as fractional recovery (F_r) against time. Data were then fit with a double exponential to determine the time constants for recovery, using the formula $F_r=(F_f*(1-\exp((-x)/\tau_f)))+(F_s*(1-\exp((-x)/\tau_s)))$; where F_f and F_s are the proportions of fast and slow recovery, respectively. τ_f and τ_s are the fast and slow constants of recovery, respectively. For those cells that fit better with only one exponential F_s was considered to be 0 for statistical analysis. The kinetics of inactivation were measured on the test pulse to 0 mV from the same protocol used for voltage-dependence of activation. The current from 90% of the peak amplitude to 20 ms after the test pulse was fitted by the Chebyshev method to the equation $i=(F_f*e^{-t/\tau_f})+(F_s*e^{-t/\tau_s})+C$, where I is the current and C is the steady-state persistent current. The presence of persistent current was measured with the same protocol as above, from 245 to 250 ms after the test pulse was started, averaging the current in the segment and then

normalizing against the peak current during the test pulse. To measure use-dependent rundown a 10 mV pulse was given from a -100 mV holding potential, at a frequency of 80 Hz. Residual linear currents were subtracted using the p/4 procedure off-line. Peak current was measured and normalized to the peak current of the first pulse, and then plotted against pulse number [34, 42]. Analysis of the recorded currents was carried out using the software packages Clampfit 9.0.2 (Axon Instruments) and Origin 7 (OriginLab).

7. Two-electrode voltage clamp recordings:

Plasmids containing the cDNAs encoding rat $Na_v1.2$, rat β1WT, or human p.R125C were linearized using Xho I ($Na_v1.2$), EcoR I (β1WT), or Apa I plus Not I (p.R125C). mRNA was synthesized from the linearized plasmids using T7 ($Na_v1.2$) or SP6 (β1WT and p.R125C) mMessage mMachine RNA Synthesis Kits (Ambion, Austin, Tx). The resultant cRNAs were resuspended in RNA resuspension buffer (5 mM HEPES, 0.1 mM EDTA, pH 7.5) and 1 µl of each preparation was analyzed by agarose-formaldehyde gel electrophoresis. Total cRNA yields for each preparation were estimated by comparison of the intensities of ethidium bromide stained bands on the gels. After being anesthetized with 3-aminobenzoic acid ethyl ester (tricaine, 0.2%, Sigma), and under aseptic conditions, lobes of ovary were removed through a paramedian incision from female *Xenopus laevis*. Muscle and peritoneum we closed together with catgut, followed by skin using the same type of suture. The lobes containing oocytes were manually teased and then washed twice in OR2 (82.5 mM NaCl, 2 mM KCl, 1 mM $MgCl_2$, 5 mM HEPES, pH 7.5), defolliculated, and separated by shaking in collagenase Type I (1.5 mg/ml, Sigma). Healthy stage V-VI oocytes were selected and incubated overnight at 18°C in Barth's medium (88 mM NaCl, 1 mM KCl, 0.82 mM $MgSO_4$, 0.33 mM $Ca(NO_3)_2$, 0.41 mM $CaCl_2$, 2.4 mM $NaHCO_3$, 10 mM HEPES, pH 7.4), supplemented with 50 µg/ml of gentamycin [22]. On the second day, oocytes were microinjected with 50 nl of cRNA in the following combinations: α subunit alone, α

plus β1WT, or α plus p.R125C. We used approximately a 5-fold concentration of α: β1, and equivalent concentrations of β1WT and p.R125C. After 16 to 48 h of incubation at 18°C, two-electrode voltage clamp recordings were performed at room temperature, using a Turbo TEC-10C amplifier (NPI Electronic, Germany). Micropipettes were obtained from capillary glass with internal filament (A-M systems, Carlsborg, WA) using a horizontal puller P-97. Electrode resistance was between 0.5 and 1.5 MΩ. Voltage pulses were applied and data recorded using Clampex and a Digidata 1322A digitizer. Residual linear currents were subtracted using the p/4 procedure. Signals were low pass filtered at 2 kHz and data sampled at 20 kHz online. Oocytes were continuously perfused with Ringer Solution (115 mM NaCl, 2.5 mM KCl, 1.8 mM $CaCl_2$, 10 mM HEPES, pH 7.2) to which choline solution was sometimes substituted for sodium to obtain adequate voltage control [22, 42, 49]. To examine the electrophysiological properties of sodium currents in oocytes, similar protocols and analyses were used as described for the mammalian cell lines with the following modifications: To determine the voltage dependence of activation the peak currents were evoked by depolarization with 90 ms pulses, from -100 mV to 55 mV in 5 mV increments, from a holding potential of -80 mV. Voltage dependence of inactivation was determined by applying 90 ms prepulses to potentials ranging from -100 to 55 mV, followed by a test pulse of 0 mV for 80 ms. To assess the time course of recovery from inactivation a pulse of 0 mV for 5 ms was followed by a recovery prepulse of variable duration to -80 mV and a test pulse to 0 mV.

8. Western Blot analysis of cell lysates:

For each experiment, stably transfected cells from a 100 mm Petri dish, or transiently transfected cells from a 60 mm dish, at 95% confluence were pelleted, resuspended, and homogenized in Tris-EGTA buffer (50 mM Tris, 10 mM EGTA, pH 8) with Complete Mini protease inhibitor tablets (Roche) and centrifuged once again. Cell

pellets were then resuspended in RIPA buffer (50 mM Tris, 10mM EDTA, 150 mM NaCl, 1.25% NP-40, 0.5% sodium deoxycholate, 0.1% SDS) and incubated on ice for 20 min. Non-solubilized proteins were removed by centrifugation and the resultant supernatant mixed with loading buffer containing SDS and β-mercaptoethanol. Proteins were separated by SDS-PAGE on a 10% polyacrylamide gel, transferred to nitrocellulose membrane and Western blot analysis performed as previously described [40]. Incubations with both primary and secondary antibodies were carried out at room temperature for 1 h. Immunoreactive bands were detected using West Dura or West Femto chemiluminescent substrate (Thermo Scientific). Rat brain membranes were prepared as previously described [40] and used as positive controls. Immunoreactive signals were quantified using ImageJ software (NIH) and normalized to the level of α-tubulin.

9. Surface biotinylation assays:

Surface biotinylation assays were performed as previously described [42] with slight modifications. Briefly, stably transfected cells were grown in tissue culture plates and membrane proteins biotinylated using the Cell Surface Labeling Accessory Pack (Thermo Scientific) following the manufacturer's instructions. All samples were loaded on a 10% SDS-PAGE gel and processed as described above.

10. Seizure induction in Scn1b$^{+/-}$ and Scn1b$^{+/+}$ mice:

Pentylenetetrazole (PTZ, Sigma) was diluted in sodium chloride physiological solution (Fluka, Sigma) at room temperature. P18-P21 *Scn1b$^{+/-}$* and *Scn1b$^{+/+}$* littermate mice were injected IP at doses between 0 and 80 mg/kg. Mice were observed for seizures in a large-sized cage that allowed exploration, with soft bedding, for 45 min, during which seizures were classified according to the Modified Racine scale [16, 51, 52,

68, 72]. Following the experiment all animals were euthanized with an overdose of IP sodium pentobarbital (Ovation Pharmaceuticals) followed by removal of vital organs.

11. Hippocampal slice recordings:

Acute brain slices were prepared from P17-19 *Scn1b*$^{+/+}$ and *Scn1b*$^{-/-}$ littermate mice. Brains were dissected and immersed in ice-cold dissection solution (in mM; 10 D-glucose, 4 KCl, 26 $NaHCO_3$, 234 sucrose, 2.5 $MgCl_2$, 1.3 $CaCl_2$) within 30 s. Each brain was then submerged in a chamber filled with ice-cold dissection solution and connected to a vibrating tissue slicer (Oxford vibratome sectioning system) for preparation of coronal hippocampal slices (400 μm thick). Slices were transferred to an incubation chamber containing circulating artificial cerebral spinal fluid (ACSF; in mM, 119 NaCl, 2.5 KCl, 1 NaH_2PO_4, 11 glucose, 26 $NaHCO_3$, 2.5 $MgCl_2$, 1.3 $CaCl_2$) saturated with 5% CO_2 and 95% O_2 mix and held at 35^o C for 1h. The slices were allowed to return to room temperature (22-24^{o}C) following the incubation period. Slices were then transferred to a recording chamber and continuously superfused with 30^{o}C ACSF. All recordings were made 1-5 hours after slicing. Patch pipettes were pulled from borosilicate glass using a Flaming/Brown Micropipette puller. Whole-cell recordings from randomly chosen neurons were carried out with a Multiclamp 700B amplifier (Axon Instruments). Patch pipettes (4-8MΩ) were filled with an internal solution (in mM; 115 K-gluconate, 20 KCl, 10 HEPES, 2 $MgCl_2$, 4 Na_2-ATP, 3 Na_3-GTP, pH = 7.26, 290 mOsM). For current-clamp, changes in membrane potential were recorded in CA1 and CA3 neurons after injecting currents ranging from -100 pA to 280 pA in 20 pA intervals. Resting membrane potentials and action potential (AP) properties were then analyzed using ClampFit 8.2. The initial AP generated in each experiment was analyzed as follows: Cell resting membrane potential was recorded as the average resting membrane potential of all traces. Internal resistance was calculated using V=IR, where V was the change in voltage from resting membrane potential to maximal negative voltage produced by the

fist injected current of -100 pA. AP threshold was calculated at the onset of the AP. AP rise time was calculated as the change in time from the onset of the AP to the maximal voltage reached. AP amplitude was calculated as the change in voltage from the threshold voltage to the maximal voltage reached. Half-decay time was measured as the time required for the AP to decay to ½ of its maximal voltage. Finally, the maximum rates of depolarization and repolarization were measured from the AP differentiated waveform.

12. Sodium current recordings and β1 immunocytochemistry in acutely dissociated CA3 hippocampal neurons:

Acutely dissociated CA3 neurons were prepared from P10-P14 *Scn1b*$^{-/-}$ and *Scn1b*$^{+/+}$ littermate mice. Brains were rapidly dissected and immersed in ice-cold high sucrose solution (in mM; 250 sucrose, 11 D-glucose, 0.5 KCl, 1 NaH_2PO_4, 2 $MgSO_4$, 2 $CaCl_2$) saturated with O_2, for 2 min. The brain was submerged in a chamber filled with ice-cold high sucrose solution and connected to a vibratome tissue slicer (World Precision instruments) to generate coronal hippocampal slices (300-350 μm thick). Slices were then transferred to a dish containing cold Na-isethionate solution (in mM; 140 Na-isethionate, 23 glucose, 15 Hepes, 2 KCl, 4 $MgCl_2$, 0.1 $CaCl_2$) and the CA3 region was isolated. CA3 areas were transferred to a chamber containing bicarbonate buffered holding solution (in mM; 126 NaCl, 2.5 KCl, 1.25 NaH_2PO_4, 10 glucose, 26 $NaHCO_3$, 2 $MgCl_2$, 2 $CaCl_2$, 1 pyruvic acid, 0.2 ascorbic acid, 0.1 N-nitro-L-arginine, 1 kynurenic acid) saturated with 5% CO_2 and 95% O_2 mix and held at room temperature (21-22 ^{o}C) for 1-6 h. To dissociate neurons, 2-3 CA3 slices were incubated in Hank's balanced salt solution (HBSS, Gibco) supplemented with 20 mM ascorbic acid, 0.2 mM ascorbic acid and 1.25 mg/ml of protease type XIV (Sigma) saturated with O_2 for 20 min. The HBSS solution was removed and the slices were rinsed 3 times using cold Na-

isethionate solution. After the final rinse, 300 µl of this solution was left to triturate the tissue using silicon coated Pasteur pipettes with progressively smaller tip sizes.

After mechanical dissociation, 100-150 µL of cellular suspension were transferred to a dry glass coverslip. For sodium current recordings the coverslip was placed inside of the recording chamber. After 5-10 min the Na-isethionate solution was replaced by extracellular solution, (in mM; 20 NaCl, 1 $BaCl_2$, 2 $MgCl_2$, 55 CsCl, 1 $CdCl_2$, 1 $CaCl_2$, 10 HEPES, 20 TEA-Cl and 100 glucose, pH 7.35 with CsOH). Voltage clamp recordings were performed in the standard whole-cell configuration, using similar conditions to those described by [35] using an Axopatch 200B voltage-clamp amplifier (Axon Instruments). Isolated sodium currents were recorded from single neurons (bipolar or pyramidal, as assessed by morphology) at 21° C. Fire-polished patch pipettes were generated from borosilicate glass capillaries (Warner Instrument Corp.) using a Sutter P-87 puller (Sutter Instrument Co.) and were filled with internal solution (in mM; 1 NaCl, 150 N-methyl-D-glucamine, 10 EGTA, 1 $CaCl_2$, 2 $MgCl_2$, 2 Na_2ATP, 0.05 GTP, 10 HEPES, and 5 glucose, pH 7.3 with CsOH). All recordings were performed within 10-60 min following plating of cells on the coverslip.

For immunocytochemistry, dissociated neurons were transferred to BD BioCoat coverslips that were pretreated with poly-D-lysine and laminin (BD Biosciences). After allowing the neurons to rest on the coverslip for 20 min the neurons were fixed with 4% paraformaldehyde for an additional 20 min. After three washes with PBS, the coverslips were incubated in block solution (5% non-fat dry milk, 1% bovine serum albumin fraction V, 0.025% Triton-X100 from Sigma, in PBS) for 1 h. Incubation overnight at 4°C with primary antibody (anti- $\beta1_{intra}$ at a 1:500 dilution in block solution) was followed by three washes with block solution and 1 h incubation at room temperature with secondary antibody (Alexa Fluor anti-rabbit 568, 1:500 dilution). After three additional washes with block solution and PBS each the coverslips were incubated for 5 min at room temperature with DAPI. Following a final wash with water for 20 min the coverslips were

mounted on glass slides using Gel/Mount (Biomeda Corp.) and placed at 4°C. Samples were viewed using a Fluoview 500 confocal laser-scanning microscope (Olympus) with 100x objective. Images (1024 x 1024 pixels) were acquired with the Olympus Optical Fluoview software, and then exported into ImageJ.

13. Statistical analyses:

Data were tested for normality using the Kolmogorov-Smirnov test, and for homogeneity of variances using the Levene test. Continuous variables with normal distribution were compared using two-tailed Student's *t*-test or ANOVA. If homogeneity of variance existed, Tukey's was selected as the *post-hoc* test, otherwise Tamhane's T2 was used. Discrete variables and continuous variables not normally distributed were compared using the Mann-Withney U test or Kruskal-Wallis H. Statistical significance was set at a $p < 0.05$. The version 13.0 for Windows of SPSS (SPSS Inc.) was used for all determinations of statistical significance.

Results

1. Clinical evaluation:

This male patient was a dizygotic twin born after cesarean section at 39 weeks of gestation following a normal, uncomplicated pregnancy. His parents are first cousins of Moroccan origin. Both parents and his brother are healthy with no reported seizures. A history of epilepsy during adolescence was reported in a maternal aunt. At age 3 months, the patient developed generalized tonic-clonic seizures after vaccination. During a subsequent hospitalization he experienced a second generalized seizure. Treatment with valproic acid was started. MRI was normal and EEG showed rolandic discharges. Five days after a new hospital admission, the patient developed fever-associated convulsions that occurred at a frequency of 2-3/week. During the following month, he experienced several generalized myoclonias each day that were often associated with fever. Valproic acid doses were increased and clobazam was added to the treatment

without a clear reduction in seizure frequency. From the age of 5 months the patient was repeatedly hospitalized for persistent myoclonias during episodes of infections. His mother reported a deterioration of psychomotor abilities. Myoclonias remained refractory to treatment with valproic acid, clonazepam, clobazam and phenytoin. Clinical examination at the age of 13 months revealed a tetrapyramidal syndrome with pronounced global hypotonia. The patient died three weeks later due to respiratory insufficiency secondary to an aspiration pneumonia.

2. Genetic analyses:

Mutation analysis for *SCN1A* was performed as described elsewhere [15]. No mutations in *SCN1A* were identified. The 6 coding exons of *SCN1B* were analyzed next. All single nucleotide polymorphisms located in the amplicons of *SCN1B* were observed homozygously, and a novel homozygous mutation was identified in exon 3 (c.373C>T), predicting a missense mutation of a highly conserved arginine residue (R) at position 125 to cysteine (C) (**Figure II.2.A** and **B**). p.R125 is located in the β1 extracellular immunoglobulin domain, 4 amino acids downstream from the previously identified p.C121W GEFS+1 mutation (**Figure II.2.C**) [65]. Both parents were found to be heterozygous carriers of the mutation, which was not observed in the 92 control individuals tested. Genotyping of 4 STR markers in a 5 Mb region surrounding *SCN1B* revealed a common haplotype in both parents that was transmitted to the child (**Figure II.2.D**). These data confirm that both mutated alleles from the child originated from the same ancestral haplotype, consistent with the consanguinity of the parents.

3. Electrophysiological characterization of p.R125C in mammalian cell lines:

Previous mutations of *SCN1B* reported in epileptic patients have shown abnormalities in β1-mediated channel gating properties when assayed in heterologous expression systems [42, 65, 70]. In the following series of experiments, we assessed the

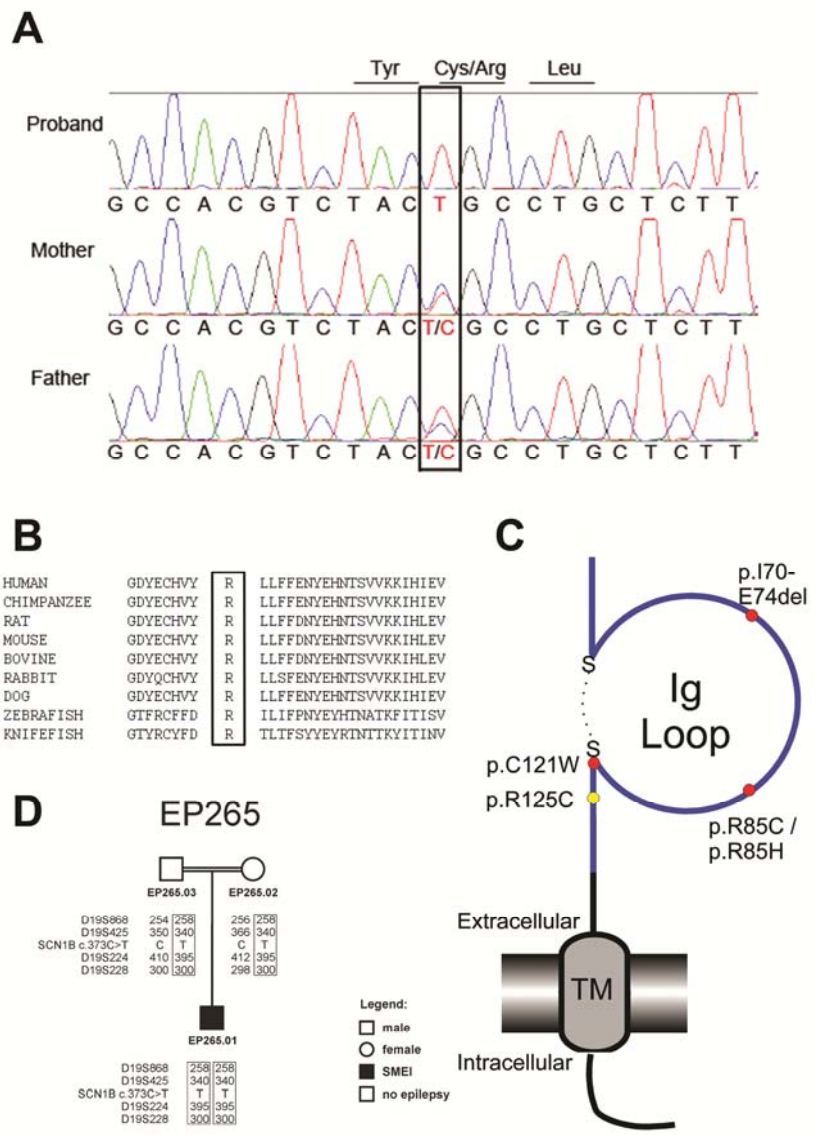

Figure II.2. *SCN1B* homozygous mutation found in Dravet Syndrome.
(**A**) Chromatogram showing the c.373C>T homozygous mutation in the *SCN1B* exon 3 amplicon in the proband (upper lane), whereas both parents are heterozygous (lower two lanes) for the mutation. The mutation results in a change of arginine (R) at position 125 to cysteine (C) in the amino acid sequence. (**B**) Alignment of the corresponding region of the sodium channel β1 subunit amino acid sequence across multiple species showing the high conservation of p.R125. (**C**) Topology of the sodium channel β1 subunit. The extracellular domain contains an immunoglobulin (Ig) loop bound by a disulfide bridge (S--S). A mutation in the distal cysteine of the disulfide bridge (p.C121, red circle) has been reported in families with GEFS+. The amino acid position of the mutation found in the proband (p.R125C) is marked by the yellow circle. Domains shared by both splice variants, β1 and β1B, are shown in blue and include only the extracellular region. β1B contains a novel domain encoded by a retained intron. The transmembrane domain (TM) of β1 is followed by a short intracellular domain. (**D**) The genotyping of 4 STR markers around the *SCN1B* site confirm the ancestral haplotype.

effect of the p.R125C β1 mutant subunit on currents expressed by $Na_v1.1$ and $Na_v1.2$ using the whole-cell patch clamp technique in transfected mammalian cells.

To examine the effects of p.R125C on sodium currents expressed by $Na_v1.1$ we transiently transfected HEK-293 cells that stably express rat $Na_v1.1$ (HEKr$Na_v1.1$) with wildtype human β1 (β1WT) or p.R125C cDNA as described in Methods. The rat $Na_v1.1$ sequence (NP_110502.1, P04774) exhibits a 98.16% amino acid identity with human $Na_v1.1$ (NP_008851.3, P35498), predicting that effects of β1 subunits should be similar on channel proteins from both species [56, 61]. We found no significant difference in sodium current density (**Figure II.3.A**), voltage-dependence of activation or inactivation (**Figure II.3.B** and **C**), kinetics of inactivation or recovery from inactivation (**Figure II.3.D**, **Table II.1**) between cells expressing β1WT (NP_001028.1, Q07699) and those transfected with the p.R125C mutant. However, we also found no significant differences between cells expressing $Na_v1.1$ alone compared to cells co-expressing β1WT subunits, in agreement with previously reported findings [12, 39, 53]. Similar results were obtained when we used HEK cells stably expressing human $Na_v1.1$ in place of the rat clone (data not shown). An effect of β1WT on the kinetics of current inactivation of $Na_v1.1$ has been previously reported [1]. In agreement with that study, we found a statistically significant difference in the rate of inactivation comparing cells expressing $Na_v1.1$ alone with those expressing β1WT using a single exponential for analysis. This difference, however, disappeared when the data were fit with two exponentials (**Table II.1**). Using two exponentials there was also no difference between the cells expressing β1WT compared with those expressing p.R125C.

As an alternative, we tested the p.R125C mutant in SNaIIa cells. We have published a number of papers using this cell line [30, 41, 42], Chinese hamster lung 1610 fibroblasts that stably expresses rat $Na_v1.2$ [67] (NP_036779.1, P04775). Previous studies have demonstrated multiple significant effects of β1 co-expression with $Na_v1.2$ in this heterologous system [30]. Stable transfection of SNaIIa cells with β1WT or p.R125C

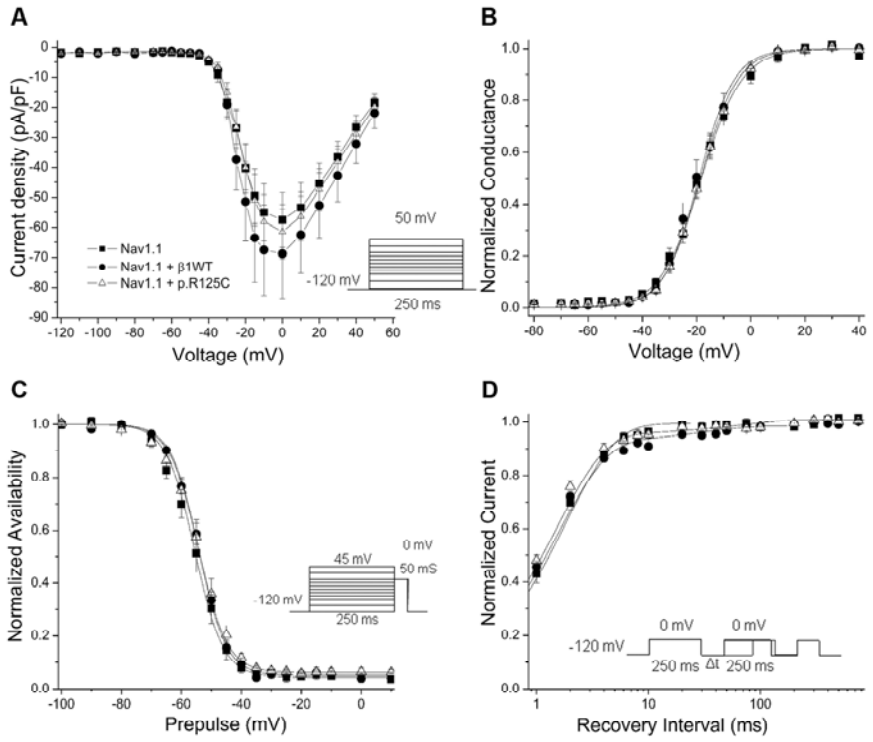

Figure II.3. p.R125C and β1WT have no effect on the properties of sodium current in HEKrNa$_v$1.1 cells. Cells stably expressing rat Na$_v$1.1 in a HEK-293 background (HEKrNa$_v$1.1) were transiently co-transfected with GFP and either β1WT (filled circles) or p.R125C (open triangles). HEKrNa$_v$1.1 cells transfected only with EGFP (filled squares) were used as negative controls. Whole-cell patch-clamp recordings of sodium currents were performed as described in Methods. (**A**) Sodium current density is unchanged in the presence and absence of β1 subunits, as is (**B**) the voltage-dependence of activation. (**C**) A similar lack of effect from either transfected β1 subunit is observed for the voltage dependence of inactivation and (**D**) recovery from inactivation. Insets depict the protocol scheme. (**A**) and (**B**) were obtained using the same protocol. Data points represent mean ± SEM, solid lines represent fit to the means. Biophysical properties are provided in **Table II.1**.

cDNA was performed as described in Methods. Whole-cell patch-clamp analysis revealed expected changes in sodium current density (**Figure II.4.A**), voltage-dependence of activation and inactivation (**Figure II.4.B** and **C**), kinetics of steady-state inactivation and recovery from inactivation (**Figure II.4.D** and **Table II.2**), persistent current (**Table II.2**), and frequency dependence at 80 Hz for β1WT (**Figure II.4.E**) [30, 42]. In contrast, cells transfected with p.R125C yielded results that were indistinguishable from untransfected SNaIIa cells (**Figure II.4.A** - **E**), suggesting a lack of

Table II.1: Biophysical parameters of sodium current in HEKrNa$_v$1.1 cells compared with HEKrNa$_v$1.1 cells co-expressing β1WT or p.R125C.

	HEKrNa$_v$1.1	**HEKrNa$_v$1.1 + β1WT**	**HEKrNa$_v$1.1 + p.R125C**
Voltage-dependence of activation			
$V_{1/2}$ (mV)	-18.27 (±1.53)	-19.09 (±1.79)	-18.49 (±0.92)
k	-7.54 (±0.35)	-6.52 (±0.54)	-6.87 (±0.26)
n	12	9	11
Voltage-dependence of inactivation			
$V_{1/2}$ (mV)	-55.52 (±1.32)	-54.18 (±0.77)	-54.30 (±1.47)
k	4.73 (±0.22)	4.59 (±0.13)	4.79 (±0.21)
C	0.04 (±0.01)	0.05 (±0.01)	0.60 (±0.01)
n	11	9	11
Kinetics of inactivation, one exponential			
τ_{slow} (ms)	0.63 (±0.06)	0.42 (±0.03)^A	0.59 (±0.03)
n	11	8	10
Kinetics of inactivation, two exponentials			
τ_{slow} (ms)	25.07 (±12.99)	6.95 (±3.18)	16.10 (±8.68)
Amplitude$_{slow}$ (%)	7.72 (±1.65)	4.43 (±2.35)	5.20 (±4.84)
τ_{fast} (ms)	0.48 (±0.05)	0.34 (±0.01)	0.46 (±0.02)
Amplitude$_{fast}$ (%)	92.27 (±1.65)	95.56 (±2.35)	94.79 (±1.45)
N	11	8	10

Data are mean ± SEM. ^{A} $p < 0.05$ compared to Na$_v$1.1.

functional expression of this mutant β1 subunit. We next attempted to express human Na$_v$1.1 cDNA in 1610 cells to analyze the effect of β1 and p.R125C on Na$_v$1.1 channels in this background. Unfortunately, numerous experiments using three different transfection methods/reagents resulted in no measurable sodium currents.

4. Cell surface expression of β1WT vs. p.R125C:

To investigate the mechanism underlying the inability of p.R125C β1 to modulate sodium currents, we evaluated the level of total expression vs. cell surface expression of p.R125C and β1WT subunit polypeptides. Experiments were performed in 1610 cells as well as in HEKrNa$_v$1.1 cells that were stably transfected with β1WT or p.R125C. To be able to confirm our results using two different antibodies, we engineered a V5-His

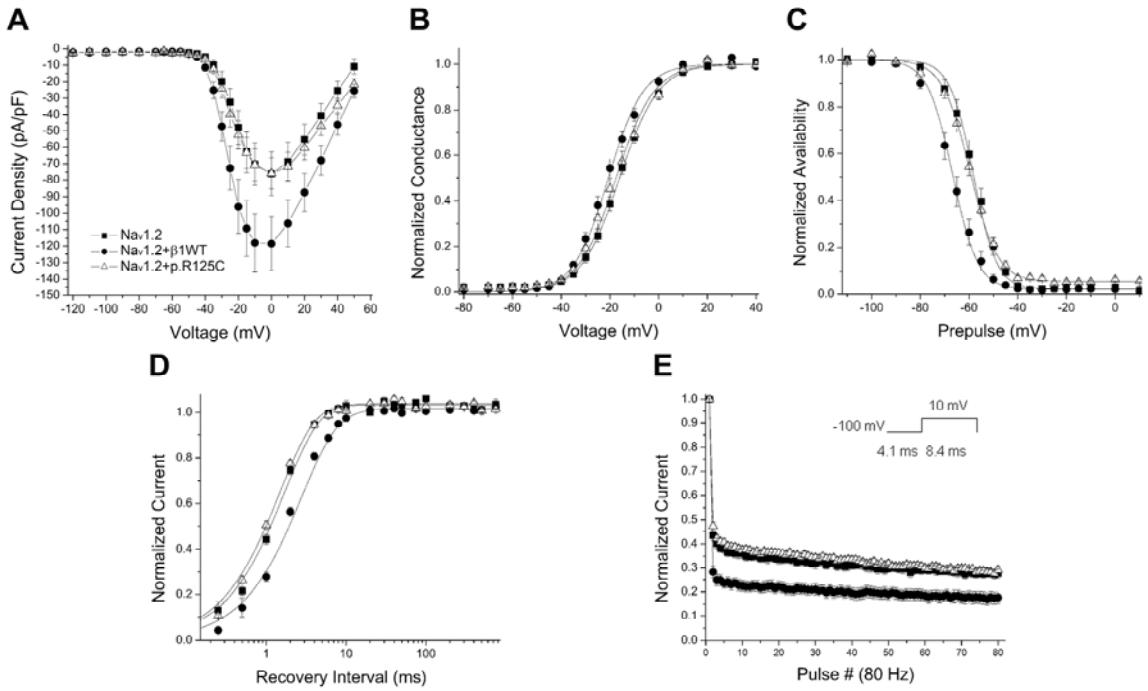

Figure II.4. p.R125C does not modulate sodium current expressed by $Na_v1.2$ in SNalla cells. SNalla cells were stably transfected with either β1WT (filled circles) or p.R125C (open triangles) and used for whole-cell patch clamp experiments as described in Methods. Untransfected cells (filled squares) were used as negative controls. β1WT (**A**) increased the current density, (**B**) negatively shifted the voltage-dependence of activation and (**C**) inactivation, (**D**) slowed the recovery from inactivation, and (**E**) reduced the availability of sodium channels under high frequency stimulation (inset shows the protocol scheme) compared to cells expressing α alone. In contrast, p.R125C did not modulate sodium current properties. Protocols for (**A**), (**B**), (**C**) and (**D**) are the same as in **Figure II.3**. Biophysical properties can be found in **Table II.2**.

epitope tag on the carboxyl-termini of β1WT and p.R125C, respectively, as described in Methods, and used these constructs to generate additional stable cell lines in 1610 and HEKrNa$_v$1.1 cells. Western blots were probed with anti-V5 antibody, as shown in **Figure II.5**, and these results were confirmed with anti-β1$_{intra}$ antibody (not shown). Similar results were obtained in cell lines expressing untagged β1 subunits with Western blots probed with anti-β1$_{intra}$ (not shown). Comparison of total cellular protein levels of β1 subunits in either 1610 cells (**Figure II.5.A**) or HEKrNa$_v$1.1 cells (not shown) showed that the p.R125C mutant was expressed at a level comparable to that of the β1WT

Table II.2: Biophysical parameters of sodium current in SNaIIa cells compared with SNaIIa cells coexpressing β1WT or p.R125C.

	SNaIIa	SNaIIa + β1WT	SNaIIa + p.R125C
Voltage-dependence of activation			
$V_{1/2}$ (mV)	-16.04 (±1.02)	-20.63 (±1.22)	-17.50 (±1.50)
k	-7.92 (±0.46)	-7.15 (±0.22)	-7.79 (±0.38)
n	17	15	18
Voltage-dependence of inactivation			
$V_{1/2}$ (mV)	-58.26 (±1.49)	-66.72 (±1.47)[A]	-59.66 (±1.05)[B]
k	4.76 (±0.12)	5.11 (±0.08)	5.59 (±0.17)
C	0.02 (±0.01)	0.02 (±0.01)	0.05 (±0.00)
n	13	14	16
Kinetics of inactivation			
τ_{slow} (ms)	4.82 (±0.75)	6.26 (±1.20)	4.71 (±1.60)
$Amplitude_{slow}$ (%)	6.41 (±0.99)	0.04 (±0.00)[C]	10.62 (±1.60)[D]
τ_{fast} (ms)	0.57 (±0.02)	0.49 (±0.04)	0.56 (±0.33)
$Amplitude_{fast}$ (%)	93.58 (±0.99)	97.15 (±0.01)[C]	89.37 (±1.60)[D]
n	12	14	10
Persistent current			
% of peak current	2.70 (±0.70)	0.00 (±0.00)[A]	1.88 (±0.41)[B]
n	12	13	14

Data are mean ± SEM. [A] $p < 0.005$ compared to $Na_v1.2$. [B] $p < 0.005$ compared to β1WT. [C] $p < 0.001$ compared to $Na_v1.2$. [D] $p < 0.001$ compared to β1WT.

subunit. The average expression levels of multiple cell clones of both 1610 and HEKrNa$_v$1.1 cells relative to α-tubulin expression were compared by densitometry. There were no significant differences in the levels of total protein expression between wildtype (0.91 arbitrary units ± 0.11, n = 9) and mutant β1 subunits (0.61 arbitrary units ± 0.25, n = 12) in all of the cell lines tested ($p = 0.293$, Student's *t*-test). In contrast, in all cell lines tested, we observed that p.R125C was poorly expressed at the cell surface compared with β1WT, both in the presence and absence of α subunits. **Figure II.5.B** shows results of surface biotinylation for one HEKrNa$_v$1.1 clone expressing β1WT, two different HEKrNa$_v$1.1 clones expressing p.R125C (samples 1 and 2), and three different 1610 clones expressing p.R125C (samples 3 - 5). The p.R125C-expressing cell lines showed barely detectable (sample 3) or no detectable (samples 1, 2, 4, and 5) levels of cell surface expression in spite of robust intracellular expression. For comparison,

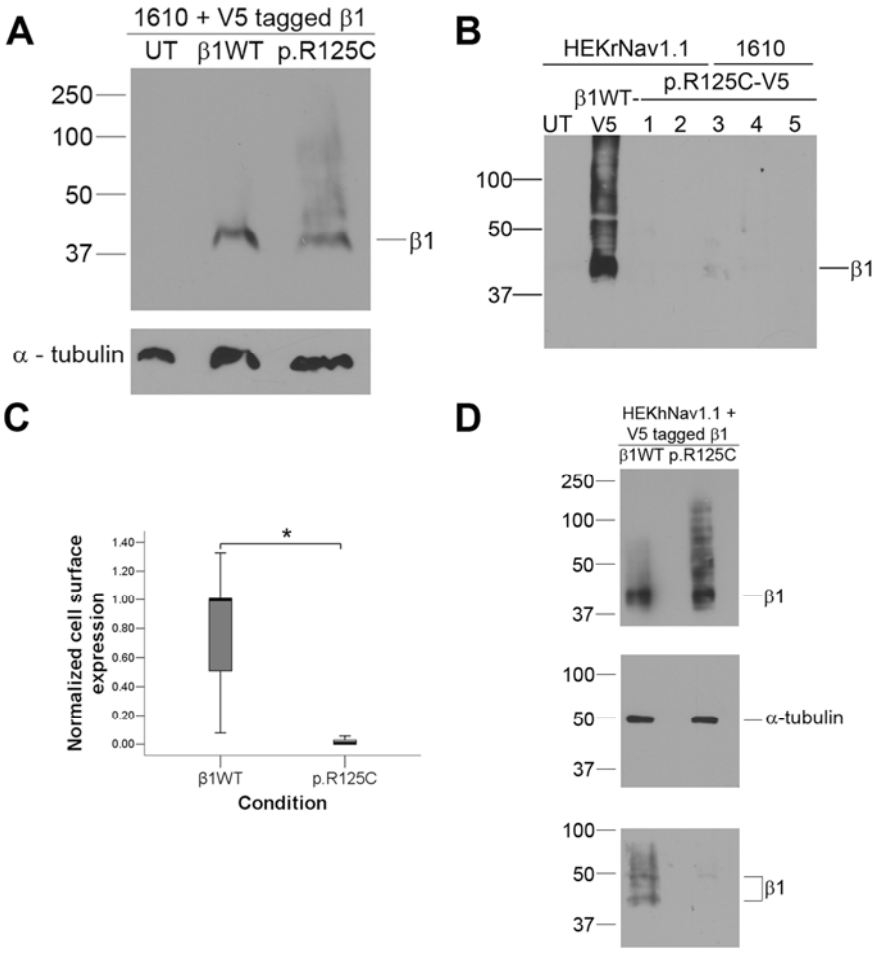

Figure II.5. p.R125C is poorly expressed at the cell surface at physiological temperatures.

(**A**) Comparison of total cellular expression of β1WT vs. p.R125C in 1610 cells. Representative Western blot of 1610 cells stably transfected with V5-tagged p.R125C (lane 3), demonstrating that the expression of the mutant protein is comparable to β1WT (lane 2). Untransfected cells (UT, lane 1) were used as a negative control. Re-probing the blot with anti-α-tubulin confirmed the presence of protein in all lanes. (**B**) Cell surface expression of β1WT vs. p.R125C. HEKrNa$_v$1.1 or 1610 cells stably transfected with V5-tagged β1WT or p.R125C were surface biotinylated, and the biotinylated proteins probed as described in Methods. Untransfected cells show no anti-V5 immunoreactivity (UT, lane 1). Cells transfected with β1WT show robust cell surface expression (lane 2). Faint or no cell surface expression was detected in multiple clones of cells transfected with the mutant p.R125C (HEKrNa$_v$1.1 cells: samples 1 and 2; 1610 cells: samples 3 - 5). For comparison, sample 4 is the same cell line used to detect total cellular expression in (**A**), p.R125C. (**C**) Box plots of band intensities measured using ImageJ for clones of HEKrNa$_v$1.1 and 1610 cells transfected with β1WT and p.R125C and processed to detect surface biotinylated proteins as described in Methods. We calculated a significant difference ($p < 10^{-6}$ Mann-Whitney U-test) between the level of cell surface expression of β1WT (n = 18 experiments) compared to p.R125C (n = 15 experiments). (**D**) p.R125C is poorly expressed at the cell surface in the presence of human Na$_v$1.1. Upper panel: Comparison of total cellular expression of β1WT vs. p.R125C in HEKhNa$_v$1.1 cells. Representative Western blot of HEKhNa$_v$1.1 cells stably transfected with V5-tagged

p.R125C (lane 2), demonstrating that the expression of the mutant protein is comparable to β1WT (lane 1). Center panel: Re-probing the blot with anti-α-tubulin confirmed equal loading of protein in both lanes. Lower panel: Cell surface expression of β1WT vs. p.R125C. HEKhNa$_v$1.1 transiently transfected with V5-tagged β1WT or p.R125C were surface biotinylated, and the biotinylated proteins probed as described in Methods. Cells transfected with β1WT show robust cell surface expression (lane 1). Faint or no cell surface expression was detected in cells transfected with the mutant p.R125C (lane 2). The blot is representative of triplicate experimental repeats. Molecular weight markers are in KDa.

sample 4 in **Figure II.5.B** is the same cell line used to demonstrate total cellular expression of the mutant subunit in **Figure II.5.A**, lane labeled "p.R125C."

Quantification of Western blot analyses of many biotinylated cell clones (in both 1610 cells and HEKrNa$_v$1.1 cells) by densitometry using ImageJ software showed that, on average, p.R125C cell surface expression was 6.7% of β1WT levels (**Figure II.5.C**; β1WT n = 18 cell clones, p.R125C n = 15 cell clones). To determine whether the cell surface expression of p.R125C was dependent on the presence of a human, rather than a rat, α subunit, we repeated the cell lysate and surface biotinylation experiments using the HEKhNa$_v$1.1 cell line. As shown in **Figure II.5.D**, both β1WT and p.R125C were expressed at comparable levels in whole cell lysates. In contrast and similar to results obtained in the HEKrNav1.1 line, only β1WT was detectable at the cell surface.

Many disease mutations have been shown to act through mechanisms involving trafficking deficiency to the cell surface (reviewed in [25]). Some of these mutants, including sodium channel α subunit mutations associated with GEFS+ and long QT syndrome [53, 60], can be rescued *in vitro* by incubation of cells at nonphysiological temperatures. To investigate whether a similar mechanism occurs with p.R125C, we grew a selected clone of V5-tagged p.R125C stably transfected 1610 cells in a humidified CO_2 incubator at 27ºC for 48 h. This same p.R125C cell clone had no detectable cell surface expression at 37^{o}C as assessed by surface biotinylation (**Figure II.6**, "37^{o}C" lane). Surface biotinylation followed by Western blot analysis of this same cell line grown at 27ºC demonstrated that p.R125C was expressed at the cell surface

following the low temperature incubation, suggesting that this mutant is trafficking deficient (**Figure II.6**, "27°C" lane).

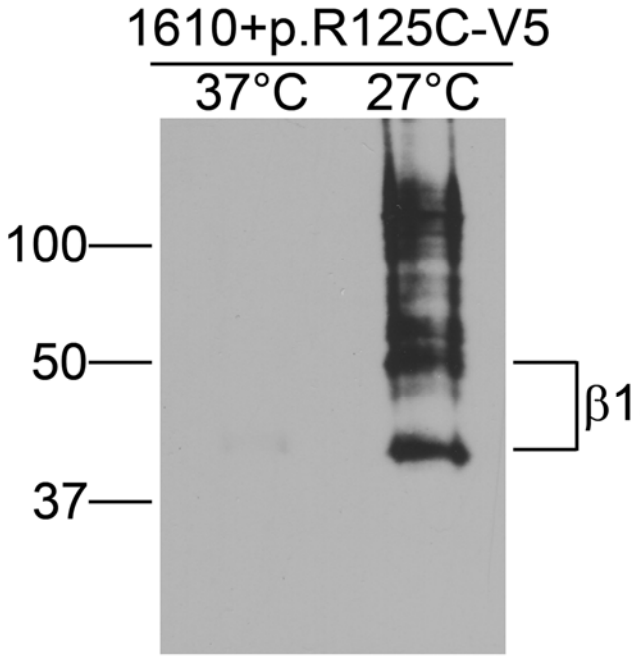

Figure II.6. Cell surface expression of p.R125C is rescued at low temperature. 1610 cells stably transfected with V5-tagged p.R125C were incubated at 37ºC or 27ºC for 48 h and then surface biotinylated as described in Methods. The resulting Western blot was probed with anti-V5 antibody. Incubation at 27ºC rescued the cell surface expression of p.R125C, resulting in the presence of β1 immunoreactive bands at 40 kDa and higher, likely representing various levels of avidin attachment, whereas no band is detectable for the cells incubated at 37 ºC. Molecular weight markers are in KDa.

5. Sodium current modulation by p.R125C in Xenopus oocytes:

We observed that the p.R125C mutant β1 subunit is expressed at significantly lower levels at the cell surface of mammalian cells grown at physiological temperatures compared with wildtype, and that this low level of surface expression is insufficient to modulate whole cell sodium currents. To determine whether p.R125C β1 would be capable of current modulation if it did reach the cell surface, we co-expressed wildtype or mutant β1 subunits with sodium channel α subunits in *Xenopus* oocytes. This model system has the advantages of expressing high levels of sodium channel α and β subunit

proteins (e.g. [22]) as well as growth under low temperature conditions [55] that, in our hands, promote p.R125C cell surface expression. We demonstrated previously that another GEFS+1 mutant, p.C121W β1, is robustly expressed in oocytes, where it modulates sodium currents similar to wildtype β1 in spite of a significant loss of functional modulation of current in mammalian cells grown at 37^{o}C [42]. We measured sodium currents expressed by rat *Scn2a* (encoding $Na_v1.2$) cRNA injected alone or currents expressed by the α subunit co-injected with rat β1WT (NP_058984.1, Q00954, 96.33% amino acid identity with human β1) or p.R125C using the two-electrode voltage clamp technique (**Figure II.7**). We observed that the effects of p.R125C β1 on sodium current expressed by *Scn2a* (**Figure II.7.A** - **C**) were indistinguishable from β1WT. To determine whether a lower level of p.R125C expression would result in the loss of current modulation by this mutant subunit in oocytes, we diluted the p.R125C mRNA stock 50-fold prior to injection. In contrast to previous results with p.C121W β1 [42], we observed no reduction in $Na_v1.2$ current modulation by p.R125C under these conditions (**Figure II.7.A** - **C**). Taken together, these data suggest that even though p.R125C is inefficiently expressed at the cell surface at physiological temperatures in mammalian cells, if this trafficking defect could be overcome, the mutant subunit would be fully capable of modulating sodium current.

6. Seizure susceptibility of mice expressing a single wild-type Scn1b allele:

Scn1b$^{-/-}$ mice have been described previously by our lab [14]. These mice are born normally but then exhibit spontaneous generalized seizures beginning in the second postnatal week, and exhibit other neurological abnormalities including ataxia, characteristics that are similar to Dravet syndrome patients. *Scn1b*$^{-/-}$ mice die in adolescence by postnatal day 21 (P21), recapitulating the small proportion of Dravet syndrome patients that die as a consequence of the disease. In contrast, *Scn1b*$^{+/-}$ mice

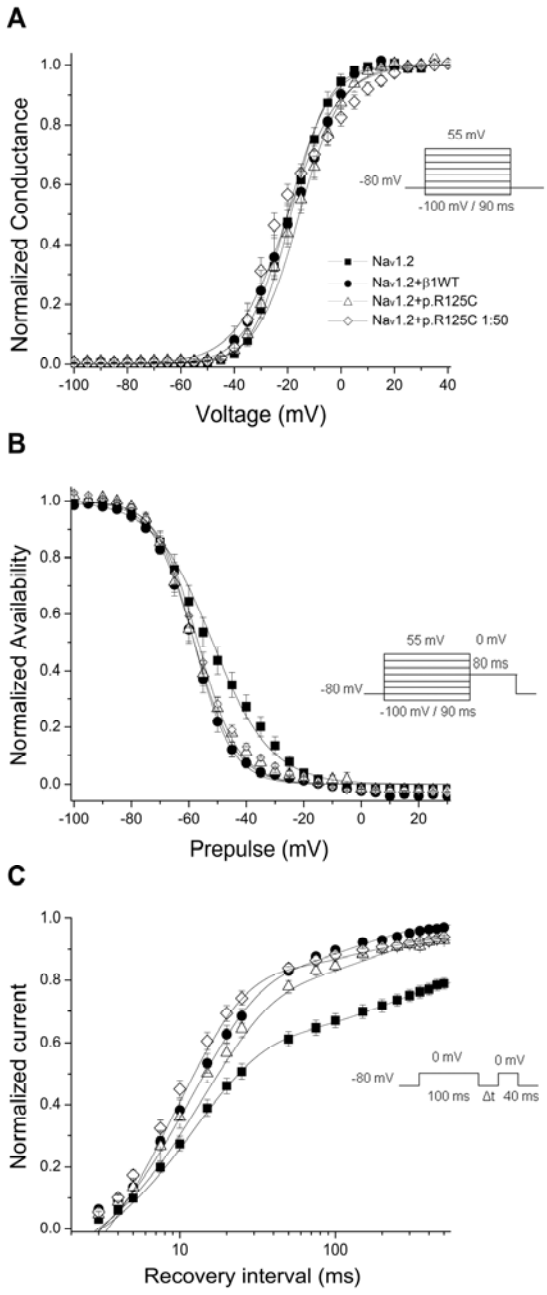

Figure II.7. p.R125C modulates sodium currents expressed by $Na_v1.2$ in *Xenopus* oocytes *Xenopus laevis* oocytes were injected with the cRNA encoding $Na_v1.2$, either alone (filled squares), with β1WT (filled circles), or with p.R125C (open triangles). The p.R125C mRNA was also diluted 1:50 before injection (open diamonds). Neither β1WT nor p.R125C had any measurable effect on the voltage dependence of activation of $Na_v1.2$. (**A**). p.R125C modulates the voltage-dependence of inactivation (**B**), and rate of recovery from inactivation (**C**) of $Na_v1.2$ currents similar to β1WT. Insets show protocol schemes. Data points represent mean ± SEM. Solid lines represent fits to the means. Biophysical properties are provided in **Table II.3**.

Table II.3: Biophysical parameters of sodium currents expressed by $Na_v1.2$ alone or $Na_v1.2$ coexpressed with β1WT or R125C in *Xenopus* oocytes.

	$Na_v1.2$	$Na_v1.2$ + β1WT	$Na_v1.2$ + p.R125C
Voltage-dependence of activation			
$V_{1/2}$ (mV)	-18.81 (±1.38)	-20.06 (±3.08)	-16.81 (±1.29)
k	-6.88 (±0.31)	-7.8 (±0.18)	-8.59 (±0.51)
n	10	7	13
Voltage-dependence of inactivation			
$V_{1/2}$ (mV)	-51.69 (±2.60)	-58.11 (±1.33)	-58.17 (±1.41)
k	10.12 (±0.31)	7.18 (±0.49)[A]	6.61 (±0.28)[A]
C	-0.01 (±0.00)	-0.02 (±0.00)	0.01 (±0.01)
n	10	9	14
Kinetics of inactivation			
τ_{slow} (ms)	7.41 (±0.68)	5.10 (±0.50)	6.05 (±0.72)
$Amplitude_{slow}$ (%)	46.42 (±3.09)	10.10 (±1.29)[A]	20.71 (±1.44)[A]
τ_{fast} (ms)	1.43 (±0.31)	0.49 (±0.04)[A]	0.68 (±0.05)[A]
$Amplitude_{fast}$ (%)	53.57 (±3.1)	89.89 (±2)[A]	79.28 (±2.11)[A]
n	10	6	9

Data are mean ± SEM. [A] $p \leq 0.001$ compared to $Na_v1.2$.

do not exhibit spontaneous behavioral seizures and live normal life spans, suggesting that the presence of a single wildtype *Scn1b* allele is sufficient for normal sodium current modulation by β1 *in vivo*. We demonstrate above that a *SCN1B* Dravet syndrome mutant, p.R125C, is inefficiently trafficked to the cell surface in transfected mammalian cells at physiological temperatures, resulting in functional *SCN1B* gene inactivation. Unlike previously described GEFS+1 patients carrying a single mutant *SCN1B* allele [54], the patient described in our study is homozygous for the p.R125C mutation. Thus, based on our heterologous expression data, we predict that this Dravet syndrome patient had a functional *SCN1B* null phenotype. Both parents of this patient are heterozygous for the mutation and do not exhibit seizures, similar to *Scn1b*$^{+/-}$ mice [14]. To investigate whether patients carrying one mutant *SCN1B* allele might be more susceptible to seizure induction in response to proconvulsive stimuli, we injected *Scn1b*$^{+/-}$ and *Scn1b*$^{+/+}$ littermates with the GABA antagonist pentylenetetrazole (PTZ) at

age P18-21, the time interval during which the seizures observed in *Scn1b*$^{-/-}$ mice are at their most severe. *Scn1b*$^{+/-}$ and *Scn1b*$^{+/+}$ mice were injected with a single dose of PTZ between 20 to 80 mg/kg, and the resulting seizures were graded according to the Modified Racine scale [16, 52], described in the legend to **Table II.4**. At 20 mg/kg we observed minor changes in the level of activity of mice of both genotypes, whereas at 40 mg/kg a minority of mice from both groups exhibited myoclonic jerks and forelimb clonus. At 60 mg/kg the majority of mice from both groups exhibited seizures between grades 2 and 6. At this dose there were no statistically significant differences in the mean time to myoclonic jerk or seizures of higher severity between *Scn1b*$^{+/-}$ mice and *Scn1b*$^{+/+}$ (**Table II.4**). Also, at 60 mg/kg there were no significant differences in the highest seizure level reached by each genotype (**Table II.4**). At a dose of 80 mg/kg, 85% of *Scn1b*$^{+/+}$ and 90% of *Scn1b*$^{+/-}$ died during status epilepticus. There were no statistical differences in the mean time to death between the two groups (**Table II.4**), or cumulative survival (**Figure II.8**). While not significant, trends in the data suggest that *Scn1b*$^{+/-}$ mice may be even less sensitive to PTZ seizure induction than their wildtype

Table II.4: Seizure parameters in *Scn1b*$^{+/+}$ and *Scn1b*$^{+/-}$ mice.

Parameter	Pentylenetetrazole dose (mg/kg)	*Scn1b*$^{+/+}$	*Scn1b*$^{+/-}$
Time to myoclonic jerk or seizure of higher severity (min)[A]	60	2.52 (±0.31)	5.79 (±1.36)
Highest seizure level[B, C]	60	6 (3.68-6.56)	6 (3.03-6.46)
Time to death (min)	80	4.92 (±1.67)	11.36 (±3.26)
n[D]		8	8

[A] Data are mean ± SEM. [B] Data are median (95% CI). [C] As measured using the Modified Racine Scale: 0 = no seizure, 1 = staring/unresponsive, 2 = focal clonic convulsion (including head nod, twitch, myoclonic jerk, backing), 3 = forelimb clonus (tonic/clonic seizure), 4 = rearing, 5 = loss of posture (including jumping, rearing, and falling), 6 = status epilepticus and death. [D] 8 mice of each genotype used for each dose.

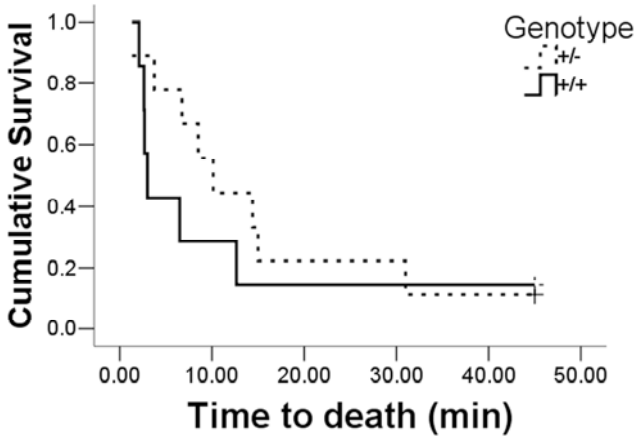

Figure II.8. Time to death due to *status epilepticus* of *Scn1b*$^{+/-}$ mice is similar to *Scn1b*$^{+/+}$ mice. Mice with either one (*Scn1b*$^{+/-}$) or two copies (*Scn1b*$^{+/+}$) of *Scn1b* were injected with pentylenetetrazole (PTZ) to induce seizures. Following a dose of 80 mg/kg the majority of mice died as a consequence of *status epilepticus.* Cumulative survival curves show no significant differences between *Scn1b*$^{+/-}$ mice (broken line, n=8) and *Scn1b*$^{+/+}$ (full line, n=8), p = 0.383, Log-rank test.

littermates. Throughout these experiments, control animals were injected with vehicle alone (0.9 % saline solution); none of these animals exhibited seizures.

7. *Scn1b*$^{-/-}$ *mice show altered electrical excitability in CA3 but not CA1 regions of the hippocampus:*

Hippocampal pyramidal neurons acutely isolated from *Scn1b*$^{-/-}$ mice have normal sodium currents [14]. To explore potential differences in electrical excitability by which a loss of functional expression of β1 may result in seizures, we performed recordings from acutely isolated hippocampal slices, a preparation in which synaptic contacts remain intact. Because *Scn1b*$^{-/-}$ mice exhibit differential expression of $Na_v1.1$ and $Na_v1.3$ in the CA3 but not in the CA1 region of the hippocampus [14], we analyzed APs in both regions. As shown in **Table II.5**, we did not observe significant differences in the excitability of *Scn1b*$^{-/-}$ CA1 neurons compared to wildtype. Measurements included the neuronal resting membrane potential, input resistance, AP threshold, AP rise time, AP peak voltage, and AP amplitude. In contrast, we observed that *Scn1b*$^{-/-}$ CA3 neurons

fired evoked APs with a significantly higher peak voltage and significantly greater amplitude compared to wildtype. The differences in AP rise time for CA3 neurons between the two genotypes approached significance ($p = 0.051$). Thus, the absence of functional β1 subunits is predicted to result in CA3 neuronal hyperexcitability *in vivo*, consistent with the severe seizure phenotype of *Scn1b*$^{-/-}$ mice as well as the severe seizure phenotype of the pediatric patient in this study.

Table II.5. Analysis of evoked action potentials in CA1 or CA3 hippocampal slices from *Scn1b*$^{+/+}$ and *Scn1b*$^{-/-}$ mice.

	***Scn1b*$^{+/+}$**	***Scn1b*$^{-/-}$**
CA1		
Resting potential (mV)	-71.99 (±1.21)	-71.78 (±0.76)
Input resistance (MΩ)	142.60 (±27.68)	141.36 (±11.23)
Threshold (mV)	-33.81 (±2.00)	-33.00 (±1.50)
Rise time (ms)	0.76 (±0.03)	0.67 (±0.03)
Peak voltage (mV)	35.48 (±1.91)	33.73 (±2.16)
Amplitude (mV)	69.29 (±2.90)	66.74 (±2.36)
N	22	19
CA3		
Resting potential (mV)	-72.96 (±0.54)	-71.74 (±0.59)
Input resistance (MΩ)	156.99 (±5.97)	161.75 (±11.06)
Threshold (mV)	-33.82 (±0.75)	-35.73 (±0.78)
Rise time (ms)	0.61 (±0.02)	0.52 (±0.01)
Peak voltage (mV)	38.77 (±1.49)	46.36 (±1.21)^{A}
Amplitude (mV)	72.59 (±1.60)	82.10 (±1.29)^{B}
N	34	21

Data are mean ± SEM. ^{A} $p = 0.001$ compared to *Scn1b*$^{+/+}$. ^{B} $p < 0.001$ compared to *Scn1b*$^{+/+}$.

8. Sodium current density in Scn1b$^{-/-}$ *CA3 bipolar neurons is similar to wildtype:*

Scn1a$^{+/-}$ mice recapitulate the phenotype of Dravet syndrome patients with *SCN1A* mutations. The mechanism of epileptogenesis in *Scn1a*$^{+/-}$ mice includes a substantial reduction in sodium current density of hippocampal bipolar, but not pyramidal, neurons [73]. We showed previously that hippocampal pyramidal neurons acutely isolated from *Scn1b*$^{-/-}$ mice have normal sodium currents compared to their

wildtype littermates [14]. To explore whether the changes in CA3 hyperexcitability observed in hippocampal slice recordings resulted from a similar mechanism as described for *Scn1a*$^{+/-}$ mice, we recorded sodium currents in bipolar neurons. We first documented the expression of β1 subunits in acutely dissociated CA3 bipolar neurons from *Scn1b*$^{+/+}$ mice by staining with anti- $\beta1_{intra}$. All of the bipolar neurons examined were positive for the presence of β1 in the cell body, with the majority of neurons also exhibiting β1 in their processes (**Figure II.9**). We then recorded peak sodium current density elicited in acutely isolated CA3 hippocampal bipolar neurons following a test pulse to -20 mV from a holding potential of -80mV, using the whole-cell patch clamp technique. In contrast to [73], we observed no significant differences in peak sodium current density between genotypes (*Scn1b* $^{-/-}$ mice : -87.24 ± 13.44 nA/pF, n = 17; *Scn1b*$^{+/+}$ littermates: -58.21 ± 9.99 nA/pF, n = 9, $p = 0.159$; Student's *t*-test). Similarly, there were no measurable differences in the capacitance (*Scn1b*$^{-/-}$: 10.73 ± 1.14 pF, n = 17; *Scn1b*$^{+/+}$ littermates: 13.37 ± 1.13 pF, n = 9, $p = 0.152$; Student's *t*-test), the voltage-dependence of activation (*Scn1b*$^{-/-}$:-45.00 ± 2.20 mV, n = 4; *Scn1b*$^{+/+}$ littermates: -42.34 ± 0.46 mV, n = 4, $p = 0.28$; Student's *t*-test), or voltage-dependence of inactivation (*Scn1b*$^{-/-}$: -58.00 ± 1.26 mV, n = 4; *Scn1b*$^{+/+}$ littermates: -61.22 ± 2.28 mV, n = 4, $p = 0.26$; Student's *t*-test) of bipolar cells between the two genotypes. Thus, while the phenotypes of *Scn1a*$^{+/-}$ and *Scn1b*$^{-/-}$ mice are remarkably similar, the mechanisms of epileptogenesis are different in these two models.

Discussion

In the present study we demonstrate for the first time a homozygous loss-of-function mutation in *SCN1B* responsible for Dravet syndrome, an epilepsy syndrome in the most severe range of the GEFS+ spectrum. *SCN1B* p.R125C results in β1 subunit polypeptides that are synthesized normally but not transported to the cell surface in mammalian fibroblasts *in vitro*. Because the patient in our study carried two mutant

SCN1B alleles, our data predict a complete loss of β1 function, resulting in a null phenotype. Trafficking of p.R125C is rescued at non-physiological temperatures in mammalian cells and p.R125C exhibits normal channel modulation in *Xenopus* oocytes,

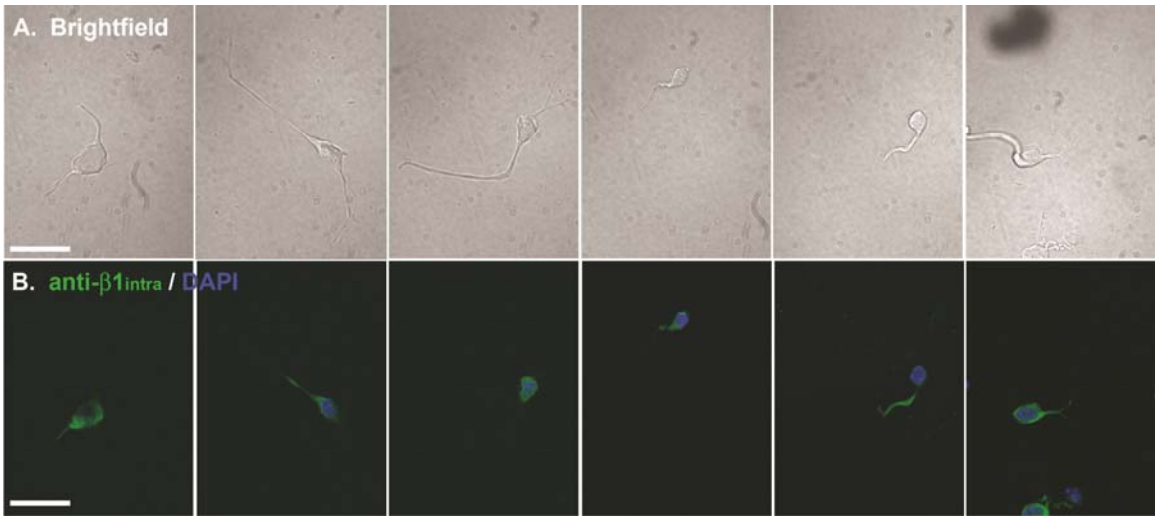

Figure II.9. β1 is expressed in hippocampal CA3 bipolar neurons.
Acutely dissociated hippocampal CA3 bipolar neurons from P10 *Scn1b*$^{+/+}$ mice were fixed with 4% paraformaldehyde and stained for β1 using anti- $\beta1_{intra}$ antibody. **(A)** Bright field images. **(B)** Anti-$\beta1_{intra}$, green; DAPI, blue. Scale bar: 20 μm.

a heterologous system that is maintained at 18^{o}C. The seizure susceptibility to administration of PTZ in *Scn1b*$^{+/-}$ mice was not significantly different from wildtype. Slice recordings from *Scn1b*$^{-/-}$ hippocampus showed increased excitability in CA3 but not CA1 neurons. In contrast to the *Scn1a*$^{+/-}$ model of Dravet syndrome [73], we did not measure significant differences in sodium current density in *Scn1b*$^{-/-}$ CA3 bipolar neurons. We conclude that one *SCN1B* allele is sufficient for the maintenance of normal electrical excitability in brain whereas the *SCN1B* null phenotype results in hyperexcitability, both in mice and in humans. These results predict that future therapeutic interventions for patients carrying trafficking mutations in *SCN1B* may include small molecule chaperones, similar to those being developed for cystic fibrosis, afibrinogenemia, and α1-antitrypsin deficiency [2, 26, 62].

Inherited as well as *de novo* mutations of ion channel genes result in several different types of epilepsy. Mutations in *SCN1B* are linked to GEFS+1, a syndrome that displays multiple seizure types in different families, and even within single individuals, bearing the mutated channel subunit [3, 54, 64, 65]. Epilepsy syndromes in GEFS+ families include febrile seizures, febrile seizures plus, mild generalized epilepsies, severe epileptic encephalopathies including myoclonic-astatic epilepsy and Dravet syndrome, temporal lobe epilepsy, and frontal lobe epilepsy [54]. Subsequently, the diverse seizure pattern of GEFS+ has also been identified in families bearing mutations in *SCN1A*, encoding $Na_v1.1$ [20, 21, 63], as well as in *GABRG2*, encoding the γ2 subunit of the $GABA_A$ receptor [5, 27, 63]. These findings have challenged the idea that a defined mutation of a single ion channel gene results in a uniform seizure type and suggest that $Na_v1.1$, sodium channel β1, and $GABA_A$ receptors may be functionally linked. Further, mutations in any of the genes encoding these proteins can result in GEFS+ spectrum diseases through disruption of inhibitory neuronal excitability.

At least 700 mutations in *SCN1A* are associated with Dravet syndrome [9, 36, 43, 59], with many of these mutations resulting in *SCN1A* haploinsufficiency. *Scn1a*$^{+/-}$ mice, that express half the normal complement of $Na_v1.1$ channels [73], and knock-in mice that carry the p.R1407X mutation, found in some patients with Dravet Syndrome [45] are animal models of this disease. *Scn1a*$^{+/-}$ mice display spontaneous seizures and sporadic deaths beginning after P21. *Scn1a*$^{-/-}$ mice develop ataxia and seizures beginning at P9 and die by P15. The loss of *Scn1a* has no measurable effects on sodium currents in isolated hippocampal pyramidal (excitatory) neurons. However, GABAergic inhibitory bipolar neurons isolated from both *Scn1a*$^{-/-}$ and *Scn1a*$^{+/-}$ mice have significantly reduced sodium current density [73]. *Scn1a*$^{RX/RX}$ mice develop ataxia and seizures during the second postnatal week and die by P20. *Scn1a*$^{RX/+}$ mice exhibit seizures from the third postnatal week and increased mortality thereafter, most probably as a consequence of status epilepticus. The *Scn1a*$^{RX/+}$ mice also exhibit

electrophysiological abnormalities of inhibitory cortical interneurons that are positive for parvalbumin. In these neurons the membrane potential is more negative, and there is a progressive decrement in spike amplitude during prolonged spike trains [45]. The behavioral and molecular phenotypes of *Scn1a*$^{-/-}$, *Scn1a*$^{+/-}$, *Scn1a*$^{RX/RX}$ and *Scn1a*$^{RX/+}$ mice are similar to that of *Scn1b*$^{-/-}$ mice, that develop generalized seizures and ataxia beginning at ~P10 and die by P21 [14]. The mechanisms of neuronal hyperexcitability between these models, however, appear to be different, as we did not detect reductions in bipolar neuron sodium current density in *Scn1b*$^{-/-}$ mice, as described for *Scn1a*$^{+/-}$ neurons [73]. Nevertheless, consistent with a functional link between *Scn1a* and *Scn1b*, *Scn1b* mice have significantly reduced $Na_v1.1$ protein expression in the hippocampus [14], suggesting that *Scn1a* and *Scn1b* may be critical partners in the regulation of hippocampal excitability. Elucidation of the mechanism causing Dravet syndrome-like seizures in *Scn1b*$^{-/-}$ mice will require a more detailed investigation in the future. Possible insights into this problem may be gleaned from our recent work with $Na_v1.1$ expressed in a heterologous system suggesting that β1 plays a dominant role in reducing sodium channel activity [1]. These results raise the possibility that disruption of β1 in inherited epilepsies may slow inactivation rates in some neurons, and thus contribute to the excessive firing associated with seizure disorders.

A mutation in *SCN1A* identified in a family with dominantly inherited GEFS+ further illustrates the importance of $Na_v1.1$-β1 interactions in the regulation of electrical excitability in brain [57]. The mutation, D1866Y, alters a conserved aspartate residue in the C-terminus of $Na_v1.1$, resulting in decreased modulation of $Na_v1.1$ by β1. Coimmunoprecipitation from transfected mammalian cells confirmed the interaction between the C-termini of wildtype $Na_v1.1$ and β1. The $Na_v1.1$ D1866Y mutation weakens this interaction, demonstrating a novel molecular mechanism involving α-β1 association leading to seizure susceptibility and adding support to the hypothesis that *SCN1A* and *SCN1B* are functionally linked in the molecular basis of epilepsy.

Mutations (p.C121W, p.I70_E74del, p.R85C, and p.R85H, **Table II.6**) in *SCN1B* cause GEFS+1 epilepsy [3, 54, 64, 65]. Interestingly, all of these mutations are located within the extracellular immunoglobulin loop domain, suggesting that β1-mediated cell adhesion is clinically relevant. We showed previously that, compared to wildtype, p.C121W increases the fraction of available sodium channels at resting membrane potentials and reduces sodium current rundown during high frequency channel activity [42]. The p.C121W mutation also disrupts β1-mediated homophilic cell-cell adhesion. Although its precise mechanism in neurons is not understood, it is generally agreed that p.C121W produces a non-functional β1 subunit [4]. We demonstrated recently that sodium channel complexes containing p.C121W may require larger than normal stimuli to open, but once activated, inactivate considerably less readily than channels containing wildtype β1, a feature that may promote repetitive firing and lead to hyperexcitability [1]. Similar to p.R125C, p.R85C and p.R85H are not detectable at the cell surface *in vitro*, although p.R85H appeared to modulate the voltage-dependence of sodium channel slow inactivation without any effect on other electrophysiological parameters. p.R85C had no detectable effects on any channel property measured, suggesting that, similar to p.R125C, this mutant β1 subunit polypeptide may not be expressed at the cell surface [70]. The p.I70_E74del mutant has not been tested functionally.

With the exception of the present report, all mutations responsible for the GEFS+ spectrum of epilepsies to date have been found to be autosomal dominant, with patients expressing one mutant and one wildtype allele. To our knowledge, this is the first report of a *SCN1B* mutation that extends the range of GEFS+ phenotypes to the most severe side of the spectrum as well as the first report of an autosomal recessive mutation resulting in a GEFS+ spectrum disease. Given that our proband was homozygous for the mutation and his parents are heterozygous and healthy, it is unlikely that p.R125C

Table II.6. Characteristics of *SCN1B* mutants associated with epilepsy

Mutation	Heterologous System	VGSC[A] α subunit tested	Results	Ref.
p.C121W	*Xenopus* oocytes	$Na_v1.2$	Similar functional modulation of α when injected at high concentration. Decreased modulation at lower concentration[B].	[42]
	1610 cells	$Na_v1.3$	Association with α. No shift in voltage-dependence of current inactivation. Decreased frequency-dependent rundown. Acceleration of recovery from fast inactivation[B]. No dominant negative effect.	[42]
	1610 cells	$Na_v1.2$	Association with α. No shift in voltage-dependence of current inactivation. No decrease in frequency- dependent rundown. Acceleration of recovery from fast inactivation[B]. Equally effective as WT in promoting cell surface expression of α subunits[B].	[42]
	HEK-293 cells HEK-293 cells	$Na_v1.4$ $Na_v1.1$	Equally effective as WT in promoting cell surface expression of α subunits[B]. Unable to accelerate recovery from inactivation[A]. Channels containing p.C121W may require larger than normal stimuli to open, but once activated, inactivate considerably less readily than channels containing wild-type $\beta1$.	[58] [1]
p.I70-E74del	N/A	N/A	N/A	[3]
p.R85C	HEK-293 cells	$Na_v1.2$	No modulation of current density. Inability to shift voltage-dependence of fast activation, fast, or slow inactivation, decrease time constant of fast inactivation, or accelerate recovery from fast inactivation[B]. No protein expression detected[B].	[70]
p.R85H	HEK-293 cells	$Na_v1.2$	No modulation of current density. Inability to shift voltage-dependence of fast activation or inactivation or accelerate recovery from fast inactivation[B]. No protein expression detected[B].	[70]
p.R125C	HEK-293 cells	$Na_v1.1$	Reduced cell surface expression[B].	Present paper

	1610 cells	$Na_v1.2$	Decreased sodium current density[B]. Inability to shift voltage-dependence of inactivation. Reduced frequency-dependent rundown, accelerated recovery from fast inactivation, increased persistent current[B]. Reduced cell surface expression[B].	Present paper
	Xenopus oocytes	$Na_v1.2$	Channel modulation similar to WT.	Present paper
p.D25N	N/A	N/A	*de novo mutation*, partial crisis	[47]
p.V138I	N/A	N/A	Family members not available, febrile convulsion	[47]
p.K208I	N/A	N/A	Family members not available, febrile convulsion	[47]
p.C211Y	N/A	N/A	Found also in controls, partial crisis	[47]
p.G213D	N/A	N/A	Found also in controls, febrile convulsion	[47]

[A] voltage-gated sodium channel. [B] Compared to β1WT.

functions as a dominant-negative. The parental phenotypes recapitulate the situation observed in mice in which animals homozygous for the *Scn1b* null mutation seize spontaneously while animals with one wildtype *Scn1b* allele appear to be neurologically normal. Like *Scn1a*$^{+/-}$ and *Scn1a*$^{RX/+}$ mice, the epileptic phenotype of *Scn1b*$^{-/-}$ mice has similarities to that observed in Dravet syndrome patients. All are normal at birth and then begin exhibiting seizures during infancy that gain in intensity. However, while seizures in patients tend to be preceded by a triggering event, e.g. fever or vaccination, they occur spontaneously in the mice. Nevertheless, patients eventually develop spontaneous seizures, which also mark the beginning of rapid disease progression. *Scn1a*$^{+/-}$, *Scn1a*$^{RX/RX}$ and *Scn1b*$^{-/-}$ mice also exhibit an ataxic gait, similar to many Dravet syndrome patients [14, 45, 73]. Thus, *Scn1a*$^{+/-}$, *Scn1a*$^{RX/+}$ and *Scn1b*$^{-/-}$ mice may represent animal models of Dravet syndrome. However, in contrast to *Scn1a*, in which haploinsufficiency results in a severe epileptic phenotype, the functional loss of both *Scn1b* alleles is required for disease. We propose that one wildtype copy of *Scn1b* is sufficient for normal control of excitability in the brain.

In summary we present the first case of Dravet syndrome due to a homozygous mutation in *SCN1B*, and show that the consequence of this mutation is the inability of β1 polypeptides to be trafficked to the surface of transfected mammalian cells. While HEK and 1610 cells certainly do not fully recapitulate the situation in neurons, our data predict that the patient carrying this mutation is a functional *SCN1B* null and that *Scn1b*$^{-/-}$ mice may be a model for Dravet syndrome. The present results from hippocampal slice recordings as well as previous results from *Scn1b*$^{-/-}$ mice [6] predict that not only deficits in excitability but abnormal cell adhesion resulting in aberrant neuronal pathfinding and fasciculation may play a role in this epileptic syndrome.

Acknowledgments

Additional experimental contributions: Dr. Lieve Claes, at the laboratory of Dr. Peter De Jonghe, Laboratory of Neurogenetics, University of Antwerp, performed genetic analyses of the proband, family members, and controls. Luis Lopez –Santiago performed and analyzed the hippocampal action potential experiments as well as the whole cell voltage clamp experiments on acutely dissociated hippocampal neurons. Emily Slat generated the β1 and p.R125C cDNA constructs. Raja Dondeti performed the seizure susceptibility experiments. Chunling Chen and Charles Gray generated and genotyped the *Scn1b* null mice. Heather O'Malley performed the immunohistochemistry experiments. All of them worked at the laboratory of Dr. Lori Isom, Department of Pharmacology University of Michigan. Fumitaka Oyama, Haruko Miyazaki, and Nobuyuki Nukina, at the RIKEN Brain Science Institute, Japan, provided anti-$\beta1_{intra}$ antibodies.

This project was funded by members of the Partnership for Pediatric Epilepsy Research, which includes the American Epilepsy Society, the Epilepsy Foundation and Parents Against Childhood Epilepsy (P.A.C.E.) to LLI. This research was also supported by NIH grant MH059980 and a grant from the Ralph C. Wilson Jr. Medical Research Foundation to LLI. GAP was supported by a predoctoral fellowship from the Epilepsy

Foundation of Greater Chicago, and by a Scholarship for Faculty Training from Los Andes University. The authors acknowledge the expert technical assistance of Mi Jung Lim, Mark Karadshi, and Ryan Deisler and are grateful for the scientific advice of Dr. Jack Parent and Dr. Miriam Meisler.

Bibliography

[1] T.K. Aman, T.M. Grieco-Calub, C. Chen, R. Rusconi, E.A. Slat, L.L. Isom, I.M. Raman, Regulation of persistent Na current by interactions between beta subunits of voltage-gated Na channels, J Neurosci 29 (2009) 2027-2042.

[2] M.D. Amaral, Therapy through chaperones: sense or antisense? Cystic fibrosis as a model disease, Journal of inherited metabolic disease 29 (2006) 477-487.

[3] D. Audenaert, L. Claes, B. Ceulemans, A. Lofgren, C. Van Broeckhoven, P. De Jonghe, A deletion in SCN1B is associated with febrile seizures and early-onset absence epilepsy, Neurology 61 (2003) 854-856.

[4] G. Avanzini, S. Franceschetti, M. Mantegazza, Epileptogenic channelopathies: experimental models of human pathologies, Epilepsia 48 Suppl 2 (2007) 51-64.

[5] S. Baulac, G. Huberfeld, I. Gourfinkel-An, G. Mitropoulou, A. Beranger, J.F. Prud'homme, M. Baulac, A. Brice, R. Bruzzone, E. LeGuern, First genetic evidence of GABA(A) receptor dysfunction in epilepsy: a mutation in the gamma2-subunit gene, Nat Genet 28 (2001) 46-48.

[6] W.J. Brackenbury, T.H. Davis, C. Chen, E.A. Slat, M.J. Detrow, T.L. Dickendesher, B. Ranscht, L.L. Isom, Voltage-gated Na+ channel beta1 subunit-mediated neurite outgrowth requires Fyn kinase and contributes to postnatal CNS development in vivo, J Neurosci 28 (2008) 3246-3256.

[7] W.J. Brackenbury, M.B. Djamgoz, L.L. Isom, An emerging role for voltage-gated Na+ channels in cellular migration: regulation of central nervous system development and potentiation of invasive cancers, Neuroscientist 14 (2008) 571-583.

[8] W.J. Brackenbury, L.L. Isom, Voltage-gated Na+ channels: potential for beta subunits as therapeutic targets, Expert Opin Ther Targets 12 (2008) 1191-1203.

[9] D.L. Burgess, Neonatal epilepsy syndromes and GEFS+: mechanistic considerations, Epilepsia 46 Suppl 10 (2005) 51-58.

[10] W.A. Catterall, S. Dib-Hajj, M.H. Meisler, D. Pietrobon, Inherited neuronal ion channelopathies: new windows on complex neurological diseases, J Neurosci 28 (2008) 11768-11777.

[11] W.A. Catterall, A.L. Goldin, S.G. Waxman, International Union of Pharmacology. XLVII. Nomenclature and structure-function relationships of voltage-gated sodium channels, Pharmacological reviews 57 (2005) 397-409.

[12] S. Cestele, P. Scalmani, R. Rusconi, B. Terragni, S. Franceschetti, M. Mantegazza, Self-limited hyperexcitability: functional effect of a familial hemiplegic migraine mutation of the Nav1.1 (SCN1A) Na+ channel, J Neurosci 28 (2008) 7273-7283.

[13] C. Chen, T.L. Dickendesher, F. Oyama, H. Miyazaki, N. Nukina, L.L. Isom, Floxed allele for conditional inactivation of the voltage-gated sodium channel beta1 subunit Scn1b, Genesis 45 (2007) 547-553.

[14] C. Chen, R.E. Westenbroek, X. Xu, C.A. Edwards, D.R. Sorenson, Y. Chen, D.P. McEwen, H.A. O'Malley, V. Bharucha, L.S. Meadows, G.A. Knudsen, A. Vilaythong, J.L. Noebels, T.L. Saunders, T. Scheuer, P. Shrager, W.A. Catterall, L.L. Isom, Mice lacking sodium channel beta1 subunits display defects in neuronal excitability, sodium channel expression, and nodal architecture, J Neurosci 24 (2004) 4030-4042.

[15] L. Claes, B. Ceulemans, D. Audenaert, K. Smets, A. Lofgren, J. Del-Favero, S. Ala-Mello, L. Basel-Vanagaite, B. Plecko, S. Raskin, P. Thiry, N.I. Wolf, C. Van Broeckhoven, P. De Jonghe, De novo SCN1A mutations are a major cause of severe myoclonic epilepsy of infancy, Human mutation 21 (2003) 615-621.

[16] T.B. Cole, C.A. Robbins, H.J. Wenzel, P.A. Schwartzkroin, R.D. Palmiter, Seizures and neuronal damage in mice lacking vesicular zinc, Epilepsy research 39 (2000) 153-169.

[17] T.H. Davis, C. Chen, L.L. Isom, Sodium channel beta1 subunits promote neurite outgrowth in cerebellar granule neurons, The Journal of biological chemistry 279 (2004) 51424-51432.

[18] J.T. den Dunnen, S.E. Antonarakis, Nomenclature for the description of human sequence variations, Hum Genet 109 (2001) 121-124.

[19] C. Dravet, M. Bureau, H. Oguni, Y. Fukuyama, O. Cokar, Severe myoclonic epilepsy in infancy: Dravet syndrome, Advances in neurology 95 (2005) 71-102.

[20] A. Escayg, A. Heils, B.T. MacDonald, K. Haug, T. Sander, M.H. Meisler, A novel SCN1A mutation associated with generalized epilepsy with febrile seizures plus--and prevalence of variants in patients with epilepsy, Am J Hum Genet 68 (2001) 866-873.

[21] A. Escayg, B.T. MacDonald, M.H. Meisler, S. Baulac, G. Huberfeld, I. An-Gourfinkel, A. Brice, E. LeGuern, B. Moulard, D. Chaigne, C. Buresi, A. Malafosse, Mutations of SCN1A, encoding a neuronal sodium channel, in two families with GEFS+2, Nat Genet 24 (2000) 343-345.

[22] A.J. Fein, L.S. Meadows, C. Chen, E.A. Slat, L.L. Isom, Cloning and expression of a zebrafish SCN1B ortholog and identification of a species-specific splice variant, BMC genomics 8 (2007) 226.

[23] T. Fujiwara, Clinical spectrum of mutations in SCN1A gene: severe myoclonic epilepsy in infancy and related epilepsies, Epilepsy research 70 Suppl 1 (2006) S223-230.

[24] E. Gennaro, F.M. Santorelli, E. Bertini, D. Buti, R. Gaggero, G. Gobbi, M. Lini, T. Granata, E. Freri, A. Parmeggiani, P. Striano, P. Veggiotti, S. Cardinali, F.D. Bricarelli, C. Minetti, F. Zara, Somatic and germline mosaicisms in severe myoclonic epilepsy of infancy, Biochemical and biophysical research communications 341 (2006) 489-493.

[25] P. Gissen, E.R. Maher, Cargos and genes: insights into vesicular transport from inherited human disease, J Med Genet 44 (2007) 545-555.

[26] N. Gregersen, Protein misfolding disorders: pathogenesis and intervention, Journal of inherited metabolic disease 29 (2006) 456-470.

[27] L.A. Harkin, D.N. Bowser, L.M. Dibbens, R. Singh, F. Phillips, R.H. Wallace, M.C. Richards, D.A. Williams, J.C. Mulley, S.F. Berkovic, I.E. Scheffer, S. Petrou, Truncation of the GABA(A)-receptor gamma2 subunit in a family with generalized epilepsy with febrile seizures plus, Am J Hum Genet 70 (2002) 530-536.

[28] L.L. Isom, K.S. De Jongh, D.E. Patton, B.F. Reber, J. Offord, H. Charbonneau, K. Walsh, A.L. Goldin, W.A. Catterall, Primary structure and functional expression of the beta 1 subunit of the rat brain sodium channel, Science 256 (1992) 839-842.

[29] L.L. Isom, D.S. Ragsdale, K.S. De Jongh, R.E. Westenbroek, B.F. Reber, T. Scheuer, W.A. Catterall, Structure and function of the beta 2 subunit of brain sodium channels, a transmembrane glycoprotein with a CAM motif, Cell 83 (1995) 433-442.
[30] L.L. Isom, T. Scheuer, A.B. Brownstein, D.S. Ragsdale, B.J. Murphy, W.A. Catterall, Functional co-expression of the beta 1 and type IIA alpha subunits of sodium channels in a mammalian cell line, The Journal of biological chemistry 270 (1995) 3306-3312.
[31] K.A. Kazen-Gillespie, D.S. Ragsdale, M.R. D'Andrea, L.N. Mattei, K.E. Rogers, L.L. Isom, Cloning, localization, and functional expression of sodium channel beta1A subunits, The Journal of biological chemistry 275 (2000) 1079-1088.
[32] J.A. Kearney, A.K. Wiste, U. Stephani, M.M. Trudeau, A. Siegel, R. RamachandranNair, R.D. Elterman, H. Muhle, J. Reinsdorf, W.D. Shields, M.H. Meisler, A. Escayg, Recurrent de novo mutations of SCN1A in severe myoclonic epilepsy of infancy, Pediatric neurology 34 (2006) 116-120.
[33] C.M. Korff, D.R. Nordli, Jr., Epilepsy syndromes in infancy, Pediatric neurology 34 (2006) 253-263.
[34] L.F. Lopez-Santiago, L.S. Meadows, S.J. Ernst, C. Chen, J.D. Malhotra, D.P. McEwen, A. Speelman, J.L. Noebels, S.K. Maier, A.N. Lopatin, L.L. Isom, Sodium channel Scn1b null mice exhibit prolonged QT and RR intervals, J Mol Cell Cardiol 43 (2007) 636-647.
[35] L.F. Lopez-Santiago, M. Pertin, X. Morisod, C. Chen, S. Hong, J. Wiley, I. Decosterd, L.L. Isom, Sodium channel beta2 subunits regulate tetrodotoxin-sensitive sodium channels in small dorsal root ganglion neurons and modulate the response to pain, J Neurosci 26 (2006) 7984-7994.
[36] C. Lossin, A catalog of SCN1A variants, Brain & development 31 (2009) 114-130.
[37] J.D. Malhotra, K. Kazen-Gillespie, M. Hortsch, L.L. Isom, Sodium channel beta subunits mediate homophilic cell adhesion and recruit ankyrin to points of cell-cell contact, The Journal of biological chemistry 275 (2000) 11383-11388.
[38] J.D. Malhotra, V. Thyagarajan, C. Chen, L.L. Isom, Tyrosine-phosphorylated and nonphosphorylated sodium channel beta1 subunits are differentially localized in cardiac myocytes, The Journal of biological chemistry 279 (2004) 40748-40754.
[39] M. Mantegazza, A. Gambardella, R. Rusconi, E. Schiavon, F. Annesi, R.R. Cassulini, A. Labate, S. Carrideo, R. Chifari, M.P. Canevini, R. Canger, S. Franceschetti, G. Annesi, E. Wanke, A. Quattrone, Identification of an Nav1.1 sodium channel (SCN1A) loss-of-function mutation associated with familial simple febrile seizures, Proceedings of the National Academy of Sciences of the United States of America 102 (2005) 18177-18182.
[40] D.P. McEwen, L.L. Isom, Heterophilic interactions of sodium channel beta1 subunits with axonal and glial cell adhesion molecules, The Journal of biological chemistry 279 (2004) 52744-52752.
[41] D.P. McEwen, L.S. Meadows, C. Chen, V. Thyagarajan, L.L. Isom, Sodium channel beta1 subunit-mediated modulation of Nav1.2 currents and cell surface density is dependent on interactions with contactin and ankyrin, The Journal of biological chemistry 279 (2004) 16044-16049.
[42] L.S. Meadows, J. Malhotra, A. Loukas, V. Thyagarajan, K.A. Kazen-Gillespie, M.C. Koopman, S. Kriegler, L.L. Isom, D.S. Ragsdale, Functional and biochemical analysis of a sodium channel beta1 subunit mutation responsible for generalized epilepsy with febrile seizures plus type 1, J Neurosci 22 (2002) 10699-10709.

[43] M.H. Meisler, J.A. Kearney, Sodium channel mutations in epilepsy and other neurological disorders, The Journal of clinical investigation 115 (2005) 2010-2017.
[44] M. Morimoto, E. Mazaki, A. Nishimura, T. Chiyonobu, Y. Sawai, A. Murakami, K. Nakamura, I. Inoue, I. Ogiwara, T. Sugimoto, K. Yamakawa, SCN1A mutation mosaicism in a family with severe myoclonic epilepsy in infancy, Epilepsia 47 (2006) 1732-1736.
[45] I. Ogiwara, H. Miyamoto, N. Morita, N. Atapour, E. Mazaki, I. Inoue, T. Takeuchi, S. Itohara, Y. Yanagawa, K. Obata, T. Furuichi, T.K. Hensch, K. Yamakawa, Na(v)1.1 localizes to axons of parvalbumin-positive inhibitory interneurons: a circuit basis for epileptic seizures in mice carrying an Scn1a gene mutation, J Neurosci 27 (2007) 5903-5914.
[46] H. Oguni, K. Hayashi, M. Osawa, Y. Awaya, Y. Fukuyama, G. Fukuma, S. Hirose, A. Mitsudome, S. Kaneko, Severe myoclonic epilepsy in infancy: clinical analysis and relation to SCN1A mutations in a Japanese cohort, Advances in neurology 95 (2005) 103-117.
[47] A. Orrico, L. Galli, S. Grosso, S. Buoni, R. Pianigiani, P. Balestri, V. Sorrentino, Mutational analysis of the SCN1A, SCN1B and GABRG2 genes in 150 Italian patients with idiopathic childhood epilepsies, Clin Genet 75 (2009) 579-581.
[48] F. Oyama, H. Miyazaki, N. Sakamoto, C. Becquet, Y. Machida, K. Kaneko, C. Uchikawa, T. Suzuki, M. Kurosawa, T. Ikeda, A. Tamaoka, T. Sakurai, N. Nukina, Sodium channel beta4 subunit: down-regulation and possible involvement in neuritic degeneration in Huntington's disease transgenic mice, Journal of neurochemistry 98 (2006) 518-529.
[49] D.E. Patton, A.L. Goldin, A voltage-dependent gating transition induces use-dependent block by tetrodotoxin of rat IIA sodium channels expressed in Xenopus oocytes, Neuron 7 (1991) 637-647.
[50] N. Qin, M.R. D'Andrea, M.L. Lubin, N. Shafaee, E.E. Codd, A.M. Correa, Molecular cloning and functional expression of the human sodium channel beta1B subunit, a novel splicing variant of the beta1 subunit, European journal of biochemistry / FEBS 270 (2003) 4762-4770.
[51] R.J. Racine, Modification of seizure activity by electrical stimulation. I. After-discharge threshold, Electroencephalography and clinical neurophysiology 32 (1972) 269-279.
[52] R.J. Racine, Modification of seizure activity by electrical stimulation. II. Motor seizure, Electroencephalography and clinical neurophysiology 32 (1972) 281-294.
[53] R. Rusconi, P. Scalmani, R.R. Cassulini, G. Giunti, A. Gambardella, S. Franceschetti, G. Annesi, E. Wanke, M. Mantegazza, Modulatory proteins can rescue a trafficking defective epileptogenic Nav1.1 Na+ channel mutant, J Neurosci 27 (2007) 11037-11046.
[54] I.E. Scheffer, L.A. Harkin, B.E. Grinton, L.M. Dibbens, S.J. Turner, M.A. Zielinski, R. Xu, G. Jackson, J. Adams, M. Connellan, S. Petrou, R.M. Wellard, R.S. Briellmann, R.H. Wallace, J.C. Mulley, S.F. Berkovic, Temporal lobe epilepsy and GEFS+ phenotypes associated with SCN1B mutations, Brain 130 (2007) 100-109.
[55] E. Sigel, F. Minier, The Xenopus oocyte: system for the study of functional expression and modulation of proteins, Molecular nutrition & food research 49 (2005) 228-234.
[56] R.D. Smith, A.L. Goldin, Functional analysis of the rat I sodium channel in xenopus oocytes, J Neurosci 18 (1998) 811-820.

[57] J. Spampanato, J.A. Kearney, G. de Haan, D.P. McEwen, A. Escayg, I. Aradi, B.T. MacDonald, S.I. Levin, I. Soltesz, P. Benna, E. Montalenti, L.L. Isom, A.L. Goldin, M.H. Meisler, A novel epilepsy mutation in the sodium channel SCN1A identifies a cytoplasmic domain for beta subunit interaction, J Neurosci 24 (2004) 10022-10034.
[58] P. Tammaro, F. Conti, O. Moran, Modulation of sodium current in mammalian cells by an epilepsy-correlated beta 1-subunit mutation, Biochemical and biophysical research communications 291 (2002) 1095-1101.
[59] J. Turnbull, H. Lohi, J.A. Kearney, G.A. Rouleau, A.V. Delgado-Escueta, M.H. Meisler, P. Cossette, B.A. Minassian, Sacred disease secrets revealed: the genetics of human epilepsy, Human molecular genetics 14 Spec No. 2 (2005) 2491-2500.
[60] C.R. Valdivia, M.J. Ackerman, D.J. Tester, T. Wada, J. McCormack, B. Ye, J.C. Makielski, A novel SCN5A arrhythmia mutation, M1766L, with expression defect rescued by mexiletine, Cardiovascular research 55 (2002) 279-289.
[61] C.G. Vanoye, C. Lossin, T.H. Rhodes, A.L. George, Jr., Single-channel properties of human NaV1.1 and mechanism of channel dysfunction in SCN1A-associated epilepsy, J Gen Physiol 127 (2006) 1-14.
[62] D. Vu, C. Di Sanza, M. Neerman-Arbez, Manipulating the quality control pathway in transfected cells: low temperature allows rescue of secretion-defective fibrinogen mutants, Haematologica 93 (2008) 224-231.
[63] R.H. Wallace, I.E. Scheffer, S. Barnett, M. Richards, L. Dibbens, R.R. Desai, T. Lerman-Sagie, D. Lev, A. Mazarib, N. Brand, B. Ben-Zeev, I. Goikhman, R. Singh, G. Kremmidiotis, A. Gardner, G.R. Sutherland, A.L. George, Jr., J.C. Mulley, S.F. Berkovic, Neuronal sodium-channel alpha1-subunit mutations in generalized epilepsy with febrile seizures plus, Am J Hum Genet 68 (2001) 859-865.
[64] R.H. Wallace, I.E. Scheffer, G. Parasivam, S. Barnett, G.B. Wallace, G.R. Sutherland, S.F. Berkovic, J.C. Mulley, Generalized epilepsy with febrile seizures plus: mutation of the sodium channel subunit SCN1B, Neurology 58 (2002) 1426-1429.
[65] R.H. Wallace, D.W. Wang, R. Singh, I.E. Scheffer, A.L. George, Jr., H.A. Phillips, K. Saar, A. Reis, E.W. Johnson, G.R. Sutherland, S.F. Berkovic, J.C. Mulley, Febrile seizures and generalized epilepsy associated with a mutation in the Na+-channel beta1 subunit gene SCN1B, Nat Genet 19 (1998) 366-370.
[66] S. Weckx, J. Del-Favero, R. Rademakers, L. Claes, M. Cruts, P. De Jonghe, C. Van Broeckhoven, P. De Rijk, novoSNP, a novel computational tool for sequence variation discovery, Genome Res 15 (2005) 436-442.
[67] J.W. West, T. Scheuer, L. Maechler, W.A. Catterall, Efficient expression of rat brain type IIA Na+ channel alpha subunits in a somatic cell line, Neuron 8 (1992) 59-70.
[68] J.M. Witkin, M. Baez, J. Yu, M.E. Barton, H.E. Shannon, Constitutive deletion of the serotonin-7 (5-HT(7)) receptor decreases electrical and chemical seizure thresholds, Epilepsy research 75 (2007) 39-45.
[69] M. Wolff, C. Casse-Perrot, C. Dravet, Severe myoclonic epilepsy of infants (Dravet syndrome): natural history and neuropsychological findings, Epilepsia 47 Suppl 2 (2006) 45-48.
[70] R. Xu, E.A. Thomas, E.V. Gazina, K.L. Richards, M. Quick, R.H. Wallace, L.A. Harkin, S.E. Heron, S.F. Berkovic, I.E. Scheffer, J.C. Mulley, S. Petrou, Generalized epilepsy with febrile seizures plus-associated sodium channel beta1

subunit mutations severely reduce beta subunit-mediated modulation of sodium channel function, Neuroscience 148 (2007) 164-174.
[71] K. Yamakawa, Na channel gene mutations in epilepsy--the functional consequences, Epilepsy research 70 Suppl 1 (2006) S218-222.
[72] I. Yilmaz, Z. Sezer, H. Kayir, T.I. Uzbay, Mirtazapine does not affect pentylenetetrazole- and maximal electroconvulsive shock-induced seizures in mice, Epilepsy Behav 11 (2007) 1-5.
[73] F.H. Yu, M. Mantegazza, R.E. Westenbroek, C.A. Robbins, F. Kalume, K.A. Burton, W.J. Spain, G.S. McKnight, T. Scheuer, W.A. Catterall, Reduced sodium current in GABAergic interneurons in a mouse model of severe myoclonic epilepsy in infancy, Nature neuroscience 9 (2006) 1142-1149.

Chapter III

Voltage-Gated Na^+ channel β1B: a secreted cell adhesion molecule involved in human epilepsy

Introduction

SCN1B, encoding VGSC channel β1 subunits, is essential for life. Deletion of this gene in mice results in severe epilepsy, ataxia, growth retardation, cardiac abnormalities, and early death [9, 10, 25]. Human mutations in *SCN1B* result in GEFS+-spectrum disorders (reviewed in [38]), Brugada Syndrome [53], and atrial fibrillation [50]. We demonstrated that patients carrying two alleles of a functional null mutation of *SCN1B*, p.R125C, have Dravet Syndrome, a pediatric encephalopathy associated with mental retardation that is the most severe GEFS+-spectrum disease [38]. *SCN1B* can be expressed as two developmentally regulated splice variants, β1 and β1B (originally called β1A) that includes part of a retained intron encoding a novel C-terminus, stop codon, and polyadenylation site [22, 41] (**Figure III.1.A**). We and others have shown than β1 is a multifunctional molecule that participates in Na^+ current modulation, channel expression and subcellular localization, cell adhesion, cellular migration, and neurite outgrowth [4, 5]. In contrast, very little is known about the structure and function of β1B. Because *Scn1b* null mice lack both splice variants, some aspects of their complex phenotype may be due to the absence of β1B, however, this has not been investigated. In addition, because all of the *SCN1B* epilepsy mutations described to date are located in the immunoglobulin (Ig) loop region common to both splice variants [37], β1B, as well

as β1, is likely involved in human brain disease. The goal of this project was to understand the structure and function of β1B and to investigate a novel human *SCN1B* epilepsy mutation (p.G257R) located in the region unique to β1B. We demonstrate that β1B is not a transmembrane protein, as originally assumed, but is a soluble protein that functions as a ligand for β1-mediated neurite outgrowth. β1B is expressed predominantly during embryonic development in human brain, with the ratio of β1:β1B mRNA in brain increasing with development into adulthood, when β1 becomes the predominant splice variant. Association of β1B with VGSC α subunits is not detectable by ^{3}H-saxitoxin (STX) binding or coimmunoprecipitation, suggesting that β1B may not modulate Na^{+} current in brain, but instead functions as a cell adhesion molecule (CAM) independent of channel function. Consistent with this, β1B stimulates neurite outgrowth of cerebellar granule neurons (CGNs) through adhesion with neuronal β1 subunits. The β1B epilepsy mutation p.G257R results in intracellular retention of β1B, generating a functional null allele. We conclude that β1B is a secreted CAM, expressed predominately in human embryonic brain, which stimulates neurite outgrowth. We hypothesize that the p.G257R mutation causes epilepsy through a mechanism that includes intracellular retention of this subunit, resulting in aberrant neuronal migration and pathfinding.

Materials and Methods

1. Clinical Samples

A group of 360 unrelated probands diagnosed with episodic neurological disease were studied. Diagnosis was performed by experienced clinicians specialized in these neurological disorders. For most patients collected, additional clinical information allowed for a better definition of the disease sub-phenotype. The ethnic origin of all study samples is known and additional affected and non-affected family members for each proband studied was also collected for the purpose of co-segregation/pedigree analysis. Informed consent was

obtained from all study participants and study protocols were approved by the ethics committees of the institutions where collections occurred. An additional cohort of 192 unrelated Tourette's patient samples was used to assess involvement of the p.G257R variant in Tourette's syndrome. The patient from pedigree 1 had tonic-clonic seizures starting from 10 years of age. The proband's mother and maternal aunt also had a history of seizures. The patient from Pedigree 2 had right temporal lobe seizure onsets with secondary generalized seizures starting at 15 years of age, sometimes preceded by an aura. Seizures were controlled by Carbamazepine. This patient was also diagnosed with Gilles de la Tourette syndrome, with facial tics and aggressive compulsions. There was no family history of epilepsy in either parent.

2. Amplicon design and PCR

Amplicons were designed to minimize the amount of intronic sequence for each amplicon, and to avoid repetitive elements. PCR primers were designed using PrimerSelect (DNASTAR) and purchased from BioCorp (Montreal). The primer sequences, amplicon sizes and amplification conditions are given in **Tables III.1** and **III.2**. Genomic DNA was isolated from blood samples and amplified using Taq DNA polymerase (Qiagen) on a PE 9700 PCR thermocycler (Perkin Elmer). Addition of Q solution (Qiagen) was done for problematic amplicons. All amplified fragments were tested by agarose gel electrophoresis.

Table III.1 PCR primers used to amplify regions of the human*SCN1B* gene

Exon	Forward primer sequence (5'>3')	Reverse primer sequence (5'>3')	Size (bp)	Protocol
1	CGCGCTCCCGGGGACATTCTAACC	CCCGGCCCCCACCCGCTGGAG	356	TD3+Q
2	CAATGGGTGCCTCTGCCTGAC	CCCACCGCCTCCCACTCGT	269	TD8
3A*	GAGAGGCCCAGGCAGTGACA	GTTCTGTACCCGGAGCGTCTGT	527	TD1
3B*	CAGCCCCTCCTGCCCACTCC	CCCGCCCCAGAGGTGTTGAG	465	TD10
4	GAGGGCCTCCAGAATGACACAGAT	CGGGCTCCGGAGTTCCTCTC	440	TD11
5	GGGGTTGGGTCGGTCTGATGATGG	AGGGCCTGAAGGGGAGCAAGAGA	222	TD8
6	GCCGAAGTCCCCCAGGTCCCTAAT	AGGAGCTGGAGGAGGCGAAAGTGG	233	TD8

*Exon 3 was amplified in two separate minimally-overlapping PCR fragments.

Table III.2 Touch-Down PCR amplification conditions

		Touch Down				Amplification				
Protocol	Initial Denaturation (1 cycle)	denat temp (30s)	anneal temp ramp (30 s)	elong temp (45 s)	cycles	denat temp (30s)	anneal temp (30 s)	elong temp (45 s)	cycles	Final Elongation (1 cycle)
TD1	94°C, 4 min	94°C	70°C to 53°C (-1°C per cycle)	72°C	17	94°C	54°C	72°C	25	72°C, 5 min
TD3	94°C, 4 min	94°C	70°C to 60°C (-1°C per cycle)	72°C	10	94°C	60°C	72°C	30	72°C, 5 min
TD8	94°C, 4 min	94°C	66°C to 59°C (-0.5°C per cycle)	72°C	14	94°C	58°C	72°C	25	72°C, 5 min
TD10	94°C, 4 min	94°C	70°C to 63°C (-0.5°C per cycle)	72°C	14	94°C	62°C	72°C	25	72°C, 5 min
TD11	94°C, 4 min	94°C	72°C to 65°C (-0.5°C per cycle)	72°C	14	94°C	64°C	72°C	25	72°C, 5 min

3. dHPLC and sequence analysis

PCR fragments were optimized for melting temperature on a model 3500HT WAVE dHPLC apparatus (Transgenomic Inc.) with Wavemaker software version 4.1.44. PCR fragments from DNA samples were amplified using the optimized conditions and the fragments were then tested on agarose gels. Amplified fragments were pooled 4x, denatured at 95ºC in a heating block for 5 min. and renatured slowly by cooling the block to 25ºC over the course of 1 hour. The pooled PCR fragments were run on the dHPLC apparatus at two different melting temperatures. The elution profiles of each sample pool were compared, and samples from 1 to 3 pools showing variant elution profiles were selected for sequence determination at the Genome Quebec Innovation Centre sequencing facility (Montreal). Sequencing reactions were performed on an ABI prism 3700 sequencing apparatus. Sequence traces were aligned using a genomic sequence contig constructed in SeqManII (DNASTAR). Base-pair variants were identified and annotated.

Publicly available predicted Single Nucleotide Polymorphisms (SNPs, from NCBI dbSNP version 132) were identified, and those found in the sequence contig were noted.

4. Genotyping

Genotyping was performed either by direct sequencing, allele specific oligonucleotide (ASO) hybridization, or Restriction fragment length polymorphism (RFLP) assay. Genotypes obtained from sequence reads were generated by Mutation Surveyor (SoftGenetics Inc.). For each ASO assay, two oligonucleotides were designed to differentiate the wild-type from the mutant alleles. The ASO assays were done essentially as described [2]. The p.G257R variant was genotyped using an MspI RFLP assay. The 465 bp fragment from amplicon 3B (**Table III.1**) was digested with MspI restriction enzyme (New England BioLabs) and the products were separated on a 1.5% agarose gel, migrated for 2.5 hours at 135V, stained with EtBr and visualized with ultraviolet light. The 257Gly allele yields digested products of 49, 87, 90, and 239 bp in size, whereas the 257Arg allele yields fragments of 49, 87 and 329 bp in size.

5. In silico *analysis*

The amino acid sequences of human β1 (GenBank accession number NP_001028.1), human β1B (NP_950238.1), rat β1 (NP_058984.1), rat β1B (AAF25186.1), and mouse β1 (NP_035452.1) were obtained from NCBI in FASTA format. The N-terminal region of mouse β1/β1B, encoded by the first three exons of *Scn1b*, was obtained by aligning the mouse β1 sequence with the human and rat sequences and comparing the common region to the mouse chromosome 7 sequence (GenBank accession number AC158993.2). The unique C-terminal region of mouse β1B was obtained by translating *in silico* the third intron of mouse *Scn1b* as found in the chromosome 7 sequence. To predict transmembrane domains, β1 and

β1B subunit amino acid sequences were analyzed using TopPred software (http://mobyle.pasteur.fr/cgi-bin/portal.py?form=toppred) [11, 49].
Alignment of human, mouse, and rat β1 and β1B amino acid sequences was performed using CLUSTALW software (http://npsa-pbil.ibcp.fr/cgi-bin/npsa_automat.pl?page=npsa_clustalw.html) [47].

6. Animals

Scn1b wild-type and null mice, congenic on the C57BL/6 background for at least 18 generations, were generated from *Scn1b*$^{+/-}$ mice as described [10]. Animals were housed in the Unit for Laboratory Animal Medicine at the University of Michigan. All procedures were performed in accordance with University of Michigan guidelines for animal use and care.

7. Antibodies

Primary antibodies used in these studies were: anti-V5 monoclonal antibody (1:1000, AbD Serotec MCA1360), mouse or rabbit anti-pan Na^+ channel antibodies (1:1000, Sigma S8809 or S6936 respectively), and anti-Na^+/K^+ ATPase β1 subunit antibody (1:2000, Thermo Scientific MA1-16732). The specificity of the anti-V5 antibody in 1610 and HEK cells has been reported previously [38]. Secondary antibodies used in these studies were HRP-conjugated goat anti-rabbit or anti-mouse (Pierce, Rockford, IL) diluted 1:2000.

8. Expression vectors and site-directed mutagenesis

The plasmid referred to as β1V5 contains a C-terminal V5-His-epitope tag and has been described previously [38]. The cDNA for human β1B was amplified by PCR and ligated into pTRACER-CMV (Invitrogen) at the EcoRI restriction site. The p.G257R mutation was introduced by site directed mutagenesis using the QuikChange II kit

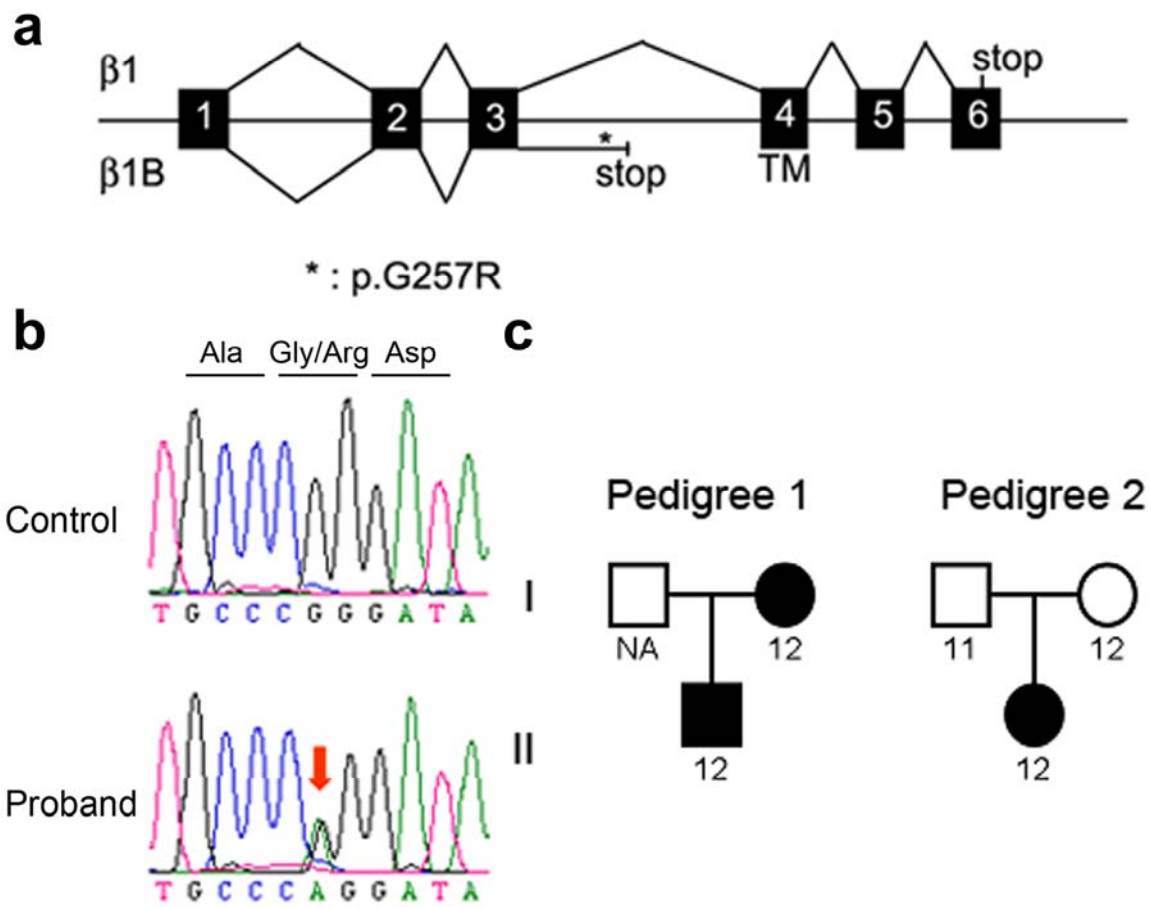

Figure III.1. A *SCN1B* mutation that affects β1B is found in two pedigrees of idiopathic epilepsy. (**A**) Genomic structure of *SCN1B*. Exons 1-6 constitute β1. Extension of exon 3 into intron 3 generates the variant, β1B. The novel 3' end of β1B does not contain a transmembrane domain (TM). * Indicates position of G257R mutation. (Not drawn to scale.) (**B**) Chromatogram showing the p.G257R heterozygous missense mutation in the epilepsy proband from pedigree 1 (lower row) whereas it is absent from a control individual (top row). (**C**) Two pedigrees segregating the p.G257R missense mutation. Pedigree 1 has epilepsy, whereas pedigree 2 has epilepsy and Tourette syndrome. Affected individuals are indicated with black symbols, normal individuals are shown with white symbols. 1, 257Gly allele; 2, 257Arg allele.

(Stratagene). V5-His epitope tags were added to the C-termini of β1B and p.G257R cDNAs using a PCR strategy followed by ligation into pcDNA3.1/V5-His TOPO TA (Invitrogen). β1V5 and β1BV5 cDNAs were also ligated into pcDNA3.1 Hygro (+). The p.R214Q, p.S248R and p.R250T mutations were introduced into β1BV5 cDNA by site-directed mutagenesis. The integrity of all plasmids was confirmed by DNA sequencing. PCR primers and conditions for

all reactions are available upon request. The cDNA for human $Na_v1.5$ corresponding to the hH1 polymorphism (GenBank accession number M77235) [26] in pRcCMV (Invitrogen) was kindly provided by Dr. Al George.

9. Cell lines

All cell lines used in this study were maintained at 37°C with 5% CO_2. Chinese hamster lung 1610 cells were maintained as described in [38]. HEK-293 cells expressing human $Na_v1.1$ (GenBank accession number NP_008851.3, HEKh$Na_v1.1$) were obtained from Glaxo-Smith-Kline under a Materials Transfer Agreement and maintained as described in [38]. Chinese Hamster Ovary cells stably expressing human $Na_v1.3$ (GenBank accession number NP_008853.3, CHOh$Na_v1.3$) were kindly provided by Dr. David Ragsdale and maintained as described in [35].

For transient transfection in HEKh$Na_v1.1$, 7.5 µg of cDNA encoding β1V5 or β1BV5 were used. 24 to 48 h later, cells were collected for biochemical experiments. Fugene 6 (Roche) was used for all transfections.

To generate stable cell lines, 2.5 µg of β subunit cDNAs were transfected and 24 h later cells were passaged into fresh medium containing selective antibiotics: G418 (400 µg/ml) for $Na_v1.5$ or V5-His-tagged β subunit cDNAs; Hygromycin (400 µg/ml) for V5-His-tagged β subunit cDNAs transfected into cell lines stably expressing α subunits; Zeocin (400 µg/ml) for wild-type or mutant β1B subunit cDNAs in pTRACER. Colonies were selected as in [19]. To confirm stable transfection of pTRACER vectors, cells were plated in Glass Slides (BD Falcon), and fixed with 4% paraformaldehyde for 20 min at RT. Samples were viewed using a Fluoview500 confocal laser-scanning microscope (Olympus) with 100x objective. Images (1024 x 1024 pixels) were acquired with the Olympus Optical Fluoview software.

10. Western blot analysis

For each experiment, stably transfected cells from a 100 mm Petri dish, or transiently transfected cells from a 60 mm dish (at 95% confluence), were processed as described in [38]. Proteins were separated by SDS-PAGE on a 10% polyacrylamide gel, transferred to nitrocellulose membrane and Western blot analysis performed using the SNAP i.d. Protein Detection System (Millipore) according to the instructions of the manufacturer.

11. Purification of β1B from conditioned media

Cells stably expressing V5-His epitope-tagged subunits were grown in one 850 cm^2 polystyrene roller bottle (Corning) containing 50 ml of media, or in twelve 150 mm x 25 mm cell culture dishes (Corning) containing 20 ml of media per dish until confluent (8-15 days). When the cells reached confluence, conditioned media were collected and centrifuged at 5000 *g* for 10 minutes. The media from culture dishes were then concentrated using an Amicon Stirred Cell Concentrator, with a Regenerated Cellulose Ultrafiltration Membrane NMWL: 10,000 (both from Amicon-Millipore), to obtain a volume of ~50 ml. Complete, EDTA-free Protease Inhibitor Cocktail (Roche) was added to the conditioned media. To purify the V5-His-tagged proteins, concentrated conditioned media were mixed with 1.2 ml total volume of His-Select HF Nickel Affinity Gel (Sigma), previously rinsed with 3 ml of deionized water and 5 ml of equilibration/washing buffer (50 mM sodium phosphate, pH 8.0, 300 mM sodium chloride, 10 mM imidazole) in a Poly-Prep Chromatography Column (Bio-Rad), and incubated for 30 minutes at RT on a Clay Adams Nutator Mixer (BD). The mix was then centrifuged at maximum speed in a swinging bucket rotor for 5 min. The supernatant was discarded by careful suction and the nickel gel resuspended in 15 ml of equilibration/washing buffer. This washing step was repeated until the supernatant after centrifugation was completely clear. The nickel gel was then resuspended in 10 ml of equilibration/washing buffer, transferred to the chromatography column, and washed with 20 ml of

equilibration/washing buffer. 4 ml of elution buffer (50 mM sodium phosphate, pH 8.0, 300 mM sodium chloride, 250 mM imidazole) were added to the gel and the eluted fraction collected in an Amicon Ultra-4 Centrifugal Filter Device with a 10,000 MWCO regenerated cellulos filter (Millipore). The filter device was then centrifuged at top speed in a swinging bucket rotor for 25 min and the non-filtered fraction collected and mixed with loading buffer containing SDS and β-mercaptoethanol at a 1:1 ratio.

12. Surface biotinylation

For surface biotinylation assays, transfected cells were grown in 4 tissue culture plates (60 mm dishes for transiently transfected or 100 mm dishes for stably transfected cell lines) and membrane proteins biotinylated as described in [38]. Immunoreactive signals were quantified using ImageJ software (NIH) and normalized to the level of Na^+/K^+ ATPase β1 subunit.

13. Coimmunoprecipitation:

200 µl of Protein G-Sepharose 4B beads (Sigma) per sample of α + β1 or α + β1B cell lines were rinsed three times with 1x PBS and split into two microcentrifuge tubes. Beads were resuspended in 250 µl of dilution buffer (60 mMTris/HCl pH 7.5, 180 mM NaCl, 1.25% Triton X-100, 6 mM EDTA pH 8 with Complete Mini Protease Inhibitor Tablets) and incubated overnight with end-over-mixing at 4°C with 4 µg of mouse or rabbit pan Na^+ channel antibody or 4 µg of mouse or rabbit IgG, as indicated in the figure legends. Cells coexpressing α + β subunits were resuspended in a 50 mM Tris, 10 mM EGTA, pH 8 solution (with Complete Mini) by scraping. The amount of sample used for each cell line were as follows: For HEKhNa$_v$1.1 cells transiently transfected or HEKhNa$_v$1.5 cells stably transfected with β1 or β1B, one 60 mm cell culture dish; for CHOhNa$_v$1.3 cells stably transfected with β1 or β1B, two 100 mm cell culture dishes. Cell suspensions were then centrifuged at 3000 *g* for 10

minutes at 4°C. Cells were washed again in Tris/EGTA solution, resuspended in 1 ml of dilution buffer and incubated 30 min on ice for lysis. After a centrifugation step to remove insoluble material, half of the supernatant was added to the beads incubated with anti-pan Na^+ channel antibody and the other half to the beads incubated with IgG. Beads with cell lysates were incubated with end-over-end mixing for 4 hours at 4°C, then washed three times with washing buffer (50 mM TRIS pH 7.5, 150 mM NaCl, 0.1% Triton X-100, 0.02% SDS, 5 mM EDTA pH 8 with Complete Mini) and once with washing buffer without Triton X-100. 35 µl of Western blot sample buffer (see Methods section in main text) were then added to the beads, triturated, and incubated at 100°C for 5 minutes. Samples were then separated by SDS-PAGE on 10% or 18% polyacrylamide gels and transferred to nitrocellulose membranes for Western blot analysis as described in the Methods section of the main text.

14. ^{3}H-STX binding:

^{3}H-STX binding was performed on intact cells, analyzed, and normalized to total cellular protein as previously described [33].

15. Deglycosylation:

5 µl of whole cell lysate from 1610-β1BV5 were treated with PGNase F (New England BioLabs P0704S) following the instructions of the manufacturer. After enzymatic deglycosilation the sample was mixed with Western blot sample buffer, separated by SDS-PAGE in a 10% polyacrylamide gel and transferred to a nitrocellulose membrane for Western blot analysis. Another 5 µl aliquot of untreated whole cell lysates was included in the Western blot analysis as a negative control.

16. Reverse-transcriptase PCR

Human Fetal frontal lobe total RNA samples (22 and 36 weeks gestation) were obtained from AMS Bio. Human postnatal frontal lobe and occipital lobe (n=4 each) total RNA samples were kindly provided by Dr. Miriam Meisler. The RT-PCR mix was prepared using 0.5 µg of RNA as template and the Titan One Tube RT-PCR System (Roche). Primers and PCR conditions available upon request.

17. Quantitative PCR

Custom Taqman MGB probes were ordered from Applied Biosystems for β1 (Product number 4331348, AILIWI2) and for β1B (Product number 4331348, AIMRUPA), both located in the region downstream of the exon 3 - intron 3 splice site. Sequences are available upon request. The equivalent efficiency of both sets of primers was confirmed. Six µg of each sample of RNA were incubated with DNase I (Invitrogen 18068-015) . cDNA was then synthetized from the processed RNA using the SuperScript First-Strand System (Invitrogen). The final volume of cDNA was then divided in two (half for the β1 assay and half for the β1B assay) and used as template for the Taqman Gene Expression Assay using the standard cycling program of a StepOnePlus Real-Time PCR System and TaqMan Gene Expression Master Mix (both from Applied Biosystems). C_T determinations were made with the StepOne Sotfware version 2.0 (Applied Biosystems). At least five repeats for each RNA sample were obtained. C_T values were then used to calculate mean C_T and SD for each sample.

18. CGN neurite outgrowth assays

Acute dissociation of cerebellar granule neurons from P14 wild-type and *Scn1b* null mice and their use in neurite outgrowth assays was described previously [12].

19. Statistical analyses

Categorical data was compared using Fisher's exact test.

For continuous data normality was tested using the Kolmogorov-Smirnov test. Group means were compared using ANOVA, withTukey's or Tamhane's T2 as *post-hoc* test. Statistical significance was set at a $P < 0.05$. SPSS v13.0 for Windows (SPSSInc.) was used for all determinations of statistical significance.

To edit the figures for this paper, images were exported to Adobe Photoshop CS3 Extended version 10.0.1 (Adobe). Besides cropping, and converting to greyscale where applicable, no other changes were made to the original images.

Results

1. A SCN1B mutation affecting β1B is found in two families with idiopathic epilepsy

Mutations in *SCN1B* are associated with human disease, including epilepsy and cardiac arrhythmia [38, 50, 53]. While one mutation specific to the region encoding β1B is linked to Brugada Syndrome [53], to date all of the *SCN1B* epilepsy mutations occur in the Ig loop domain shared by β1 and β1B [39]. To test the hypothesis that *SCN1B* mutations specifically affecting β1B and not β1 may cause epilepsy as well as arrhythmia, all *SCN1B* exons and intron 3, that is retained in β1B [22, 41], were amplified by PCR as part of a screening study of 150 genes in 360 unrelated patients with episodic brain disorders (118 with epilepsy, 110 with migraine, 66 with bipolar disorder, 35 with Tourette's syndrome, 25 with essential tremor, 4 with episodic ataxia, one with episodic vertigo and one with episodic syncope). A total of 14 *SCN1B* variants were identified, of which five resulted in amino acid substitutions in the unique region encoding β1B (**Table III.3**). Of these, three had minor allele frequencies (MAF) > 0.1 (p.L210P, p. S248R, and p.R250T) and occurred in all cohorts of patients. A variant (p.R214Q) had MAF = 0.005 but was also present in four out of eight cohorts. One variant (p.G257R) was identified in two unrelated probands with idiopathic

epilepsy (MAF = 0.002) as a heterozygous mutation (**Figure III.1.B**). One of those probands belonged originally to the Tourette's cohort, but upon further clinical investigation this patient was found to be comorbid for epileptic seizures, suggesting that this variant was associated with an epilepsy phenotype. Clinical characteristics of all probands are given in the Methods section.

To further examine whether the p.G257R variant was associated with Tourette's syndrome, an additional 192 unrelated Tourette's probands were genotyped (data not shown). The variant was not detected in this additional cohort, suggesting that p.G257R is not associated with increased risk of Tourette's syndrome. We screened an additional 187 normal control samples for the portion of intron 3 pertaining to the β1B splice isoform. One individual was found that had the p.G257R missense.

To examine segregation of p.G257R, additional samples from the probands' available family members were genotyped. For pedigree 1, both the proband and her mother carried the mutation and suffered from epilepsy. For pedigree 2, the mutation was inherited from the mother but there was no reported history of seizures in either parent (**Figure III.1.C**). The frequency of the mutated allele giving rise to the p.G257R missense mutation in patients with epilepsy (3 in 236 alleles) was significantly higher than the frequency in people without epilepsy (2 in 1242 - including healthy controls and probands with other neurological diseases; $P = 0.032$ Fisher's exact test). Thus, a *SCN1B* mutation in the region unique to β1B is linked with human epilepsy, possibly as a risk factor, given its presence in healthy controls, suggesting that wild-type β1B is critical for proper development of neuronal excitability.

2. Na^+ channel β1B is a secreted protein

The topology of β1 is well understood [17], however, less is known about β1B. *In silico* analyses of the predicted amino acid sequences of human β1 and β1B were performed using the Goldman Engelman Steitz hydrophobicity scale as described in Methods. In contrast to

Table III.3. Identified human *SCN1B* variants

							Allelic frequencies by cohort*										
							Epilepsy		Migraine		Bipolar		Tourette		ET		
Exon	position	dbSNP	Allele 1	Allele 2	impact	MAF	1	2	1	2	1	2	1	2	1	2	Total
1	chr19:40213619	none	G	T	g.+15 after the end of exon 1	nd	nd	nd	nd	nd	nd	nd	nd	nd	nd	nd	nd
3	chr19:40216664	rs55742440	T	C	Leu210Pro	0.394	136	94	132	86	83	45	38	32	30	20	696
3	chr19:40216676	none	G	A	Arg214Gln	0.005	227	1	219	1	122	2	69	1	50	0	692
3	chr19:40216779	none	C	A	Ser248Arg	0.147	197	33	184	34	109	19	54	16	47	3	696
3	chr19:40216784	none	G	C	Arg250Thr	0.149	198	34	185	33	108	20	54	16	46	4	698
3	chr19:40216804	none	G	A	Gly257Arg	0.002	231	1	220	0	128	0	69	1	50	0	700
5	chr19:40222354	rs28365107	T	G	g. -25 before the start of x05	nd	nd	nd	nd	nd	nd	nd	nd	nd	nd	nd	nd
5	chr19:40222365	rs28365109	C	A	g. -14 before the start of x05	nd	nd	nd	nd	nd	nd	nd	nd	nd	nd	nd	nd
5	chr19:40222457	rs28365106	C	T	g. +6 after the end of x05	nd	nd	nd	nd	nd	nd	nd	nd	nd	nd	nd	nd
5	chr19:40222507	none	G	T	g. +59 after the end of x05	nd	nd	nd	nd	nd	nd	nd	nd	nd	nd	nd	nd
6	chr19:40222530	rs28365105	C	G	g. -18 before the start of x06	nd	nd	nd	nd	nd	nd	nd	nd	nd	nd	nd	nd
6	chr19:40222577	rs2278995	T	C	3'UTR +42 after the stop codon	0.135	197	31	179	33	106	20	54	14	47	3	684
6	chr19:40222621	rs2278996	A	C	3'UTR +86 after the stop codon	nd	nd	nd	nd	nd	nd	nd	nd	nd	nd	nd	nd
6	chr19:40222718	none	C	A	3'UTR +184 after the stop codon	nd	nd	nd	nd	nd	nd	nd	nd	nd	nd	nd	nd

*number of chromosomes from each disease cohort with either allele 1 or 2; nd, not done

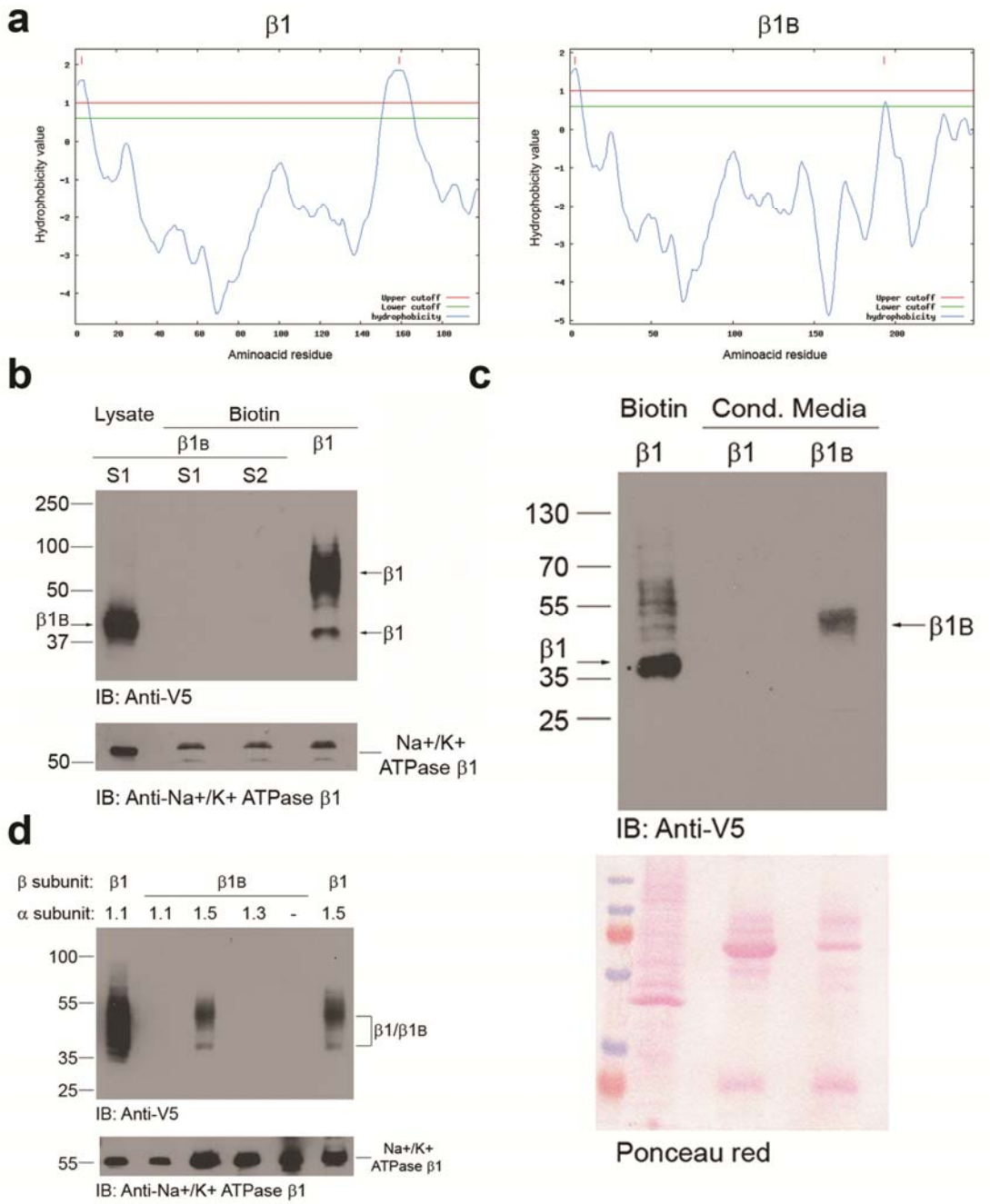

Figure III.2. β1B is a secreted protein. (**A**) Hydrophobicity plots analyzing the amino acid sequences of human β1 (left panel) or β1B (right panel) show identical N-terminal signal peptides. β1, but not β1B, contains a transmembrane domain. (**B**) β1 but not β1B is expressed at the cell surface. Upper panel: Lane 1 (β1B Lysate S1) demonstrates robust β1B protein expression in the whole-cell lysates of 1610-β1BV5. This same cell clone (β1B Biotin S1) showed that β1B is not expressed at the cell surface. An

independent 1610-β1BV5 clone (S2) gave a similar result. A biotinylated sample from 1610-β1V5 (Biotin β1) was used as positive control. (**C**) β1B but not β1 is expressed in conditioned media. Upper panel: Conditioned media collected from 1610-β1V5 (Cond. Media β1, lane 2) or 1610-β1BV5 (Cond. Media β1B, lane 3). A surface biotinylated sample of 1610-β1V5 cells (Biotin β1) was used as a positive control. Lower panel: Ponceau red staining of the nitrocellulose membrane shows the presence of protein in all lanes. (**D**) β1B is expressed at the cell surface in the presence of $Na_v1.5$. Upper panel: Cell surface biotinylation samples from cell lines expressing $Na_v1.1$, $Na_v1.3$, or $Na_v1.5$ with β1BV5 (β1B-1.1, β1B-1.3 and β1B-1.5 lanes, respectively). Surface biotinylation samples from cells coexpressing $Na_v1.1$ or $Na_v1.5$ with β1V5 (β1-1.1 and β1-1.5 lanes, respectively) were used as positive controls. A sample from 1610-β1BV5 cells (β1B"–" lane) served as a negative control. Lower panels in (**B**) and (**D**): A Western blot of the same samples probed with an antibody to the Na^+/K^+ ATPase β1 subunit served as loading control for surface proteins. All blots are representative of triplicate experimental repeats. Molecular weight markers in kilodaltons. Arrows indicate β1 or β1B immunoreactive bands.

β1 [17], a hydrophobic transmembrane domain was not predicted for β1B (**Figure III.2.A**). The predicted β1B amino acid sequences from rat and mouse were analyzed similarly for hydrophobicity (**Figure III.3**). In contrast to predicted amino acid sequences for β1 from these species, which are highly conserved (**Figure III.4.A**), very little similarity was found in the C-terminal region unique to β1B, suggesting that the sequence of this domain is species specific (**Figure III.4.B**). Importantly, none of theseunique β1B sequences contained a predicted transmembrane domain, suggesting that β1B may be a secreted protein (**Figure III.3**).

To investigate whether β1B is indeed a secreted protein we stably transfected Chinese hamster lung 1610 fibroblasts with a V5-His epitope-tagged human β1B cDNA construct (1610-β1BV5). Protein expression at the cell surface was assessed by surface biotinylation, probing the final Western blot with anti-V5 antibody. 1610 cells stably expressing β1V5 (1610-β1V5) were used as a positive control [38] and, as expected, β1V5 was detected at the cell surface (**Figure III.2.B**). In contrast, β1BV5 was not detected at the cell surface despite abundant levels of β1BV5 protein in the whole cell lysate sample (**Figure III.2.B**). We next assayed conditioned media by Western blot to test for the presence of β1B. Anti-V5 immunoreactive bands were present in conditioned

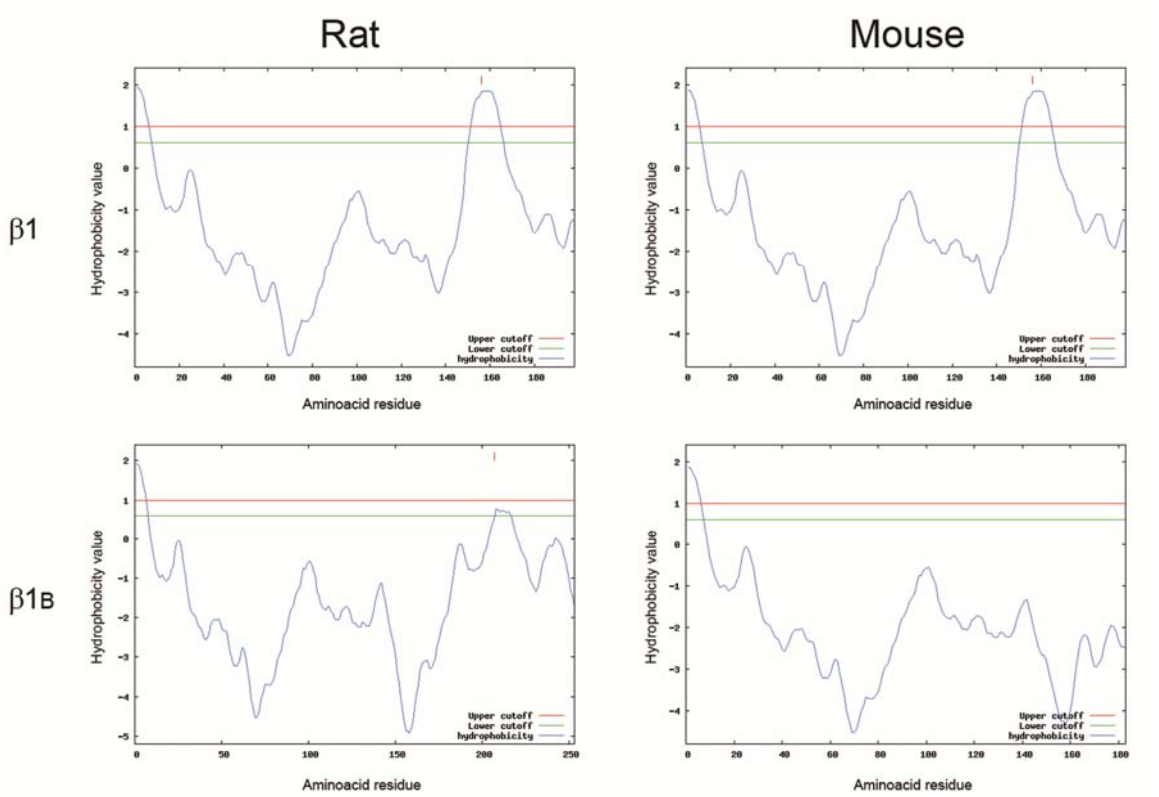

Figure III.3. Rat and mouse β1B are predicted to be secreted proteins. The predicted amino acid sequences of rat and mouse β1 (upper panels) contain signal peptide and transmembrane domains. In contrast, rat and mouse β1B (lower panels) contain a signal peptide but no transmembrane domain. Hydrophobicity analyses were performed using TopPred software as described in Methods.

media from 1610-β1BV5 cells, while, as expected, no bands were detected in media from 1610-β1V5 cells despite high levels of protein present on the Ponceau red stained blot (**Figure III.2.C**).

While performing this project we noticed that the migration of β1B on SDS-PAGE was variable, over a size range of approximately 26 kDa (the predicted molecular weight of non-glycosylated β1B) to 45 KDa, with the majority of experiments showing the ~45 kDa band. Interestingly, the same clonal line of 1610-β1BV5 cells yielded bands of different sizes in different experiments, and we were unable to identify the source of this variability. We hypothesized that these bands might represent different glycosylation

Figure III.4. The unique C-terminal region of β1B is not conserved between species. (**A**) Alignments of the predicted amino acid sequences of the C-terminal region of β1 encoded by exons 4 and 5 in human, rat and mouse using the CLUSTALW algorithm. (**B**) Alignments of the predicted amino acid sequences of the unique C-terminal region of β1B encoded by retained intron 3 in human, rat and mouse using the CLUSTALW algorithm. Numbers above all alignments correspond to the human sequence.

states of β1B and that enzymes present in the culture medium or experimental solutions might result in artifactual deglycosylation of this protein. To test this, whole cell lysates of 1610-β1BV5 cells were treated with PNGase F and samples were then analyzed by Western Blot. PNGase F treatment resulted in collapse of the β1B immunoreactive band from ~45 to ~26 KDa (**Figure III.5**), suggesting that the various immunoreactive β1B bands identified in the conditioned media represent different glycosylation states. Because we do not yet have a specific anti-human β1B antibody, we were not able to assess the glycosylation state of native β1B in human brain, however, this will be the

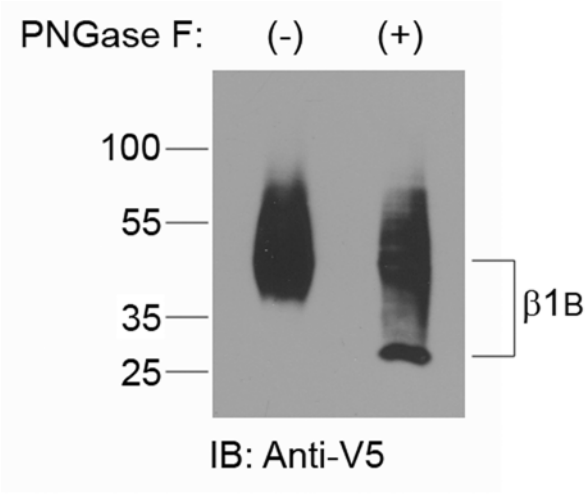

Figure III.5. β1B is a glycoprotein. Western blot of 1610-β1BV5 whole cell lysates before (left lane) and after (right lane) treatment with PNGase F. This blot is representative of three experimental repeats. Molecular weight markers are given in kilodaltons. Arrows indicate β1B immunoreactive bands. The lower immunoreactive band is consistent with the molecular weight of fully deglycosylated β1B (~26 kDa).

focus of future investigation. Native rat β1B migrates at ~45 kDa [22], thus we are reasonably confident that this will be the case for human β1B.

Taken together, these data suggest that both β1 and β1B are glycoproteins, however β1 has transmembrane topology while β1B is secreted.

The experiments in **Figure III.2** (panels **B** and **C**), demonstrate that β1B is secreted from cells that do not express Na^+ channels. We then decided to test the ability of β1B to associate with different α subunits. To test whether the presence of a VGSC α subunit may result in retention of β1B at the cell surface, we performed surface biotinylation assays on cell lines coexpressing human β1BV5 with human $Na_v1.1$, $Na_v1.3$, or $Na_v1.5$. Similar to 1610 cells, β1B was not detected at the surface of cells coexpressing $Na_v1.1$or $Na_v1.3$ (**Figure III.2.D**), suggesting that β1B is secreted in spite of the presence of these channels. In contrast, cell surface β1B expression was detected in biotinylated samples from cells coexpressing $Na_v1.5$ and β1B (**Figure**

III.2.D), suggesting that β1B may be selectively retained at the cell surface by this channel.

β1 associates with multiple VGSC α subunits and increases their functional expression [14, 19, 22]. For example, β1 associates with $Na_v1.2$ and this association is functionally detected by increased Na^+ current density and by increased cell surface ^{3}H-saxitoxin (STX) binding [18, 32]. Rat β1B increases the cell surface expression of rat $Na_v1.2$ in transfected cells, suggesting that these subunits functionally associate [23]. Similarly, human β1B co-expression increases Na^+ current density generated by human $Na_v1.5$ [52]. Here, we tested whether human β1B affects the cell surface expression of human $Na_v1.3$. Because $Na_v1.3$ is predominately expressed in fetal brain [8] it is most relevant to β1B physiology. Chinese hamster ovary fibroblasts stably expressing human $Na_v1.3$ (CHOh$Na_v1.3$) [34] were transfected with human β1 or β1B cDNAs. [^{3}H]-STX binding to intact cells was used to assay Na^+ channel cell surface expression [32]. Because STX is membrane impermeant, binding to intact cells measures only cell surface and not intracellular channels [30, 32]. As expected, β1 significantly increased cell surface ^{3}H-STX binding compared to $Na_v1.3$ alone ($Na_v1.3$ + β1: 8.93 ± 0.72 fmol/mg vs. $Na_v1.3$ alone: 5.53 ± 0.65 fmol/mg, n = 9 for each subunit combination, P < 0.001). In contrast, β1B did not significantly increase cell surface ^{3}H-STX binding compared with untransfected cells ($Na_v1.3$ + β1B: 5.90 ± 0.92 fmol/mg) (**Figure III.6.A**), suggesting that human $Na_v1.3$ and β1B do not functionally associate.

Because *SCN1B* mutations affecting the region specific to β1B are linked to cardiac arrhythmia [52] and epilepsy (shown here), we tested the effects of human β1B co-expression on human $Na_v1.1$, a common target of genetically determined epilepsy [36], and on human $Na_v1.5$, the α subunit most prevalent in heart and a target of inherited arrhythmia [8, 42, 44]. For unknown reasons, we were unable to establish stable β1V5- or β1BV5-expressing cell lines using HEKh$Na_v1.1$ cells [38]. Thus, all

experiments with this cell line were performed following transient transfection of β1V5 or β1BV5 cDNA. We were able to establish stable β subunit-expressing lines using HEK cells stably transfected with human $Na_v1.5$ (HEKh$Na_v1.5$). The effects of β1 or β1B on cell surface expression of $Na_v1.1$ or $Na_v1.5$ were then studied using cell surface biotinylation assays. Western blots were quantified by densitometry and normalized to the cell surface levels of α subunit in cells expressing no β subunits. Neither β1 nor β1B affected the levels of cell surface expression of $Na_v1.1$ compared to cells expressing α subunit alone (1.67 ± 0.13 versus 1.49 ± 0.34 versus 1.00 ± 0.41 arbitrary units respectively, n = 3 for each condition, P = 0.36, **Figure III.6.B**). The lack of functional modulation of human $Na_v1.1$ by β1 in this cell line was reported previously [38]. Similarly, neither β subunit affected the cell surface levels of human $Na_v1.5$ detectable with this assay (HEKh$Na_v1.5$: 1 ± 0.17; HEKh$Na_v1.5$ + β1: 0.77 ± 0.06; HEKh$Na_v1.5$ + β1B: 0.75 ± 0.00, n = 3 for each condition, P = 0.27, **Figure III.6.B**).

We next examined whether β1B associates with $Na_v1.1$, $Na_v1.3$, or $Na_v1.5$ using coimmunoprecipitation assays. In these experiments, anti-pan Na^+ channel antibody was used for the immunoprecipitation step from Triton X-100-solubilized whole cell lysates and Western blots were probed with anti-V5 to detect associated β subunits. β1 co-precipitated with $Na_v1.1$, (**Figure III.6.C**), $Na_v1.3$ (**Figure III.6.D**), and $Na_v1.5$ (**Figure III.6.E**). In contrast, β1B association was not detected with any α subunit (**Figure III.6.C - E**). Western blots of whole cell lysates from each cell line coexpressing α and β1BV5 subunits demonstrated the presence of β1B in all three (**Figure III.6.F**). Lack of association between $Na_v1.5$ and β1B in the coimmunoprecipitation assay contrasts with our result showing cell surface retention of β1B in the presence of $Na_v1.5$, and with a previous report of functional β1B-$Na_v1.5$ association [51]. One possible explanation for this discrepancy is that the interaction between β1B and $Na_v1.5$ is disrupted by detergent solubilization.

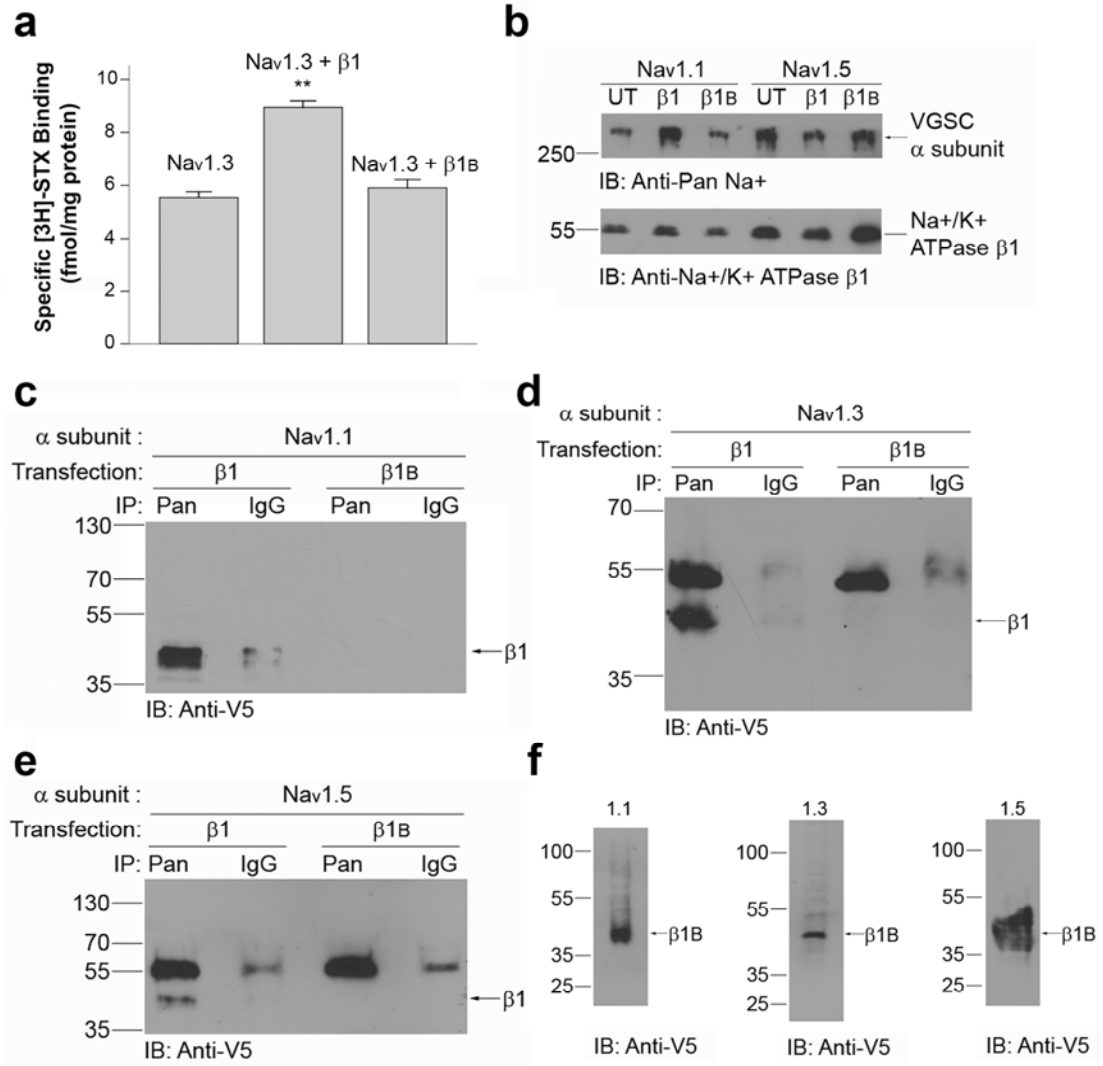

Figure III.6. Association of β1B with $Na_v1.1$, $Na_v1.3$ or $Na_v1.5$ is not detectable. (**A**) [^{3}H]-STX binding to intact cells stably expressing $Na_v1.3$, $Na_v1.3$ + β1V5 ($Na_v1.3$+β1), or $Na_v1.3$ + β1BV5 ($Na_v1.3$+β1B). Specific binding data were normalized to protein concentration. Data presented as mean ± SE. Significance: ** $P < 0.001$. (**B**) Surface biotinylation comparison of cell surface expression of $Na_v1.1$ or $Na_v1.5$ in the presence of β1 versus β1B. Representative Western blot analysis of surface biotinylation assays of cells stably expressing $Na_v1.1$ or $Na_v1.5$ alone ($Na_v1.1$ UT or $Na_v1.5$ UT), $Na_v1.1$ or $Na_v1.5$ with β1V5 ($Na_v1.1$ β1 or $Na_v1.5$ β1), or $Na_v1.1$ or $Na_v1.5$ with β1BV5 ($Na_v1.1$ β1B or $Na_v1.5$ β1B) probed with anti-pan Na^+ channel antibody. Analysis of the same membrane with anti-Na^+/K^+ ATPase β1 subunit antibody served as loading control. (**C**-**E**) Coimmunoprecipitation from cells stably coexpressing $Na_v1.1$ (**C**), $Na_v1.3$ (**D**) or $Na_v1.5$ (**E**) with β1V5 or β1BV5, as indicated, was performed using anti-pan Na^+ channel antibody for immunoprecipitation followed by anti-V5 to probe the Western blot. Immunoprecipitation with non-immune IgG was performed as a negative control. (**F**) Western blots of equal aliquots of whole cell lysates of β1B expressing cells used in panels **C** – **E** to demonstrate the presence of β1B. Molecular weight markers are given in kilodaltons. Arrows indicate immunoreactive β1 or β1B bands.

These results suggest that β1B may associate selectively, but perhaps transiently or with low affinity, with some VGSC α subunits but not others. Further, if β1B associates with $Na_v1.5$, this suggests that the function of β1B in heart, where $Na_v1.5$ is the principal Na^+ channel, may be different than its function in brain, where $Na_v1.1$ and $Na_v1.3$ are predominately expressed.

3. Expression patterns of β1 and β1B in human brain are developmentally regulated

We demonstrated previously that β1 and β1B mRNA have complementary expression patterns in rat brain. β1B is expressed predominantly during embryonic rat brain development, with levels decreasing after birth. In contrast, β1 expression is low in embryonic rat brain, but becomes dominant over β1B in postnatal brain [22]. To determine whether this developmental expression pattern is conserved in humans we performed reverse transcriptase PCR (RT-PCR) using primers specific for β1 or β1B and human frontal lobe total RNA as template. Samples were obtained from both human embryonic brain (22 weeks and 36 weeks of gestation) and human postnatal brain (age range: 9-56 years). In addition, we obtained occipital lobe total RNA from the postnatal subjects. RNA from *Scn1b* null mouse brain was used as a negative control. At the earliest time point assayed, 22 weeks of gestation, both variants were detected, although higher levels of β1B were detected compared to β1. As development progressed, the level of β1B appeared to remain relatively constant while the level of β1 increased (**Figure III.7.A**). To quantify these results we prepared cDNA from each RNA sample and performed quantitative PCR using the Taqman assay. Ratios of β1 to β1B were compared using the $2^{-\Delta CT}$ method. At 22 weeks of gestation β1:β1B= 0.08 (mean $2^{-\Delta CT}$ ± SD: 0.08 ± 0.15). At 36 weeks of gestation β1B and β1 levels were similar (β1:β1B

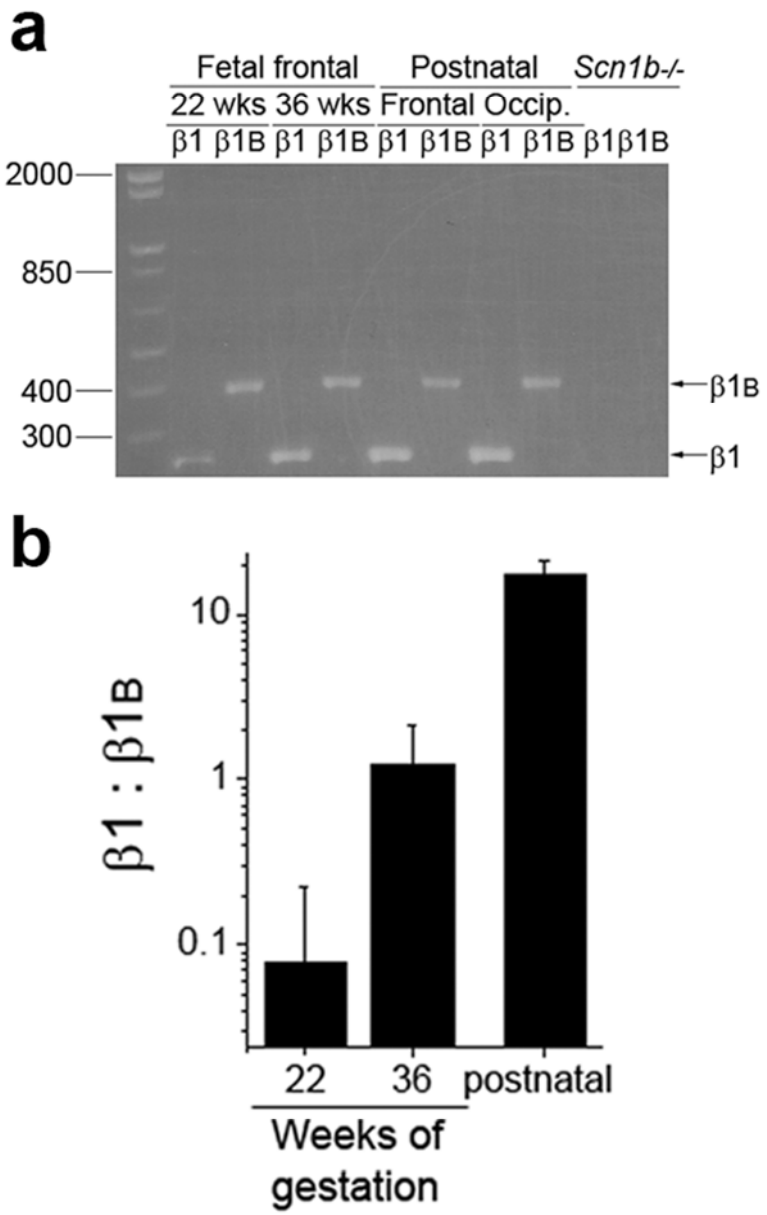

Figure III.7. β1B is the predominant *SCN1B* splice variant during human fetal brain development. (**A**) Reverse-transcriptase PCR using primers for β1 or β1B performed with total RNA as template from human embryonic frontal lobe (22 weeks gestation: lanes 1 and 2; or 36 weeks gestation: lanes 3 and 4), postnatal frontal lobe (lanes 5 and 6), or postnatal occipital lobe (lanes 7 and 8). Samples of total RNA from *Scn1b* null mouse brain were analyzed in parallel as negative controls (lane 9 and 10). The gel shown is representative of triplicate experimental repeats. Nucleic acid markers are shown in base pairs. Arrows indicate migration of β1 and β1B bands. (**B**) Quantitative PCR was performed with cDNAs generated from the RNA frontal lobe samples using the Taqman assay as described in Methods. Ratios of β1 to β1B were compared using the $2^{-\Delta CT}$ method for each time point. Values are presented as mean ± SD. Note the logarithmic scale on the y-axis.

4. β1B stimulates neurite outgrowth in CGNs through β1 adhesion

VGSC β subunits contain a single extracellular Ig loop domain and function as CAMs [27, 28, 31]. β1 promotes CGN neurite outgrowth *in vitro* and *in vivo* through *trans* homophilic cell adhesive interactions [3, 4, 12]. Because β1 and β1B contain identical Ig loop domains, we hypothesized that β1B may function as a secreted CAM to promote neurite outgrowth. Previous results using an engineered soluble β1 extracellular domain support this idea [12]. To test this hypothesis, we investigated the ability of β1B to promote neurite outgrowth of CGNs. CGNs were isolated from P14 C57BL/6 mice and plated on monolayers of untransfected 1610 cells (as a negative control), 1610-β1V5 cells (as a positive control), or 1610-β1BV5 cells, as described in Methods. After 24 hours of incubation cells were fixed, immunostained with anti-GAP43, and the length of the longest neurite measured. Consistent with previous results [4, 12], the mean neurite length of CGNs plated on 1610-β1V5 cells (64.88 ± 2.63 μm SE) was significantly greater than CGNs plated on 1610 cells (40.64 ± 1.70 μm). Importantly, the mean neurite length of CGNs plated on 1610-β1BV5 cells (69.43 ± 2.46 μm) was also statistically greater than CGNs plated on 1610 cells, and not significantly different from cells plated on 1610-β1V5 cells (n = 300 for each group, P< 0.001; **Figure III.8.A**). Thus, similar to β1, β1B functions as a CAM in neurite outgrowth. In contrast to β1, however, we propose that β1B functions as a secreted rather than as a transmembrane CAM.

The neurite outgrowth promoting activity of β1 is abolished in CGNs isolated from *Scn1b* null mice [12], demonstrating that *trans* homophilic β1-β1 interactions are required. To test if a similar requirement of β1 expression on the neuron exists for β1B signaling, we compared neurite outgrowth of CGNs isolated from *Scn1b* null mice vs. wild-type controls plated on β1B-secreting monolayers. In agreement with our previous studies [12], the mean neurite length of WT CGNs plated on 1610-β1V5 cells (75.46 ± 2.44 μm) was statistically greater than for *Scn1b* null CGNs (36.42 ± 1.45 μm). In a

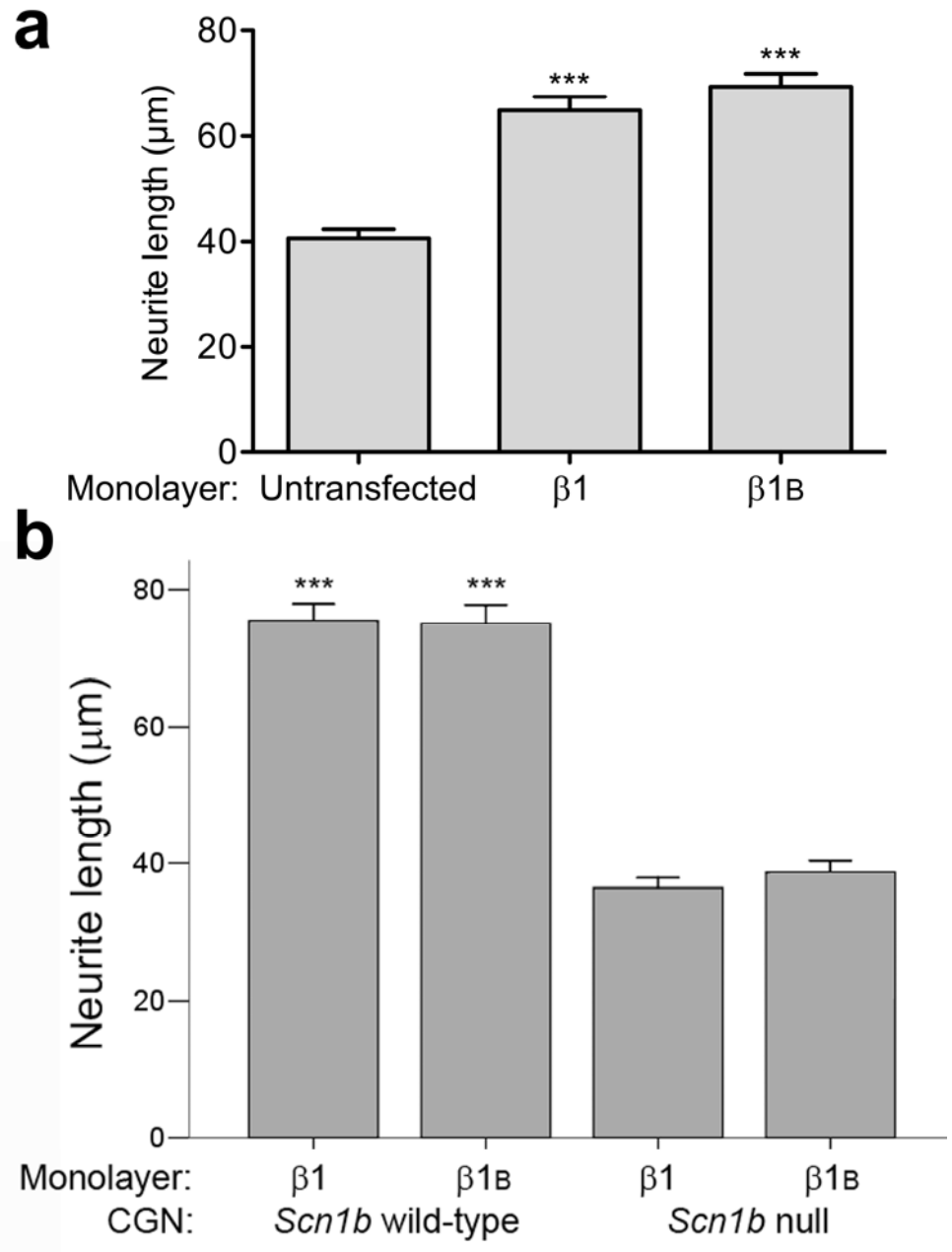

Figure III.8. β1B stimulates neurite outgrowth of CGNs.(**A**) Neurite lengths of CGNs isolated from wild-type mice grown on 1610 cells (Untransfected) or 1610 cells stably expressing β1V5 (β1) or β1BV5 (β1B) measured as described in Methods. Significance: *** *P*< 0.001. (**B**) Neurite lengths of CGNs from wild-type and *Scn1b* null mice grown on 1610 cells stably expressing β1V5 or β1BV5. Significance: *** *P*< 0.001. All data are presented as mean ± SE.

similar manner the mean neurite length of WT CGNs plated on 1610-β1BV5 cells (75.06 ± 2.71 μm) was significantly higher than that of null CGNs (38.66 ± 1.69 μm, n = 300, P< 0.001; **Figure III.8.B**). There was no significant difference between the mean neurite lengths of WT or null CGNs plated on 1610-β1V5 cells versus those on 1610-β1BV5 cells. These data demonstrate that the neurite outgrowth promoting ability of β1B requires interaction with β1 subunits present at the neuronal surface, similar to the mechanism described for β1 [3, 4].

5. β1B p.G257R is a trafficking deficient mutation resulting in a functional null allele

To investigate the mechanism by which β1B p.G257R could cause seizures we stably transfected 1610 cells with V5-His-tagged p.G257R cDNA (1610-p.G257RV5). In contrast to wild-type β1BV5, p.G257RV5 was not detected in conditioned media (**Figure III.9.A**) despite high levels of expression of the protein in the whole cell lysates (**Figure III.9.B**) and in the Ponceau red stained blot (**Figure III.9.A**). We used surface biotinylation assays to determine whether p.G257RV5 might be present at the cell surface. As demonstrated in **Figure III.9.B**, p.G257RV5 was detected in the whole cell lysate but not in the conditioned media or on the cell surface. From these data we concluded that p.G257R is a trafficking deficient mutant. To confirm that the trafficking deficiency of p.G257R is specifically pathogenic we tested three other *SCN1B* non-seizure related polymorphic variants containing amino acid substitutions in β1B found in our cohort of patients: p.R214Q, p.S248R, p.R250T. These variants were present in each disease cohort and hence were not associated with epilepsy (**Table III.3**). To facilitate detection of these proteins, V5-His epitope tags were inserted at their C-termini, similar to p.G257RV5. 1610 cells were stably transfected and conditioned media were collected. In contrast to p.G257RV5, all three variants were detected in the conditioned media similar to wild-type β1BV5 (**Figure III.9.C**). These results suggest that the lack of

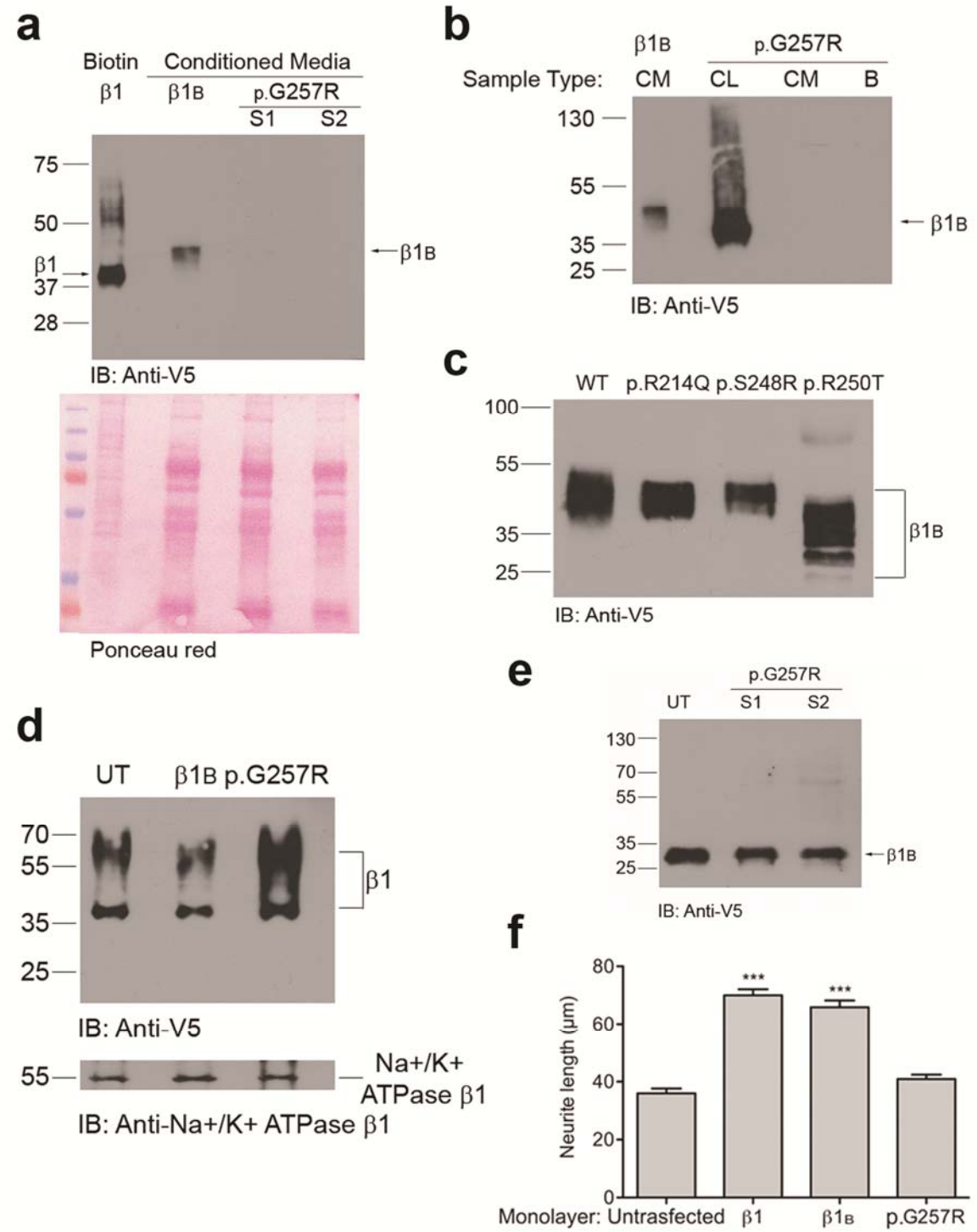

Figure III.9. β1B p.G257R is a trafficking deficient mutant. (**A**) β1B but not p.G257R is detected in conditioned media. Upper panel: Conditioned media from 1610- β1BV5 (Cond. Media β1B) or 1610-p.G257RV5 (Cond. Media p.G257R S1 and S2, 2 independent cell clones). A surface biotinylated sample from 1610-β1V5 (Biotin β1) was used as a positive control. Lower panel: Ponceau red staining of the nitrocellulose membrane. (**B**) p.G257R is retained intracellularly. Western blot analysis of whole-cell

lysate (p.G257R CL), surface biotinylated cells (p.G257R B), or conditioned media (p.G257R CM) from the same 1610-p.G257RV5 cell clone. Conditioned media from 1610-β1BV5 cells (β1B CM) shows normal secretion of β1B. (**C**) β1B polymorphic variants are secreted. p.R214Q, p.S248R, and p.R250T are normally secreted into conditioned media similar to wild-type β1B. (**D**) p.G257R does not interfere with the cell surface expression of β1. Upper panel: Surface biotinylation assays of 1610-β1V5 and either β1B or p.G257R. 1610-β1V5 cells (UT lane) used as positive control. Lower panel: Western blot of the same samples with an antibody to the Na^+/K^+ ATPase β1 subunit served as loading control for surface proteins. (**E**) p.G257R does not interfere with normal secretion of β1B. Conditioned media from two independent 1610-β1BV5 clones and p.G257R (p.G257R S1 and S2). Conditioned media from 1610-β1BV5 cells (UT) was used as positive control. (**F**) p. G257R does not stimulate neurite outgrowth. Neurite lengths of CGNs isolated from wild-type mice grown on 1610 cells (Untransfected),1610 cells stably expressing β1V5 (β1), 1610 cells stably expressing β1BV5 (β1B), or 1610 cells stably expressing p.G257RV5. Data are mean ± SE. Significance: *** $P< 0.001$. All Western blots are representative of three experimental repeats. Molecular weight markers are given in kilodaltons.

secretion of p.G257R is a pathogenic change and not a normal variability present in β1B polymorphisms.

To test whether p.G257R may inhibit β1 cell surface expression via a dominant-negative function, 1610-β1V5 cells were stably transfected with cDNA encoding either β1B or p.G257R in pTRACER. This plasmid encodes EGFP under control of a separate promoter than that used for the multiple cloning site. After stable transfection, greater than 99% of the 1610-β1V5 cells coexpressing β1B or p.G257R showed green fluorescence, confirming β1B or p.G257R protein expression (**Figure III.10**). Surface biotinylation assays were subsequently performed on 1610-β1V5 cells or 1610-β1V5 cells coexpressing either wild-type β1B or p.G257R in pTRACER. Surface expression of similar levels of β1V5 surface expression, indicating that co-expression of β1B or β1V5 was detected by probing the Western blots with anti-V5 antibody. All lanes showed p.G257R did not interfere with β1 trafficking to the plasma membrane (**Figure III.9.D**). A similar strategy was used to assess whether p.G257R functioned as a dominant-negative for wild-type β1B secretion. Stably transfected 1610-β1BV5 cells were transfected with p.G257R in pTRACER. Western blots of conditioned media were

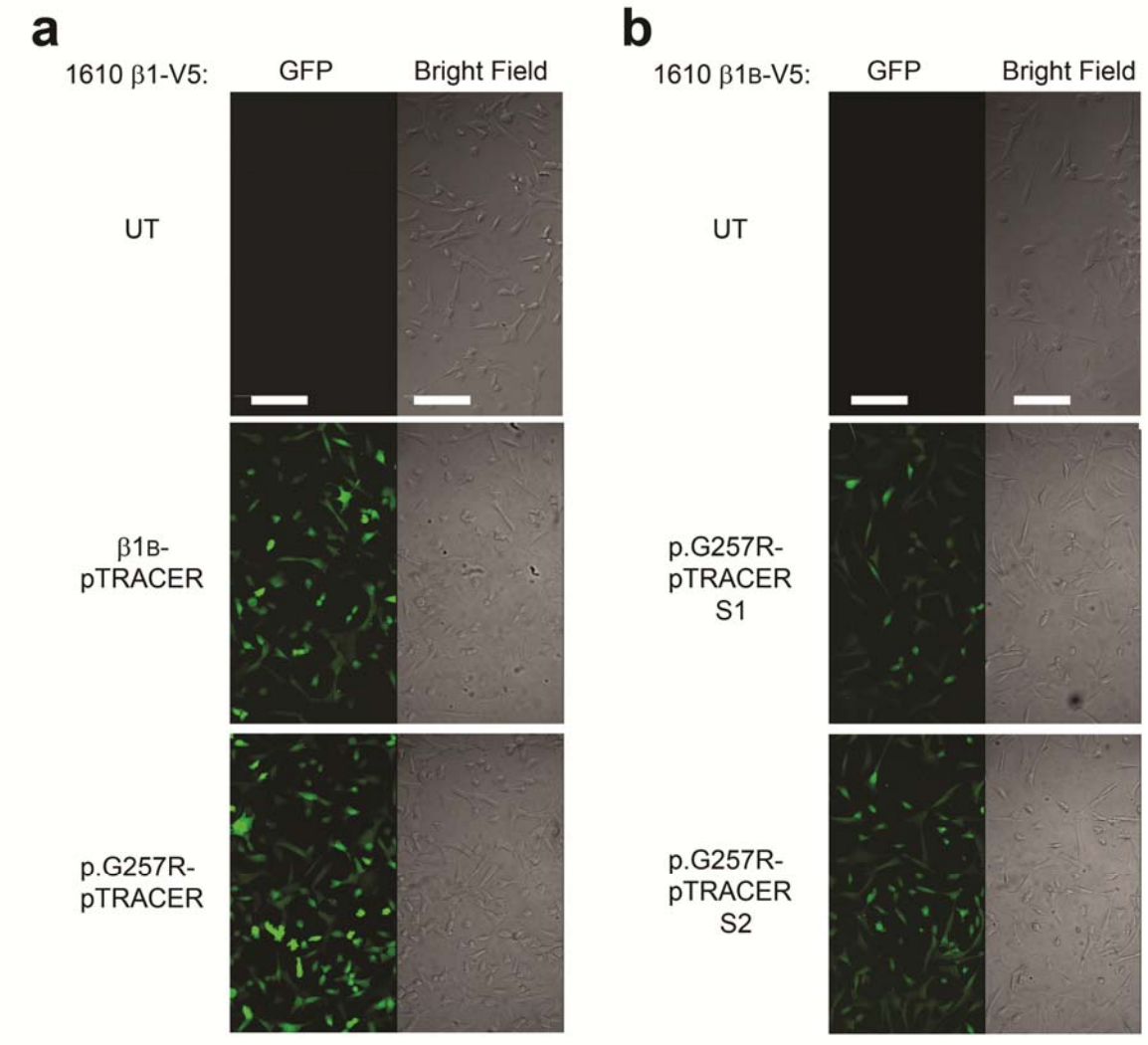

Figure III.10. Confirmation of expression of β1B or p.G257R in pTRACER in 1610-β1V5 cells or 1610-β1BV5 cells, as indicated. 1610-β1V5 cells or 1610-β1BV5 cells were stably transfected with the pTRACER constructs, fixed with 4% paraformaldehyde, and monitored for GFP fluorescence (left panels) and bright field images (right panels), as indicated, using confocal microscopy. UT indicates untransfected cells. Scale bars, 100 μm.

probed with anti-V5 to detect wild-type β1B secretion. Conditioned media collected from 1610-β1BV5 cells were used as a positive control. Comparable levels of anti-V5

immunoreactive bands were detected in all lanes, demonstrating that p.G257R does not interfere with wild-type β1B secretion (**Figure III.9.E**).

Consistent with the observed intracellular retention of p.G257RV5, wild-type CGNs plated on 1610-p.G257RV5 cell monolayers had mean neurite lengths that were indistinguishable from those plated on untransfected 1610 cells (1610-p.G257RV5: 40.87 ± 1.56 μm vs. 1610: 35.96 ± 1.63 μm, *n* = 300 and 200, respectively) and significantly shorter than CGNs plated on 1610-β1V5 (70.02 ± 2.07 μm, *n* = 300) or 1610-β1BV5 (65.89 ± 2.31 μm, *n* = 300, *P*< 0.001) (**Figure III.9,F**). These results demonstrate that p.G257R is a functional null allele.

Discussion

In spite of an extensive literature demonstrating dramatic effects of β1 subunit coexpression on Na^+ current in heterologous systems, the major role of *SCN1B in vivo* appears to be cell adhesion rather than current modulation [39]. Studies with *Scn1b* null mice show that this gene plays significant roles in promoting neuronal migration, neurite extension, and axonal fasciculation in brain and corticospinal tract [3, 4]. In contrast, the observed effects of *Scn1b* deletion on neuronal Na^+ current are cell type specific and subtle [1, 3, 10, 48]. Na^+ current is required for *Scn1b*-mediated neurite outgrowth [3], but we argue that *Scn1b*-mediated modulation of Na^+ current is not. Localization of $Na_v1.6$ to the axon initial segment is modulated by *Scn1b* and is critical for *Scn1b*-mediated neurite outgrowth in CGNs [3]. However, we argue that this effect can be attributed to *Scn1b*-mediated adhesive interactions and not *Scn1b*-mediated Na^+ current modulation.

The present results emphasize that understanding the physiological role of *Scn1b* in brain must include consideration of the functions of β1B in addition to those of β1. This is under-appreciated in the field, as most studies have considered only β1. Our

results showing that β1B is a secreted CAM expressed in embryonic brain that may not associate with neuronal VGSC α subunits suggest that this splice variant may play critical roles in *Scn1b* function during brain development through non-conducting cell adhesive mechanisms. Interestingly, because β1B is a secreted CAM, it may play autocrine or paracrine roles in neuronal pathfinding. Deletion of β1B may make a significant contribution to the severe neurological *Scn1b* null phenotype. This phenotype includes not only *Scn1b* null mice but also the functional null *SCN1B* p.R125C mutation linked to Dravet syndrome in humans [38]. Prior to the present study, all reported *SCN1B* mutations linked to human epilepsy were found to be located in the Ig loop domain that is shared between β1 and β1B. These results suggest that cell adhesion is clinically relevant, and importantly, that disruption of either splice variant may result in human brain disease. Novel evidence provided here demonstrates that β1B p.G257R (located in the retained intronic region unique to β1B) also associates with human epilepsy, strengthening the hypothesis that β1B is a critical player in brain development.

CAMs are critical for normal nervous system development and for synaptic plasticity in adulthood. Dysregulation of NCAM expression or signaling is associated with a number of brain disorders, including depression, anxiety, bipolar disorder and schizophrenia [see [6] for review]. Deletion of Nr-CAM in mice results in an altered behavioral phenotype reflective of increased impulsivity [29]. Deletion of the CAM Lsamp in mice leads to heightened reactivity to novelty [7] and conditional deletion of L1-CAM in brain results in decreased anxiety-like behavior [24]. Epilepsy and neuropsychiatric disease have a bidirectional relationship of comorbidity [13, 15, 20, 40, 46] and thus may share common genetic mechanisms. *SCN1B*-dependent neuronal pathfinding may be critical to abnormal brain development in both neurological and psychological disease. Expression of multiple *SCN1B* splice variants, including a secreted form, is also consistent with other members of the Ig superfamily of CAMs [21, 43]. For example,

increased expression of secreted forms of NCAM is associated with bipolar disorder and depression [6]. In a similar way, modulation of β1B secretion may have pathological consequences in brain, as suggested here for β1B p.G257R.

We did not detect biochemical or functional association of human β1B with human VGSC α subunits, including $Na_v1.1$, $Na_v1.3$, and $Na_v1.5$. These results strengthen the argument that the β1B splice variant functions as a CAM independent of the ion-conducting pore. Intriguingly, however, β1B was sequestered at the cell surface by $Na_v1.5$ but not by $Na_v1.1$ or $Na_v1.3$. This result implies that β1B and $Na_v1.5$ associate functionally (but perhaps transiently or with low affinity), in agreement with a previous study showing modulation of $Na_v1.5$ currents in heterologous cells by β1B [53]. A *SCN1B* mutation linked to Brugada syndrome disrupts the current modulatory properties of β1B [53], supporting the idea that β1B function in human heart may be different than in brain. In addition to heart, $Na_v1.5$ is expressed in a population of limbic neurons in brain [16]. It is possible that differential β1B expression in specific brain areas may result in different effects on excitability and neurite outgrowth depending on which Na^+ channel α subunits are co-expressed. These data, in concert with our recent results showing specific partnering of $Na_v1.6$ and β1 subunits in cerebellum [3], raise the possibility that certain VGSC α and β subunits form selective partnerships in excitable cells.

The epilepsy-linked mutation *SCN1B* p.G257R results in intracellular retention of β1B. This mechanism is consistent with that of *SCN1B* p.R125C, linked to Dravet syndrome, that results in intracellular retention of β1 and, presumably, β1B as well [37]. It is interesting to consider that defective β1/ β1B trafficking may be a common mechanism of some *SCN1B* epilepsy mutations, resulting in functional null alleles including reduced secretion of β1B. In addition to abolishing β1/β1B function, retention of these subunits in the cytoplasm may inhibit signaling or trafficking of other proteins or induce cellular stress leading to neural degeneration. Thus, *SCN1B* gene dosage

appears to be critical for brain disease. Heterozygous expression of one mutant and one wild-type *SCN1B* allele results in mild to moderate GEFS+ spectrum disorders with incomplete penetrance in human patients, with symptom severity likely depending on genetic background and/or epigenetic factors. In this sense the pedigrees presented in our study are similar to those reported previously [45, 53], and is compatible with the presence of the mutation in healthy controls. In contrast, inheritance of two mutant *SCN1B* alleles affecting the region common to β1 and β1B results in Dravet syndrome, the most severe, and sometimes fatal, disorder of the GEFS+ spectrum. If, as predicted by the present results, secreted β1B regulates neurite extension in developing human brain through cell adhesive interactions, gene dosage will be critically important, as varying levels of *SCN1B* expression are predicted to regulate gradients of β1B in the extracellular matrix, which may then serve as attractive or repulsive signals. The contribution of β1B to brain development is not yet known, however, our results shed new light on the role of this subunit in *SCN1B* function and present a fresh perspective on the biology of these multi-functional subunits.

Acknowledgements

Additional experimental contributions: William Brackenbury carried out the neurite outgrowth assays, Chunling Chen generated the *Scn1b* null mice and provided advice on many of the biochemistry, molecular, and cell biology experiments. Both of them are at the laboratory of Dr. Lori Isom, Department of Pharmacology, University of Michigan. Ron G. Lafréniere, Guy A. Rouleau (both at Centre of Excellence in Neuromics, Université de Montreal and Emerillon Therapeutics Inc., Montreal, Canada), and Patric Cossette (at the Department of Medicine, Université de Montreal, and CHUM-Hôpital Notre-Dame, Montreal, Canada) collected the patient data and samples, performed the genetic screening and cloned β1B into p.TRACER.

This research was supported by NIH grant MH059980 to LLI and by members of the Partnership for Pediatric Epilepsy Research, which includes the American Epilepsy Society, the Epilepsy Foundation and Parents Against Childhood Epilepsy to LLI. GAP was supported by a predoctoral fellowship from the Epilepsy Foundation of Greater Chicago and the University of Michigan Cardiovascular Center Inaugural Predoctoral Fellowship. WJB was supported by a postdoctoral fellowship from the Epilepsy Foundation. The authors acknowledge the expert technical assistance of T.J. O'Shea, Raja Dondeti, Julie Jones, Guy Lenk, Yoshihiro Morishima and are grateful for the scientific advice of Dr. Jack Parent and Dr. Miriam Meisler.

Bibliography

[1] T.K. Aman, T.M. Grieco-Calub, C. Chen, R. Rusconi, E.A. Slat, L.L. Isom, I.M. Raman, Regulation of persistent Na current by interactions between beta subunits of voltage-gated Na channels, J Neurosci 29 (2009) 2027-2042.

[2] S. Bourgeois, D. Labuda, Dynamic allele-specific oligonucleotide hybridization on solid support, Anal Biochem 324 (2004) 309-311.

[3] W.J. Brackenbury, J.D. Calhoun, C. Chen, H. Miyazaki, N. Nukina, F. Oyama, B. Ranscht, L.L. Isom, Functional reciprocity between Na+ channel Nav1.6 and beta1 subunits in the coordinated regulation of excitability and neurite outgrowth, Proceedings of the National Academy of Sciences of the United States of America 107 (2010) 2283-2288.

[4] W.J. Brackenbury, T.H. Davis, C. Chen, E.A. Slat, M.J. Detrow, T.L. Dickendesher, B. Ranscht, L.L. Isom, Voltage-gated Na+ channel beta1 subunit-mediated neurite outgrowth requires Fyn kinase and contributes to postnatal CNS development in vivo, J Neurosci 28 (2008) 3246-3256.

[5] W.J. Brackenbury, L.L. Isom, Voltage-gated Na+ channels: potential for beta subunits as therapeutic targets, Expert Opin Ther Targets 12 (2008) 1191-1203.

[6] L.H. Brennaman, P.F. Maness, NCAM in neuropsychiatric and neurodegenerative disorders, Adv Exp Med Biol 663 (2010) 299-317.

[7] E.H. Catania, A. Pimenta, P. Levitt, Genetic deletion of Lsamp causes exaggerated behavioral activation in novel environments, Behav Brain Res 188 (2008) 380-390.

[8] W.A. Catterall, A.L. Goldin, S.G. Waxman, International Union of Pharmacology. XLVII. Nomenclature and structure-function relationships of voltage-gated sodium channels, Pharmacol Rev 57 (2005) 397-409.

[9] C. Chen, T.L. Dickendesher, F. Oyama, H. Miyazaki, N. Nukina, L.L. Isom, Floxed allele for conditional inactivation of the voltage-gated sodium channel beta1 subunit Scn1b, Genesis 45 (2007) 547-553.

[10] C. Chen, R.E. Westenbroek, X. Xu, C.A. Edwards, D.R. Sorenson, Y. Chen, D.P. McEwen, H.A. O'Malley, V. Bharucha, L.S. Meadows, G.A. Knudsen, A. Vilaythong, J.L. Noebels, T.L. Saunders, T. Scheuer, P. Shrager, W.A. Catterall, L.L. Isom, Mice lacking sodium channel beta1 subunits display defects in neuronal excitability, sodium channel expression, and nodal architecture, J Neurosci 24 (2004) 4030-4042.

[11] M.G. Claros, G. von Heijne, TopPred II: an improved software for membrane protein structure predictions, Comput Appl Biosci 10 (1994) 685-686.

[12] T.H. Davis, C. Chen, L.L. Isom, Sodium channel beta1 subunits promote neurite outgrowth in cerebellar granule neurons, The Journal of biological chemistry 279 (2004) 51424-51432.

[13] T.J. Dixon-Salazar, L.C. Keeler, D.A. Trauner, J.G. Gleeson, Autism in several members of a family with generalized epilepsy with febrile seizures plus, Journal of child neurology 19 (2004) 597-603.
[14] A.J. Fein, L.S. Meadows, C. Chen, E.A. Slat, L.L. Isom, Cloning and expression of a zebrafish SCN1B ortholog and identification of a species-specific splice variant, BMC genomics 8 (2007) 226.
[15] J.J. Gargus, Ion channel functional candidate genes in multigenic neuropsychiatric disease, Biol Psychiatry 60 (2006) 177-185.
[16] H.A. Hartmann, L.V. Colom, M.L. Sutherland, J.L. Noebels, Selective localization of cardiac SCN5A sodium channels in limbic regions of rat brain, Nature neuroscience 2 (1999) 593-595.
[17] L.L. Isom, K.S. De Jongh, D.E. Patton, B.F. Reber, J. Offord, H. Charbonneau, K. Walsh, A.L. Goldin, W.A. Catterall, Primary structure and functional expression of the beta 1 subunit of the rat brain sodium channel, Science 256 (1992) 839-842.
[18] L.L. Isom, T. Scheuer, A.B. Brownstein, D.S. Ragsdale, B.J. Murphy, W.A. Catterall, Functional co-expression of the β1 and type IIA α subunits of sodium channels in a mammalian cell line., J. Biol. Chem. 270 (1995) 3306-3312.
[19] L.L. Isom, T. Scheuer, A.B. Brownstein, D.S. Ragsdale, B.J. Murphy, W.A. Catterall, Functional co-expression of the beta 1 and type IIA alpha subunits of sodium channels in a mammalian cell line, The Journal of biological chemistry 270 (1995) 3306-3312.
[20] A. Jacoby, A. Thapar, The contribution of seizures to psychosocial ill-health, Epilepsy Behav 15 Suppl 1 (2009) S41-45.
[21] D.C. Jones, A. Roghanian, D.P. Brown, C. Chang, R.L. Allen, J. Trowsdale, N.T. Young, Alternative mRNA splicing creates transcripts encoding soluble proteins from most LILR genes, Eur J Immunol 39 (2009) 3195-3206.
[22] K.A. Kazen-Gillespie, D.S. Ragsdale, M.R. D'Andrea, L.N. Mattei, K.E. Rogers, L.L. Isom, Cloning, localization, and functional expression of sodium channel beta1A subunits, The Journal of biological chemistry 275 (2000) 1079-1088.
[23] K.A. Kazen-Gillespie, D.S. Ragsdale, M.R. D'Andrea, L.N. Mattei, K.E. Rogers, L.L. Isom, Cloning, localization, and functional expression of sodium channel β1A subunits, J. Biol. Chem. 275 (2000) 1079-1088.
[24] J.W. Law, A.Y. Lee, M. Sun, A.G. Nikonenko, S.K. Chung, A. Dityatev, M. Schachner, F. Morellini, Decreased anxiety, altered place learning, and increased CA1 basal excitatory synaptic transmission in mice with conditional ablation of the neural cell adhesion molecule L1, J Neurosci 23 (2003) 10419-10432.
[25] L.F. Lopez-Santiago, L.S. Meadows, S.J. Ernst, C. Chen, J.D. Malhotra, D.P. McEwen, A. Speelman, J.L. Noebels, S.K. Maier, A.N. Lopatin, L.L. Isom, Sodium channel Scn1b null mice exhibit prolonged QT and RR intervals, J Mol Cell Cardiol 43 (2007) 636-647.
[26] J.C. Makielski, B. Ye, C.R. Valdivia, M.D. Pagel, J. Pu, D.J. Tester, M.J. Ackerman, A ubiquitous splice variant and a common polymorphism affect heterologous expression of recombinant human SCN5A heart sodium channels, Circulation research 93 (2003) 821-828.
[27] J.D. Malhotra, K. Kazen-Gillespie, M. Hortsch, L.L. Isom, Sodium channel beta subunits mediate homophilic cell adhesion and recruit ankyrin to points of cell-cell contact, The Journal of biological chemistry 275 (2000) 11383-11388.
[28] J.D. Malhotra, M.C. Koopmann, K.A. Kazen-Gillespie, N. Fettman, M. Hortsch, L.L. Isom, Structural requirements for interaction of sodium channel beta 1

subunits with ankyrin, The Journal of biological chemistry 277 (2002) 26681-26688.
[29] L.D. Matzel, J. Babiarz, D.A. Townsend, H.C. Grossman, M. Grumet, Neuronal cell adhesion molecule deletion induces a cognitive and behavioral phenotype reflective of impulsivity, Genes Brain Behav 7 (2008) 470-480.
[30] D.P. McEwen, C. Chen, L.S. Meadows, L.F. Lopez-Santiago, L.L. Isom, The voltage-gated Na+ channel β3 subunit does not mediate trans homophilic cell adhesion or associate with the cell adhesion molecule contactin, Neurosci Lett in press (2009).
[31] D.P. McEwen, L.L. Isom, Heterophilic interactions of sodium channel beta1 subunits with axonal and glial cell adhesion molecules, The Journal of biological chemistry 279 (2004) 52744-52752.
[32] D.P. McEwen, L.S. Meadows, C. Chen, V. Thyagarajan, L.L. Isom, Sodium channel β1 subunit-mediated modulation of Nav1.2 currents and cell surface density is dependent on interactions with contactin and ankyrin, J Biol Chem 279 (2004) 16044-16049.
[33] D.P. McEwen, L.S. Meadows, C. Chen, V. Thyagarajan, L.L. Isom, Sodium channel beta1 subunit-mediated modulation of Nav1.2 currents and cell surface density is dependent on interactions with contactin and ankyrin, The Journal of biological chemistry 279 (2004) 16044-16049.
[34] L.S. Meadows, Y.H. Chen, A.J. Powell, J.J. Clare, D.S. Ragsdale, Functional modulation of human brain Nav1.3 sodium channels, expressed in mammalian cells, by auxiliary beta 1, beta 2 and beta 3 subunits, Neuroscience 114 (2002) 745-753.
[35] L.S. Meadows, J. Malhotra, A. Loukas, V. Thyagarajan, K.A. Kazen-Gillespie, M.C. Koopman, S. Kriegler, L.L. Isom, D.S. Ragsdale, Functional and biochemical analysis of a sodium channel beta1 subunit mutation responsible for generalized epilepsy with febrile seizures plus type 1, J Neurosci 22 (2002) 10699-10709.
[36] M.H. Meisler, J.A. Kearney, Sodium channel mutations in epilepsy and other neurological disorders, J Clin Invest 115 (2005) 2010-2017.
[37] G. Patino, W.J. Brackenbury, L.L. Isom, The β1B splice variant of the voltage-gated sodium channel SCN1B is a soluble protein with a possible role in axon pathfinding Program No. 517.12. 2009 Neuroscience Meeting Planner. Chicago, IL: Society for Neuroscience, 2009. Online.
[38] G.A. Patino, L.R. Claes, L.F. Lopez-Santiago, E.A. Slat, R.S. Dondeti, C. Chen, H.A. O'Malley, C.B. Gray, H. Miyazaki, N. Nukina, F. Oyama, P. De Jonghe, L.L. Isom, A functional null mutation of SCN1B in a patient with Dravet syndrome, J Neurosci 29 (2009) 10764-10778.
[39] G.A. Patino, L.L. Isom, Electrophysiology and beyond: Multiple roles of Na(+) channel beta subunits in development and disease, Neuroscience letters (2010).
[40] E. Pauli, H. Stefan, [Emotional and affective disorders, anxiety and personality disorders in epilepsies], Nervenarzt 80 (2009) 1440-1451.
[41] N. Qin, M.R. D'Andrea, M.L. Lubin, N. Shafaee, E.E. Codd, A.M. Correa, Molecular cloning and functional expression of the human sodium channel beta1B subunit, a novel splicing variant of the beta1 subunit, European journal of biochemistry / FEBS 270 (2003) 4762-4770.
[42] C.A. Remme, A.A. Wilde, C.R. Bezzina, Cardiac sodium channel overlap syndromes: different faces of SCN5A mutations, Trends Cardiovasc Med 18 (2008) 78-87.

[43] G. Rougon, O. Hobert, New insights into the diversity and function of neuronal immunoglobulin superfamily molecules, Annu Rev Neurosci 26 (2003) 207-238.
[44] Y. Ruan, N. Liu, S.G. Priori, Sodium channel mutations and arrhythmias, Nat Rev Cardiol 6 (2009) 337-348.
[45] I.E. Scheffer, L.A. Harkin, B.E. Grinton, L.M. Dibbens, S.J. Turner, M.A. Zielinski, R. Xu, G. Jackson, J. Adams, M. Connellan, S. Petrou, R.M. Wellard, R.S. Briellmann, R.H. Wallace, J.C. Mulley, S.F. Berkovic, Temporal lobe epilepsy and GEFS+ phenotypes associated with SCN1B mutations, Brain 130 (2007) 100-109.
[46] S.J. Spence, M.T. Schneider, The role of epilepsy and epileptiform EEGs in autism spectrum disorders, Pediatr Res 65 (2009) 599-606.
[47] J.D. Thompson, D.G. Higgins, T.J. Gibson, CLUSTAL W: improving the sensitivity of progressive multiple sequence alignment through sequence weighting, position-specific gap penalties and weight matrix choice, Nucleic Acids Res 22 (1994) 4673-4680.
[48] M. Uebachs, T. Opitz, M. Royeck, G. Dickhof, M.T. Hostmann, L.L. Isom, H. Beck, Efficacy loss of the anticonvulsant carbamazepine in mice lacking sodium channel β subunits via paradoxical effects on persistent sodium currents, J Neurosci (2010) In press.
[49] G. von Heijne, Membrane protein structure prediction. Hydrophobicity analysis and the positive-inside rule, J Mol Biol 225 (1992) 487-494.
[50] H. Watanabe, D. Darbar, D.W. Kaiser, K. Jiramongkolchai, S. Chopra, B.S. Donahue, P.J. Kannankeril, D.M. Roden, Mutations in sodium channel beta1- and beta2-subunits associated with atrial fibrillation, Circ Arrhythm Electrophysiol 2 (2009) 268-275.
[51] H. Watanabe, D. Darbar, D.W. Kaiser, K. Jiramongkolchai, S. Chopra, B.S. Donahue, P.J. Kannankeril, D.M. Roden, Mutations in Sodium Channel β1- and β2-Subunits Associated With Atrial Fibrillation, Circulation: Arrhythmia and Electrophysiology 2 (2009) 268-275.
[52] H. Watanabe, T.T. Koopmann, S. Le Scouarnec, T. Yang, C.R. Ingram, J.J. Schott, S. Demolombe, V. Probst, F. Anselme, D. Escande, A.C. Wiesfeld, A. Pfeufer, S. Kaab, H.E. Wichmann, C. Hasdemir, Y. Aizawa, A.A. Wilde, D.M. Roden, C.R. Bezzina, Sodium channel beta1 subunit mutations associated with Brugada syndrome and cardiac conduction disease in humans, J Clin Invest 118 (2008) 2260-2268.
[53] H. Watanabe, T.T. Koopmann, S. Le Scouarnec, T. Yang, C.R. Ingram, J.J. Schott, S. Demolombe, V. Probst, F. Anselme, D. Escande, A.C. Wiesfeld, A. Pfeufer, S. Kaab, H.E. Wichmann, C. Hasdemir, Y. Aizawa, A.A. Wilde, D.M. Roden, C.R. Bezzina, Sodium channel beta1 subunit mutations associated with Brugada syndrome and cardiac conduction disease in humans, The Journal of clinical investigation 118 (2008) 2260-2268.

Chapter IV

Conclusions

The work presented in this thesis makes significant contributions to two important areas of sodium channel biology: sodium channel subunit structure and the pathophysiology of *SCN1B* mutations in epilepsy. Our novel findings on the structure and function of sodium channel β1B subunits have changed the field and introduced a new perspective on these multifunctional proteins, including their role in human brain development and disease.

1. The subunit structure of voltage-gated sodium channels

Currently, there are 14 genes described that encode VGSC subunits: 10 encoding α and 4 encoding β subunits [4]. Whereas most of the genes encoding α subunits give rise to multiple splice variants, *SCN1B* is so far the only β subunit gene found be alternatively spliced in the coding region [17, 28] [7]. Prior to our work, all of the splice variants encoded by α subunit genes, as well as the β 1 - 4 subunits, were shown to be transmembrane proteins [4, 13, 14, 22, 37]. Based on this information, it was assumed that short strings of hydrophobic amino acids present in the C-terminus of the β1B splice variant represented a transmembrane domain [17]. Importantly, our new results, presented here, prove that β1B lacks a transmembrane domain and is instead a soluble protein that is secreted into the extracellular medium. These results are the first

description of a soluble VGSC subunit. A soluble voltage-gated potassium channel subunit of unknown function has been described previously in the rat kidney, but unlike β1B, this subunit is intracellular [1], and it is unlikely that it could have similar functions as β1B.

The stoichiometry of VGSCs is known only for rat brain, from which channels were purified to theoretical homogeneity. These data showed that VGSCs are heterotrimers, consisting of one α central, pore-forming subunit associated with one covalently and one non-covalently linked β subunit [11, 12]. Based on these data, it has been assumed that the same configuration holds true for VGSCs in other tissues and species. However, whether this 1:1:1 stoichiometry occurs in all areas, all cell types, and all subcellular compartments of the CNS is unknown. The presence of a soluble β subunit lends greater complexity to the possible combinations of VGSC subunits and thus VGSC function. For example, secreted β1B interacts with neuronal β1 *in trans* to promote neurite outgrowth in cerebellar granule neurons. In spite of our results suggesting that β1B does not associate with neuronal VGSC α subunits, if neuronal β1 subunits that bind β1B are also associated with α, then β1B may associate indirectly with the VGSC complex. This idea fits with our new understanding of VGSCs as multi-protein complexes composed of ion-conducting proteins, cell adhesion molecules, transmembrane proteases, extracellular matrix molecules, and signaling proteins [27]. Interestingly, while we have no evidence of β1B association with neuronal α subunits, our biochemical results suggest that β1B may interact transiently with $Na_v1.5$, in agreement with previous results showing modulation of Nav1.5 current by β1B [32]. Similarly, it is possible that the electrophysiological properties of $Na_v1.1$ or $Na_v1.3$ (or those of other tetrodotoxin-sensitive α subunits) may be transiently modulated by β1B or indirectly modulated through β1–β1B *trans* interactions. Alternatively, β1B may function exclusively in subcellular domains where β1 is present in the absence of α subunits.

2. Pathophysiology of SCN1B mutations

A number of *SCN1B* mutations located in the Ig loop domain are linked with mild to moderate GEFS+ epilepsy syndromes (reviewed in [26]). Our results have expanded the spectrum of epileptic syndromes linked to *SCN1B* to include Dravet Syndrome (the most severe type of GEFS+) and idiopathic epilepsies. We have also demonstrated that a mutation affecting only the β1B splice variant, and not β1, (p.G257R) is linked to neurological disease. Interestingly, the two *SCN1B* mutations we studied, p.R125C and p.G257R, have a common pathogenic mechanism: they are both trafficking-deficient. While p.R125C was tested on the β1 backbone, we predict that this Ig loop domain mutation affects both β1 and β1B, resulting in intracellular retention of both subunits. Immunocytochemical experiments suggest that the mutants p.R85H and p.R85C are also trafficking-deficient [35]. We predict that the trafficking deficiency demonstrated for these mutations, using the β1 backbone, also occurs for β1B. Taken together, these results suggest that trafficking deficiency, resulting in functional null alleles, might be a common mechanism for some cases of β1/β1B dysfunction.

Because *Scn1b* null mice lack β1 and β1B, it is not possible to determine which subunit is most critical for normal functioning of the CNS. Similar to *Scn1b* null mice, the p.R125C proband is predicted to lack β1 and β1B function [26]. It is tempting to point to the p.G257R mutation as a cause of epilepsy to argue that β1B is the most critical *SCN1B* subunit in terms of CNS function. However, caution is necessary in addressing this question. An on-going project in our lab is the generation of mice expressing only the β1B splice variant. Once these mice are available, their neurologic phenotype will help to start answering critical *SCN1B* structure-function questions.

Whereas most of the literature regarding *SCN1B* mutations and epilepsy has focused on the changes that the mutation causes in the modulation of the

electrophysiological characteristics of selected VGSC α subunits in heterologous systems, our *ex vivo* recordings of neurons from wild-type or *Scn1b* null mice have evidenced only subtle changes in sodium current. A large body of work from our lab has also demonstrated that VGSC β subunits are multifunctional. In addition to modulation of sodium current, β subunits function as CAMs, and in the case of β1B (with its limited ability to associate with α subunits) this might be the predominant function *in vivo*. Similar to the question regarding the relative functional importance of *SCN1B* splice variants, the question of which function, electrophysiology versus cell adhesion, is most relevant *in vivo* is difficult to answer. In the end, both splice variants and both functions are likely critical in brain – although with differential cell type specific, subcellular domain specific, temporal components.

Importantly, our results demonstrate that the mechanism of epileptogenesis due to *SCN1B* mutations is different from that due to *SCN1A* mutations. Multiple lines of evidence point to diverse mechanisms underlying a common disease phenotype. *Scn1a*$^{+/-}$ mice exhibit a severe neurological phenotype [36] that is similar to *Scn1b* null mice [5] and Dravet Syndrome patients (either due to heterozygous *SCN1A* or homozygous *SCN1B* mutations) [3, 9, 19, 34] and that is not very dissimilar to that of the *Scn1a* null mice [36]. *Scn1b*$^{+/-}$ mice, on the other hand, have a normal neurological phenotype. These data suggest that while only one copy of *SCN1B* is required for normal brain function, severe epilepsy results from *SCN1A* haploinsufficiency. $Na_v1.1$, encoded by *SCN1A*, is a key VGSC in the generation of action potentials in hippocampal inhibitory neurons [24, 36]. Consistent with this, GABAergic neurons from *Scn1a*$^{+/-}$ hippocampus exhibit dramatic reductions in sodium current density compared to wild-type cells [36]. This loss of function is proposed to be responsible for seizures present in both the mouse model and in human patients with *SCN1A* mutations. In contrast, electrophysiological recordings from *Scn1b* null neurons, including hippocampal bipolar

neurons[26], have demonstrated only minor differences in sodium current compared to wild-type, suggesting a different mechanism of seizure induction. Finally, while epileptic syndromes linked to *SCN1A* mutations do not respond to (and can be exacerbated by) treatment with sodium channel blocking drugs [6], patients described in our study of the β1B p.G257R mutation were successfully treated with carbamazepine, again suggesting different mechanisms of epilepsy. Together, these data suggest that while seizures due to *SCN1A* mutations may be caused by neuronal cell type-specific changes in sodium current, seizures due to *SCN1B* mutations likely have a different underlying cause. Based on results from our laboratory demonstrating the importance of *Scn1b* in the correct migration and tract formation of cortical and cerebellar neurons [2], we propose that aberrant β1/ β1B CAM function leading to neuronal pathfinding errors may be responsible for the development of neuronal hyperexcitability resulting in seizures.

3. Unanswered questions and future directions

One of the most puzzling aspects of *SCN1B* mutations and epilepsy is the observation that, while the majority of human epilepsy patients with such mutations are heterozygous, *Scn1b*$^{+/-}$ mice do not exhibit seizures, and may even have a higher seizure threshold than wild-type according to our PTZ seizure-induction experiments[26]. If *SCN1B* haploinsufficiency in human subjects results in seizures, then why is it necessary for mice to be missing both *Scn1b* alleles to cause the epileptic phenotype? Genetic background and epigenetics are likely critical here. In support of this, many of the *SCN1B* mutations reported to cause epilepsy or cardiac arrhythmia (including our two studies) have incomplete penetrance. Another possibility, not mutually exclusive with the one above, is based on key biological differences between a null allele (resulting in gene deletion) and a mutated allelle (resulting in production of an abnormal protein).

Importantly, a mutant protein may be either loss-of-function (similar to a deleted allele) or gain-of-function. Our results in heterologous systems predict that β1 p.C121W [21], β1 p.R125C, and β1B p.G257R result in partial to complete loss-of-function. However, the possibility exists that these mutations may result in gain-of-function *in vivo*. Current work in our laboratory aims to determine if the presence of these mutated proteins may be detrimental to the function of neurons, or even cause cellular stress and apoptosis through the activation of the unfolded protein response [38].

A very pressing question is how do we translate our findings to the clinical realm? Our results open new avenues for clinical research that must be followed in the hope of developing the best treatments possible for patients with *SCN1B* mutations. So far all the patients reported with *SCN1B* mutations present with either epilepsy or cardiac arrhythmia, but there are no known reports of a patient with both types of pathology. One reason for this might be that the epileptic syndromes in this context predominate during childhood and adolescence whereas the cardiac arrhythmias (Brugada syndrome, conduction disease, and atrial fibrillation) usually make their appearance from the third to fourth decades of life onwards [31, 32]. Complicating this lack of overlap in age of presentation is that the clinical manifestations of both the epileptic syndromes and the cardiac arrhythmias can be subtle. Most patients with epilepsy due to *SCN1B* mutations present with febrile seizures, which are the most common type of seizure during childhood. By the same token, people presenting with cardiac arrhythmia associated with *SCN1B* mutations can be asymptomatic for many years. To address this question it will be necessary to perform systematic electrocardiographic studies in epilepsy patients with *SCN1B* mutations. Such studies will not be easy because the arrhythmias described can be episodic. Thus, it might be important to perform the electrocardiographic studies in settings known to induce rhythm disorders, like fever and sleep for Brugada syndrome [15, 25, 29, 30]. The possible association of epilepsy and cardiac arrhythmia in the same

subject as a consequence of one mutation has the potential to explain some of the sudden unexplained death in epilepsy (SUDEP) cases due to cardiac arrhythmia [20, 23].

Previous results from our laboratory have demonstrated a function for β1 and β1B as CAMs during tract formation in the CNS. Since abnormalities in brain development and function can result not only in neurological syndromes but in psychiatric ones as well, exemplified by the significant comorbidity between epilepsy and psychiatric syndromes [8, 10], it will be important to explore the possible role of *SCN1B* mutations and polymorphisms in behavioral phenotypes. Such work is ongoing in our laboratory with *Scn1b*$^{+/-}$ mice. In addition, whether β1 and β1B function as CAMs during development of the peripheral nervous system remains to be explored. In support of this possibility a previous study has demonstrated peripheral nerve abnormalities in patients with the p.C121W mutation [18]. If such a role proves true it could also be important for the cardiac arrhythmia phenotype as a proportion of patients with Brugada syndrome demonstrate a reduction in sympathetic innervation of the heart [16, 33].

In conclusion, my graduate work has made a number of important contributions to the understanding of the role of sodium channel β subunits in brain development and disease. The results from these projects, which will continue in our laboratory, and of the proposed human studies promise to bring us closer to targeted and effective therapies for patients with *SCN1B* mutations and to a better understanding of VGSC physiology. Undoubtedly, many new questions will also arise. But we look forward both to pursuing those new challenges and continuing to apply them for the benefit of our patients.

Bibliography

[1] A.H. Beesley, B. Ortega, S.J. White, Splicing of a retained intron within ROMK K+ channel RNA generates a novel set of isoforms in rat kidney, Am J Physiol 276 (1999) C585-592.

[2] W.J. Brackenbury, T.H. Davis, C. Chen, E.A. Slat, M.J. Detrow, T.L. Dickendesher, B. Ranscht, L.L. Isom, Voltage-gated Na+ channel beta1 subunit-mediated neurite outgrowth requires Fyn kinase and contributes to postnatal CNS development in vivo, J Neurosci 28 (2008) 3246-3256.

[3] R.H. Caraballo, N. Fejerman, Dravet syndrome: a study of 53 patients, Epilepsy research 70 Suppl 1 (2006) S231-238.

[4] W.A. Catterall, A.L. Goldin, S.G. Waxman, International Union of Pharmacology. XLVII. Nomenclature and structure-function relationships of voltage-gated sodium channels, Pharmacological reviews 57 (2005) 397-409.

[5] C. Chen, R.E. Westenbroek, X. Xu, C.A. Edwards, D.R. Sorenson, Y. Chen, D.P. McEwen, H.A. O'Malley, V. Bharucha, L.S. Meadows, G.A. Knudsen, A. Vilaythong, J.L. Noebels, T.L. Saunders, T. Scheuer, P. Shrager, W.A. Catterall, L.L. Isom, Mice lacking sodium channel beta1 subunits display defects in neuronal excitability, sodium channel expression, and nodal architecture, J Neurosci 24 (2004) 4030-4042.

[6] A.V. Delgado-Escueta, B.F. Bourgeois, Debate: Does genetic information in humans help us treat patients? PRO--genetic information in humans helps us treat patients. CON--genetic information does not help at all, Epilepsia 49 Suppl 9 (2008) 13-24.

[7] S.D. Dib-Hajj, S.G. Waxman, Genes encoding the beta 1 subunit of voltage-dependent Na+ channel in rat, mouse and human contain conserved introns, FEBS letters 377 (1995) 485-488.

[8] T.J. Dixon-Salazar, L.C. Keeler, D.A. Trauner, J.G. Gleeson, Autism in several members of a family with generalized epilepsy with febrile seizures plus, Journal of child neurology 19 (2004) 597-603.

[9] C. Dravet, M. Bureau, H. Oguni, Y. Fukuyama, O. Cokar, Severe myoclonic epilepsy in infancy: Dravet syndrome, Advances in neurology 95 (2005) 71-102.

[10] J.J. Gargus, Ion channel functional candidate genes in multigenic neuropsychiatric disease, Biol Psychiatry 60 (2006) 177-185.

[11] R.P. Hartshorne, W.A. Catterall, The sodium channel from rat brain. Purification and subunit composition, The Journal of biological chemistry 259 (1984) 1667-1675.

[12] R.P. Hartshorne, D.J. Messner, J.C. Coppersmith, W.A. Catterall, The saxitoxin receptor of the sodium channel from rat brain. Evidence for two nonidentical beta subunits, The Journal of biological chemistry 257 (1982) 13888-13891.

[13] L.L. Isom, K.S. De Jongh, D.E. Patton, B.F. Reber, J. Offord, H. Charbonneau, K. Walsh, A.L. Goldin, W.A. Catterall, Primary structure and functional expression of the beta 1 subunit of the rat brain sodium channel, Science 256 (1992) 839-842.

[14] L.L. Isom, D.S. Ragsdale, K.S. De Jongh, R.E. Westenbroek, B.F. Reber, T. Scheuer, W.A. Catterall, Structure and function of the beta 2 subunit of brain

sodium channels, a transmembrane glycoprotein with a CAM motif, Cell 83 (1995) 433-442.
[15] S. Kalra, S.B. Iskandar, S. Duggal, R.D. Smalligan, Fever-induced ST-segment elevation with a Brugada syndrome type electrocardiogram, Ann Intern Med 148 (2008) 82-84.
[16] T. Kawaguchi, M. Nomura, T. Tujikawa, Y. Nakaya, S. Ito, 123I-metaiodo-benzylguanidine myocardial scintigraphy in the Brugada-type ECG, J Med Invest 53 (2006) 95-102.
[17] K.A. Kazen-Gillespie, D.S. Ragsdale, M.R. D'Andrea, L.N. Mattei, K.E. Rogers, L.L. Isom, Cloning, localization, and functional expression of sodium channel beta1A subunits, The Journal of biological chemistry 275 (2000) 1079-1088.
[18] M.C. Kiernan, A.V. Krishnan, C.S. Lin, D. Burke, S.F. Berkovic, Mutation in the Na+ channel subunit SCN1B produces paradoxical changes in peripheral nerve excitability, Brain 128 (2005) 1841-1846.
[19] C. Korff, L. Laux, K. Kelley, J. Goldstein, S. Koh, D. Nordli, Jr., Dravet syndrome (severe myoclonic epilepsy in infancy): a retrospective study of 16 patients, Journal of child neurology 22 (2007) 185-194.
[20] B.N. McLean, S. Wimalaratna, Sudden death in epilepsy (SUDEP) recorded in amublatory EEG, J Neurol Neurosurg Psychiatry (2007).
[21] L.S. Meadows, J. Malhotra, A. Loukas, V. Thyagarajan, K.A. Kazen-Gillespie, M.C. Koopman, S. Kriegler, L.L. Isom, D.S. Ragsdale, Functional and biochemical analysis of a sodium channel beta1 subunit mutation responsible for generalized epilepsy with febrile seizures plus type 1, J Neurosci 22 (2002) 10699-10709.
[22] K. Morgan, E.B. Stevens, B. Shah, P.J. Cox, A.K. Dixon, K. Lee, R.D. Pinnock, J. Hughes, P.J. Richardson, K. Mizuguchi, A.P. Jackson, beta 3: an additional auxiliary subunit of the voltage-sensitive sodium channel that modulates channel gating with distinct kinetics, Proceedings of the National Academy of Sciences of the United States of America 97 (2000) 2308-2313.
[23] L. Nashef, N. Hindocha, A. Makoff, Risk factors in sudden death in epilepsy (SUDEP): the quest for mechanisms, Epilepsia 48 (2007) 859-871.
[24] I. Ogiwara, H. Miyamoto, N. Morita, N. Atapour, E. Mazaki, I. Inoue, T. Takeuchi, S. Itohara, Y. Yanagawa, K. Obata, T. Furuichi, T.K. Hensch, K. Yamakawa, Na(v)1.1 localizes to axons of parvalbumin-positive inhibitory interneurons: a circuit basis for epileptic seizures in mice carrying an Scn1a gene mutation, J Neurosci 27 (2007) 5903-5914.
[25] O. Ozeke, D. Aras, B. Geyik, B. Deveci, T. Selcuk, Brugada-type electrocardiographic pattern induced by fever, Indian Pacing Electrophysiol J 5 (2005) 146-148.
[26] G.A. Patino, L.R. Claes, L.F. Lopez-Santiago, E.A. Slat, R.S. Dondeti, C. Chen, H.A. O'Malley, C.B. Gray, H. Miyazaki, N. Nukina, F. Oyama, P. De Jonghe, L.L. Isom, A functional null mutation of SCN1B in a patient with Dravet syndrome, J Neurosci 29 (2009) 10764-10778.
[27] G.A. Patino, L.L. Isom, Electrophysiology and beyond: Multiple roles of Na(+) channel beta subunits in development and disease, Neuroscience letters (2010).
[28] N. Qin, M.R. D'Andrea, M.L. Lubin, N. Shafaee, E.E. Codd, A.M. Correa, Molecular cloning and functional expression of the human sodium channel beta1B subunit, a novel splicing variant of the beta1 subunit, European journal of biochemistry / FEBS 270 (2003) 4762-4770.
[29] A. Shalev, L. Zeller, O. Galante, A. Shimony, H. Gilutz, R. Illia, Symptomatic Brugada unmasked by fever, Isr Med Assoc J 10 (2008) 548-549.

[30] M. Unlu, F. Bengi, B. Amasyali, S. Kose, Brugada-like electrocardiographic changes induced by fever, Emerg Med J 24 (2007) e4.
[31] H. Watanabe, D. Darbar, D.W. Kaiser, K. Jiramongkolchai, S. Chopra, B.S. Donahue, P.J. Kannankeril, D.M. Roden, Mutations in sodium channel beta1- and beta2-subunits associated with atrial fibrillation, Circ Arrhythm Electrophysiol 2 (2009) 268-275.
[32] H. Watanabe, T.T. Koopmann, S. Le Scouarnec, T. Yang, C.R. Ingram, J.J. Schott, S. Demolombe, V. Probst, F. Anselme, D. Escande, A.C. Wiesfeld, A. Pfeufer, S. Kaab, H.E. Wichmann, C. Hasdemir, Y. Aizawa, A.A. Wilde, D.M. Roden, C.R. Bezzina, Sodium channel beta1 subunit mutations associated with Brugada syndrome and cardiac conduction disease in humans, The Journal of clinical investigation 118 (2008) 2260-2268.
[33] T. Wichter, P. Matheja, L. Eckardt, P. Kies, K. Schafers, E. Schulze-Bahr, W. Haverkamp, M. Borggrefe, O. Schober, G. Breithardt, M. Schafers, Cardiac autonomic dysfunction in Brugada syndrome, Circulation 105 (2002) 702-706.
[34] M. Wolff, C. Casse-Perrot, C. Dravet, Severe myoclonic epilepsy of infants (Dravet syndrome): natural history and neuropsychological findings, Epilepsia 47 Suppl 2 (2006) 45-48.
[35] R. Xu, E.A. Thomas, E.V. Gazina, K.L. Richards, M. Quick, R.H. Wallace, L.A. Harkin, S.E. Heron, S.F. Berkovic, I.E. Scheffer, J.C. Mulley, S. Petrou, Generalized epilepsy with febrile seizures plus-associated sodium channel beta1 subunit mutations severely reduce beta subunit-mediated modulation of sodium channel function, Neuroscience 148 (2007) 164-174.
[36] F.H. Yu, M. Mantegazza, R.E. Westenbroek, C.A. Robbins, F. Kalume, K.A. Burton, W.J. Spain, G.S. McKnight, T. Scheuer, W.A. Catterall, Reduced sodium current in GABAergic interneurons in a mouse model of severe myoclonic epilepsy in infancy, Nature neuroscience 9 (2006) 1142-1149.
[37] F.H. Yu, R.E. Westenbroek, I. Silos-Santiago, K.A. McCormick, D. Lawson, P. Ge, H. Ferriera, J. Lilly, P.S. DiStefano, W.A. Catterall, T. Scheuer, R. Curtis, Sodium channel beta4, a new disulfide-linked auxiliary subunit with similarity to beta2, J Neurosci 23 (2003) 7577-7585.
[38] K. Zhang, R.J. Kaufman, Protein folding in the endoplasmic reticulum and the unfolded protein response, Handb Exp Pharmacol (2006) 69-91.